QUANTIFYING THE IMPACT OF ROCKFALL ON THE MOBILITY OF CRITICAL TRANSPORTATION CORRIDORS

FINAL PROJECT REPORT

by

Keith Cunningham
University of Alaska, Fairbanks (UAF)
Ben Leshchinsky, Michael Olsen, Katherine Holtan
Oregon State University (OSU)
Kristen Smith, Joseph Wartman
University of Washington (UW)

Sponsorship
Pactrans and Oregon DOT

for

Pacific Northwest Transportation Consortium (PacTrans)
USDOT University Transportation Center for Federal Region 10
University of Washington
More Hall 112, Box 352700
Seattle, WA 98195-2700

In cooperation with the U.S. Department of Transportation,
Office of the Assistant Secretary for Research and Technology

DISCLAIMER

This report's contents reflect the views of the authors, who are responsible for the facts and the accuracy of the information presented herein. This document is disseminated under the sponsorship of the U.S. Department of Transportation's University Transportation Centers Program, in the interest of information exchange. The Pacific Northwest Transportation Consortium, the U.S. Government and matching sponsor assume no liability for the contents or use thereof.

TECHNICAL REPORT DOCUMENTATION PAGE

1. Report No.	**2. Government Accession No.**	**3. Recipient's Catalog No.**

4. Title and Subtitle Quantifying the Impact of Rockfall on the Mobility of Critical Transportation Corridors	**5. Report Date** 11/30/2020 **6. Performing Organization Code**
7. Author(s) and Affiliations Keith W. Cunningham – University of Alaska 0000-0002-6979-7893 Ben Leshchinsky – Oregon State University 0000-0003-3890-1368 Michael J. Olsen – Oregon State University 0000-0002-2989-5309 Joseph Wartman – University of Washington 0000-0001-7659-7198	**8. Performing Organization Report No.** 2018-M-UAF-1
9. Performing Organization Name and Address PacTrans Pacific Northwest Transportation Consortium University Transportation Center for Federal Region 10 University of Washington More Hall 112 Seattle, WA 98195-2700	**10. Work Unit No. (TRAIS)** **11. Contract or Grant No.** 69A3551747110
12. Sponsoring Organization Name and Address United States Department of Transportation Research and Innovative Technology Administration 1200 New Jersey Avenue, SE Washington, DC 20590	**13. Type of Report and Period Covered** Sept 1, 2018 - August 31, 2020 **14. Sponsoring Agency Code**

15. Supplementary Notes

Report uploaded to: www.pactrans.org

16. Abstract

This work developed a framework to assist transportation planners and managers (and others) in making informed resource allocation decisions based on the risks that rockfalls pose to the mobility of critical highway corridors. Transportation agencies, already faced with difficult asset management decisions, will benefit from a data-driven framework that synthesizes objective, quantitative identification of unstable slopes, mitigation strategies, and historical data related to debris volumes and closure times. Such an analysis will enable identification of which slopes pose the greatest risk to highway closure from infrastructure damage, thus providing an objective approach for optimizing resource allocation and potential mitigation strategies. In particular, proactive slope remediation is typically beneficial, but the benefits are not well quantified. This framework will quantify the benefit of intervention for rockfall activity and, more importantly, the cost-efficacy (accounting for mobility loss) from a risk perspective.

17. Key Words Rockfall Impacts on Mobility (RIM), Rockfall Activity Index (RAI)		**18. Distribution Statement** No restrictions.	
19. Security Classification (of this report) Unclassified.	**20. Security Classification (of this page)** Unclassified.	**21. No. of Pages** 75	**22. Price** N/A

Form DOT F 1700.7 (8-72) **Reproduction of completed page authorized.**

SI* (MODERN METRIC) CONVERSION FACTORS

APPROXIMATE CONVERSIONS TO SI UNITS				
Symbol	**When You Know**	**Multiply By**	**To Find**	**Symbol**
		LENGTH		
in	inches	25.4	millimeters	mm
ft	feet	0.305	meters	m
yd	yards	0.914	meters	m
mi	miles	1.61	kilometers	km
		AREA		
in^2	square inches	645.2	square millimeters	mm^2
ft^2	square feet	0.093	square meters	m^2
yd^2	square yard	0.836	square meters	m^2
ac	acres	0.405	hectares	ha
mi^2	square miles	2.59	square kilometers	km^2
		VOLUME		
fl oz	fluid ounces	29.57	milliliters	mL
gal	gallons	3.785	liters	L
ft^3	cubic feet	0.028	cubic meters	m^3
yd^3	cubic yards	0.765	cubic meters	m^3
		NOTE: volumes greater than 1000 L shall be shown in m^3		
		MASS		
oz	ounces	28.35	grams	g
lb	pounds	0.454	kilograms	kg
T	short tons (2000 lb)	0.907	megagrams (or "metric ton")	Mg (or "t")
		TEMPERATURE (exact degrees)		
°F	Fahrenheit	5 (F-32)/9 or (F-32)/1.8	Celsius	°C
		ILLUMINATION		
fc	foot-candles	10.76	lux	lx
fl	foot-Lamberts	3.426	candela/m^2	cd/m^2
		FORCE and PRESSURE or STRESS		
lbf	poundforce	4.45	newtons	N
lbf/in^2	poundforce per square inch	6.89	kilopascals	kPa

APPROXIMATE CONVERSIONS FROM SI UNITS				
Symbol	**When You Know**	**Multiply By**	**To Find**	**Symbol**
		LENGTH		
mm	millimeters	0.039	inches	in
m	meters	3.28	feet	ft
m	meters	1.09	yards	yd
km	kilometers	0.621	miles	mi
		AREA		
mm^2	square millimeters	0.0016	square inches	in^2
m^2	square meters	10.764	square feet	ft^2
m^2	square meters	1.195	square yards	yd^2
ha	hectares	2.47	acres	ac
km^2	square kilometers	0.386	square miles	mi^2
		VOLUME		
mL	milliliters	0.034	fluid ounces	fl oz
L	liters	0.264	gallons	gal
m^3	cubic meters	35.314	cubic feet	ft^3
m^3	cubic meters	1.307	cubic yards	yd^3
		MASS		
g	grams	0.035	ounces	oz
kg	kilograms	2.202	pounds	lb
Mg (or "t")	megagrams (or "metric ton")	1.103	short tons (2000 lb)	T
		TEMPERATURE (exact degrees)		
°C	Celsius	1.8C+32	Fahrenheit	°F
		ILLUMINATION		
lx	lux	0.0929	foot-candles	fc
cd/m^2	candela/m^2	0.2919	foot-Lamberts	fl
		FORCE and PRESSURE or STRESS		
N	newtons	0.225	poundforce	lbf
kPa	kilopascals	0.145	poundforce per square inch	lbf/in^2

*SI is the symbol for the International System of Units. Appropriate rounding should be made to comply with Section 4 of ASTM E380.
(Revised March 2003)

TABLE OF CONTENTS

List of Abbreviations xi

Acknowledgments xiii

Executive Summary xiv

CHAPTER 1.Introduction 1

1.1. Project Background 2

1.1.1. Lidar Evaluation and Digital Surface Modeling 2

1.1.2. The Rockfall Activity Index (RAI) 3

1.1.3. Photogrammetry from Unmanned Aircraft Systems (UAS) 4

1.1.4. Slope Morphology and Climate Change 5

1.2. Technology Transfer 6

CHAPTER 2.The Rockfall Impacts on Mobility (RIM) database 7

2.1. Existing Rockfall Databases 7

2.2. Database Objectives and Specifications 9

2.2.1. ODOT Unstable Slopes Database 9

2.2.2. ODOT TripCheck 10

2.2.3. Alaska DOT GAM Program: Rockslopes 12

2.2.4. AKDOT Geo-Event Tracker 15

2.2.5. Washington Department of Natural Resources Database 18

2.2.6. NASA Landslide Viewer 19

2.3. Database Management 21

2.4. The RIM Database 22

2.4.1. Database Structure 24

2.4.2. Challenges 26

2.5. Analysis Results 27

2.5.1. Closure Times 27

2.5.2. Costs 31

2.5.3. Closure Times and Costs 32

2.6. Conclusions 35

CHAPTER 3.Study Site And Data 37

3.1. Data Collection 38

CHAPTER 4.Mitigation Assessment 41
4.1. Introduction 41
4.2. Background 44
4.2.1. Regional Geology 44
4.2.2. Local Geology 44
4.2.3. Study Site 46
4.2.4. Data Acquisition 49
4.2.5. Data Processing 49
4.3. Observations 50
4.3.1. Site Characteristics 50
4.3.2. Data Acquisition and Preparation 52
4.4. Findings 53
4.4.1. Hazard Data 53
4.4.2. Change Data 62
4.5. Discussion 66
4.5.1. Excavation Damage 70
4.5.2. Data Error 70
4.5.3. RAI Hazard 70
CHAPTER 5.Summary of chapters' ConClusions 72
References 75
Bibliography 78
Appendix A: RockFalls in the News 84

LIST OF FIGURES

Figure 2.1 Map of the Unstable Slopes Database (Oregon Signed Routes Layer from Road Inventory and Classification Services Unit (RICS) and ODOT) 9
Figure 2.2 Rockfalls per year observed in Oregon from the ODOT Unstable Slopes database. 10
Figure 2.3 Map of the Rockslide TripCheck Database from 2015 on (Oregon Signed Routes Layer from Road Inventory and Classification Services Unit (RICS) and ODOT) 11
Figure 2.4 ODOT TripCheck database..................... 12
Figure 2.5 Map of AKDOT&PF rockslides (Roads from AKDOT&PF) 13
Figure 2.6 AKDOT GAM database web viewer. https://akdot.maps.arcgis.com/apps/MapSeries/index.html?appid=0be74f9ba168424eac48983da02e0250..................... 13
Figure 2.7 AKDOT rock slopes event frequency per year. 14
Figure 2.8 AKDOT rock xlopes frequency per rockfall history score..................... 14
Figure 2.9 Map of the AKDOT&PF Geo-Event Tracker (Roads from AKDOT)..................... 15
Figure 2.10 AKDOT GAM data viewer 16
Figure 2.11 Rockfall frequency by year in Alaska 16
Figure 2.12 Map of the WADNR landslides database (Roads from WSDOT) 18
Figure 2.13 WADNR landslide database interface. 19
Figure 2.14 Map of NASA landslides. https://maps.nccs.nasa.gov/arcgis/apps/webappviewer/index.html?id=824ea5864ec8423fb985b33ee6bc05b7 20
Figure 2.15 NASA landslide database rockfall/rockslide event frequency by year. 20
Figure 2.16 NASA Landslide Viewer..................... 21
Figure 2.17 RIM database rockfall locations 23
Figure 2.18 Example media articles of highway closures due to rockfalls..................... 23
Figure 2.19 Histogram of dates of rockslides in the RIM database. 24
Figure 2.20 Estimated rockfall volumes versus associated closure times catalogued in the RIM database. An associated power-law regression line is shown. 28
Figure 2.21 Estimated rockfall volumes versus associated closure times catalogued in the RIM database distinguished by reported rockfall volumes (green squares) and estimated rockfall volumes (blue circles). An associated power-law regression line for each is shown. 29
Figure 2.22 Plot of event size versus closure time. See Table 2 for interpretation of the codes. In order to apply different regression modes, all 0's were modified to be 0.0000001..................... 30
Figure 2.23 AKDOT Geo Event Tracker event size score vs. closure duration score. See Table 2 for definitions of the codes. 31
Figure 2.24. AKDOT rock event size versus cost..................... 32
Figure 2.25. Estimated repair costs versus closure times attained from the ODOT Unstable Slopes database. 33
Figure 2.26. Closure times and costs from the AKDOT Geo Event Rockslide and Landslide database. 34
Figure 2.27. Plot of repair costs versus annual maintenance costs. Entries with 0's have been removed. 34

Figure 2.28 Plot of estimated closure times and repair costs. Entries with 0's have been removed.. 35
Figure 3.1 Location of the study sites in Alaska... 37
Figure 4.1 Geologic map of Alaska with an inset of 1:250,000. The Healy Quadrangle encompassing the study area is circled in black (Wilson et al. 2005). 45
Figure 4.2 Location map obtained from Google Earth of the Glitter Gulch study site outside of Denali National Park in Alaska. State Route 3, also known as AK Interstate 4, more commonly referred to as the George Parks Highway, is the affected transportation route. This route borders the Nenana River, a tributary to the Tanana River that drains the northern slopes of Denali. 47
Figure 4.3 Aerial lidar DEM of the study area (circled in orange) obtained from the state of Alaska's Department of Geological and Geophysical Surveys on 8/20/18......... 48
Figure 4.4 Oblique photograph taken in August 2018 of the study slope at MP 241 on the George Parks Highway near Glitter Gulch, Alaska. The image was captured with a DJI Phantom 4 drone flown by Jake Dafne. Sugar Loaf Mountain is in the distance, and the Nenana River is in the foreground. 51
Figure 4.5 RAI classes (A) and RAI scores (B) for the 2012 scan of the study slope at MP 241 on the George Parks Highway near Glitter Gulch, Alaska. 54
Figure 4.6 RAI classes (A) and RAI scores (B) for the 2013 scan of the study slope at MP 241 on the George Parks Highway near Glitter Gulch, Alaska. 55
Figure 4.7 RAI classes (A) and RAI scores (B) for the 2014 scan of the study slope at MP 241 on the George Parks Highway near Glitter Gulch, Alaska. 57
Figure 4.8 RAI classes (A) and RAI scores (B) for the 2015 scan of the study slope at MP 241 on the George Parks Highway near Glitter Gulch, Alaska. Planned mitigation areas are circled in blue for scaling and black for trim blasting............ 58
Figure 4.9 RAI classes (A) and RAI scores (B) for the 2017 scan of the study slope at MP 241 on the George Parks Highway near Glitter Gulch, Alaska. 60
Figure 4.10 RAI classes (A) and RAI scores (B) for the 2018 scan of the study slope at MP 241 on the George Parks Highway near Glitter Gulch, Alaska. 61
Figure 4.11 Map of the slope near MP 240.5 on the George Parks Highway in Denali, Alaska. The change data from August 2012 to August 2013 are highlighted, with red representing a loss and blue representing a gain. Gains around the perimeter may represent differences in cropping of the annual data. The map shows the change data overlying the point cloud in grey; the 2012 data were not colored RGB, so an overlay with a true color image was not generated. 63
Figure 4.12 Map of the slope near MP 240.5 on the George Parks Highway in Denali, Alaska. The change data from August 2013 to August 2014 are highlighted, with red representing a loss and blue representing a gain. Gains around the perimeter may represent differences in cropping of the annual data. Map A shows the change data overlaying the point cloud in grey, while map B shows the change data overlaying a true color point cloud from 2013 data, with the points created during a hole-filling algorithm colored fuchsia. 64
Figure 4.13 Map of the slope near MP 240.5 on the George Parks Highway in Denali, Alaska. The change data from August 2014 to August 2015 are highlighted, with red representing a loss and blue representing a gain. Gains around the perimeter may represent differences in cropping of the annual data. Map A

shows the change data overlaying the point cloud in grey, while map B shows the change data overlaying a true color point cloud from 2014 data, with the points created during a hole-filling algorithm colored fuchsia. 65
Figure 4.14 Map of the slope near MP 240.5 on the George Parks Highway in Denali, Alaska. The change data from August 2015 to August 2017 are highlighted, with red representing a loss and blue representing a gain; the large change is largely a result of a 2016 slope maintenance project in which scaling and trim-blasting were done on the slope in conjunction with re-paving of the highway. The planned areas for work during the project are circled, in yellow for scaling and black for trim blasting. Gains around the perimeter may represent differences in cropping of the annual data. Map A shows the change data overlaying the point cloud in grey, while map B shows the change data overlaying a true color point cloud from 2015 data, with the points created during a hole-filling algorithm colored fuchsia. 67
Figure 4.15 Map of the slope near MP 240.5 on the George Parks Highway in Denali, Alaska. The change data from August 2017 to August 2018 are highlighted, with red representing a loss and blue representing a gain. The planned areas for work during the 2016 maintenance project are circled, in yellow for scaling and black for trim blasting. Gains around the perimeter may represent differences in cropping of the annual data. Map A shows the change data overlaying the point cloud in grey, while map B shows the change data overlaying a true color point cloud from 2017 data, with the points created during a hole-filling algorithm colored fuchsia 68
Figure 4.16 Point cloud generation of the 2018 study slope with hole filling outputs colored fuchsia. 71

LIST OF TABLES

Table 2.1 Comparative table of fields available in different databases and summary info (e.g., number of rockfall records, duration of span) 8
Table 2.2 Event type in the AKDOT&PF GAM database... 17
Table 2.3 Example fields of information in the RIMS database. 25
Table 4.1 Data acquisition equipment used by the PacTrans research team. The 2012 data are excluded, as they were captured by David Evans and Associates using a proprietary mobile system, the TITAN Mobile Laser Scanner................................ 49
Table 4.2 Point cloud statistics for each of the six scans, as well as successive cloud registrations. 52
Table 4.3 Annual rock fall activity data for the slope near MP 240.5 on the George Parks Highway in Denali, Alaska, from 2012 to 2018 as measured with the RAI software. Values are losses in m^3 as determined by the change detection algorithm. 69
Table A.1 Example media articles on rockfall 84

LIST OF ABBREVIATIONS

3-D:	Three-dimensional
AADT	Average annual daily traffic
AKDOT&PF:	Alaska Department of Transportation & Public Facilities
COOLR:	Cooperative Open Online Landslide Repository
DEM:	Digital elevation model
DOT:	Department of transportation
DSM:	Digital surface model
FHWA:	Federal Highway Administration
GAM:	Geotechnical Asset Management
GIS:	Geographic information system
GLC:	Global Landslide Catalog
GNSS:	Global Navigation Satellite System
Lidar:	Light detection and ranging
MP:	Mile post
NASA:	National Aeronautics and Space Administration
ODOT:	Oregon Department of Transportation
PacTrans:	Pacific Northwest Transportation Consortium
RAI:	Rockslope Activity Index
REF:	Rockslope Evolution Framework
RGB:	Red green blue
RHRS:	Rockfall Hazard Rating System
RIM:	Rockfall Impacts on Mobility
RMHR:	Rockfall Hazard Rating System
RMS:	Root mean square
SfM:	Structure from motion
TLS:	Terrestrial laser scan
UAS:	Unmanned Aircraft System
UTIC:	UAS and Terrestrial Imagery Combination
WADNR:	Washington State Department of National Resources
WSDOT:	Washington State Department of Transportation

ACKNOWLEDGMENTS

This research was funded by the Pacific Northwest Transportation Consortium (PacTrans). PacTrans is a consortium of university transportation centers located in Washington, Oregon, Idaho, and Alaska. The lead research agency was the University of Alaska Fairbanks (UAF), with Keith Cunningham serving as Principal Investigator. Co-investigators were Michael Olsen and Ben Leshchinsky from Oregon State University (OSU) and Joseph Wartman from the University of Washington (UW). Several students participated in this research. At the University of Washington, a visiting student, Nikki Shobert, assisted with the image collection and processing. Students from Oregon State University who assisted with this project included Andrew Senogles, Nick Mathews, Erzhuo Che, and Amy Atkinson. We greatly appreciate the many people who contributed and shared the databases that assisted with the Rockfall Impacts on Mobility (RIMS) database from Alaska Department of Transportation & Public Facilities (AK DOT&PF), Oregon Department of Transportation (O)DOT, Washington State Department of Transportation (WSDOT), National Aeronautics and Space Administration (NASA), and the U.S. Geological Survey. Finally, we acknowledge and appreciate the support of Leica Geosystems, David Evans and Associates, MicroSurvey Inc., and Maptek I-Site in providing the hardware and/or software utilized in this study. Field support was provided by the Natural Hazards Reconnaissance Facility (known as "RAPID"), which is supported under National Science Foundation Grant No. CMMI-1611820

.

EXECUTIVE SUMMARY

This work developed a valuable framework to assist transportation planners and managers (and others) in making informed resource allocation decisions based on the risks that rockfalls pose to the mobility of critical highway corridors. Transportation agencies, already faced with difficult asset management decisions, will benefit from a data-driven framework that synthesizes objective, quantitative identification of unstable slopes, mitigation strategies, and historical data related to debris volumes and closure times. We call this framework the Rockfall Impacts on Mobility (RIM) database. This analysis will enable identification of which slopes pose the greatest risk to highway closure from infrastructure damage, thus providing an objective approach for optimizing resource allocation and potential mitigation strategies. In particular, proactive slope remediation is typically beneficial, but the benefits are not well quantified. This framework will quantify the benefits of intervention for rockfall activity and, more importantly, the cost-efficacy (accounting for mobility loss) from a risk perspective. The public, as both user and taxpayer, will benefit from implementation of the results.

The RIM database developed in this research provides several unique opportunities to understand how rockfalls and landslides affect the highway network. This database presents regressions that enable planners to evaluate the economic costs associated with debris removal, repairs, and closures necessitated by rockfalls and landslides. These data may be used by planners to identify the routes most vulnerable to closures caused by landslides and rockfalls. They will also enable data-driven, economic cost-benefit analyses of slope mitigation techniques by identifying areas prone to repeat failures.

We performed an analysis of rockfall magnitudes and frequency for an Alaska site that was subject to typical rockfall mitigation practices to understand the effectiveness of mitigation efforts. An analysis of a 2016 scaling mitigation indicated that rockfall activity was reduced by approximately 50 percent in the years immediately following the project. This analysis, which focused on the Glitter Gulch study site, also showed that given the rockfall activity between 2012 and 2018, the Rockslope Activity Index (RAI) score was useful in identifying hazardous areas. For each change epoch, significant losses on the slope were identified by the RAI score as being of at least moderate hazard. However, significant failures were not scaled accordingly; one recommendation is that there should be a metric that clumps potential failures into clusters that could have a higher rating.

This report describes both general impacts of rockfalls and landslides on mobility and associated costs, as well as the actual efficacy of rockfall mitigation efforts typically employed in practice. All of these data-driven results suggest that the strategic data collection and database development of rockfall impacts and the efficacy of rockfall mitigation may lead to more strategic decision-making by planners. The results presented herein are a good start toward that effort.

CHAPTER 1. INTRODUCTION

Critical transportation corridors are essential for community well-being, resilience, commerce, and tourism. The states of Alaska, Washington, Idaho, and Oregon rank among the top five most mountainous states, with transportation corridors located in areas of significant geohazards. These hazards include landslides, rockfall, debris flows, frozen debris lobes, and slope instability due to thawing permafrost. Rockfalls and rockslides recently closed major highways in Alaska, Washington, Idaho, and Oregon.

During road closures, motorists and freight traffic are required to utilize limited, significantly lengthier alternative routes, which quickly become congested with increased traffic. Moreover, mitigation, maintenance, and repair can take weeks to months.

Understanding the frequency and magnitude of geohazards affecting transportation was the goal of this research. We built a practical, data-driven framework to assess the impacts of rockfall and debris slides on highway mobility. These data and framework can aid planners, engineers, and managers in making better-informed, quantitative decisions regarding mitigation and potential closures for repairs and maintenance.

Specifically, our research team worked toward the following with our data-driven and proactive framework:

- Quantify the mobility impacts of rockfalls by using the Rockfall Impacts on Mobility (RIM) database. By utilizing data mining techniques, we developed a database of unstable slopes. Data sources included historical records and trending news. Important to this database was mobility information such as closure times and mitigation strategies (rerouting).
- Develop fragility curves relating rockfall and debris volumes to closure times. The risks that rockfalls pose to the mobility of critical corridors were established by developing fragility curves relating rockfall debris volumes to highway closure and detour times based on data available from cooperators at the Oregon Department of Transportation (ODOT), Washington State Department of Transportation (WSDOT), and Alaska Department of Transportation & Public Facilities (AKDOT&PF).
- Assess the effectiveness of slope mitigation techniques, quantitatively and rigorously. In previous PacTrans research, we developed detailed morphologic databases for sites that had been mitigated and adjacent sites that had not. Standards for mitigation techniques,

such as “scaling,” are often implemented and performed on the basis of subjective judgment. Closure during these mitigation efforts can significantly affect mobility.

The data-driven approach incorporates site data and mitigation strategies related to corridor closures and impacts. This framework will provide planners with the necessary tools to make better-informed, quantitative decisions about mitigation and potential closures.

1.1. Project Background

Assessing rockfall and landslide risk poses significant challenges to transportation departments (DOTs) that must decide how to allocate limited funds for system-wide asset management and safety improvements. Slope assessment has traditionally been laborious, unsafe, and costly. Current best practices for management do not necessarily facilitate proactive methods for slope data collection, analysis, and management to identify and remediate hazardous conditions before a failure occurs.

A key factor limiting slope assessment has been inadequate data and observation systems. This is particularly true for the Pacific Northwest because of the region's vast and mountainous terrain. Without baseline data and monitoring systems, analysis of changing factors that affect transportation infrastructure is not feasible. To address this concern, in 2012 Pactrans and Alaska DOT supported a multi-institution, interdisciplinary project to collect baseline laser-scan surveys at two locations in Alaska with a long history of rockfall and landslide events. This team was led by the University of Alaska Fairbanks, with technical expertise in laser scanning from Oregon State University and geologic engineering from the University of Washington.

The research sites selected were both in Alaska. The first of these sites, the Long Lake corridor, was located northeast of Anchorage along the Glenn Highway. The second site, known as Glitter Gulch, was located immediately north of the tourist village at the Denali National Park entrance, hence the kitschy name.

1.1.1. Lidar Evaluation and Digital Surface Modeling

Laser scans using light detection and ranging (lidar) technology were the first step in evaluating the magnitude and frequency of rockfall activity. This first set of scans was completed by using mobile laser scanning technology for 10 miles of highway at each site. Subsequent scans at the sites identified to be most critical from the mobile lidar baseline data set were evaluated in greater detail by using terrestrial laser scan technology in 2013 (Phase I), 2014

(Phase II), 2015 (Phase III), and 2017 (Phase IV), producing a rich data set that can be used to develop a more precise and quantifiable geohazard risk assessment.

The first phase evaluated and developed tools to use lidar data to assess slope hazards and risk in a geotechnical asset management framework. The models derived from the laser scan data helped in visualizing various geologic features, including rock types, fracturing, weathering, and talus accumulations. The slope morphology was of particular interest in the digital elevation models (DEMs), especially for unstable, rock cantilever overhangs. Limitations of the mobile lidar scanning techniques were revealed; those primarily involved insufficient scan detail (resolution) from the currently available technology when traveling at highway speeds, vegetation interfering with scan data, and the blocking (occlusion) of laser scans by shadows cast by barriers, guard rails, and vegetation. However, benefits were identified in terms of efficient coverage across large sections of highway, safe data collection, and the ability of the data to be utilized for multiple purposes in addition to slope assessment.

Cantilever overhangs and other complex features created scanning occlusions in the DEMs, thus helping to focus the team's investigation on scientific solutions to scanning occlusions. This led to the publication of an article in the well-regarded journal *Remote Sensing* (Olsen et al. 2015) that described a new approach for detecting individual rockfall clusters to automate the development of magnitude-frequency curves, which are used to assess risk.

Another scientific shortcoming identified in the first phase was that existing rockfall hazard assessment models were inadequate for the detailed lidar DEM data because they were too coarse and subjective. Detailed change analysis identified specific locations of individual rockfall activity, talus accumulation, minute volumetric changes of the slope, overall volumetric change, and overall trends in morphology. This temporal analysis could then be further developed with more data to examine more complex phenomena such as geologic fracturing, freeze-thaw cycles, soil ratcheting, and the mitigation effects from regular DOT slope maintenance. Measurement of the rock slope change was the first step in developing a rock slope stability model capable of quantitative forecasts.

1.1.2. The Rockfall Activity Index (RAI)

The ability to measure change in slope surfaces and to quantify it with precise detail led the team to develop an enhanced analysis of slope stability and the impacts of rock structure and weathering. By tracking morphology, it is also possible to quantify slope roughness across multiple scales. Changes in morphology and roughness can be precisely calculated to infer changes in slope volume and the kinetic energy released with slope changes. These components became part of the Rockfall Activity Index (RAI) [Dunham et al. 2017] developed to model rock slope dynamics.

The RAI is a point cloud-derived, high-resolution, morphology-based method for assessing rockfall hazards. The RAI is applied in a two-step procedure. In the first step, morphological indices (local slope and roughness derived from a high-resolution, three-dimensional point cloud) are used as an indicator to classify the erosion and mass wasting processes acting on rock slopes. In the second step, the slope morphology classifications are used with estimated instability rates to map rockfall activity across a slope face. The RAI method has been implemented as a simple and computationally efficient algorithm, making it repeatable and easy to apply across rock slopes of virtually any size. The method provides an estimate of rockfall kinetic energy release along rock slope segments and detailed mapping of rock slope morphology and kinetic energy release areas. Although this quantitative formulation suggests a high degree of engineering precision, it should be recognized that variability and uncertainty exist in the parameters used to compute the RAI. Dunham et al. 2017 also discussed other established methods of assessing rock slope stability.

1.1.3. Photogrammetry from Unmanned Aircraft Systems (UAS)

Pactrans later sponsored the team's Phase III research with a new project to evaluate the quality of additional photogrammetric data collected with a drone (unmanned aircraft system or UAS) in addition to a third set of repeat terrestrial laser scans. The additional data also helped the team develop a quantifiable rockfall and slope stability model utilizing change detection techniques to forecast future slope behavior. This research effort also provided an opportunity to test and further refine the RAI system to support the point clouds acquired from drones.

The researchers rigorously examined the photogrammetric data captured by a commercial-grade drone. The data indicated that the resulting photogrammetry surface models were comparable to the lidar scans in many ways and of reasonable accuracy for slope morphology assessment, provided that adequate survey control was provided.

The photogrammetry process, called structure from motion (SfM), uses the motion parallax of the drone's changing position to generate detailed three-dimensional models of the slope surfaces. While the SfM technique is not necessarily new, its application to terrain modeling is new, especially with the perspective that an airborne platform can achieve over-terrestrial imaging. The drone demonstrated that its "aloft" perspective generated digital surface model (DSM) data of critical cantilever overhangs. Additionally, the point cloud density of the SfM model was found to be comparable to the lidar scanner but was also found to be more consistent in terms of point cloud density and mesh quality. Finally, unlike with lidar, which could only be operated from a narrow road shoulder, the drone could quickly fly above the road and in an offset position orthogonal from the target, making it safer to operate while collecting high-quality data in a shorter amount of time (accounting for the time required for survey control).

The last step in the photogrammetry research was to fuse the drone DEM with the lidar DEM. The results were effective, with the drone data filling occlusions in the lidar data, and the lidar data helping to "control" the draping of the drone DSM point cloud. Thus, a denser and more complete DEM was generated in the Phase III data collection without the problematic occlusions from the rock cantilever overhangs.

1.1.4. Slope Morphology and Climate Change

The most recently completed phase (Phase IV) of the project, "Transportation Corridor Resilience in the Face of a Changing Climate," compared the quantitative slope changes the team had measured since 2012 at Long Lake and Glitter Gulch with historical weather data and forecasted climate trends. The progressive failures observed in rock slopes must be quantified and projected by using a rational, data-driven engineering approach to capture the influence of climate change on rockfall activity. The change in rock slope morphology at the study sites showed continuous rockfall, talus accumulation, and overall progressive mass wasting. It is understood that rockfall events may be tied to freeze/thaw cycling and intense precipitation, suggesting that the influence of a changing climate is important in future rockfall activity.

On the basis of the repeat laser scans and the RAI approach, a framework for assessing projected rockslope activity based on changes in time-dependent classification and DEM evolution was developed, entitled the Rockslope Evolution Framework (REF). This prototype was used to project the potential impacts of a changing climate, using temperature increase as a proxy, on increasing rockfall activity. The results showed that the yearly RAI for a given site may increase significantly more than the observed activity rate. That is, the slow and gradual increase of activity due to climate change may result in significant increases in rockfall impacts –

a direct threat to the safety and resilience of critical corridors. In light of this possibility, the creation of a more resilient critical infrastructure will require adaptation of planning tools for rockfall today (the RAI) and the future (the REF). By considering the looming threats of climate change, we enable planners and engineers to make data-driven solutions for a more resilient future.

1.2. Technology Transfer

The insights and tools developed through this research have led to additional opportunities. The research team is currently working with Oregon DOT to implement the RAI methodology in its workflows for monitoring unstable slopes. Oregon DOT was the first DOT to purchase a mobile lidar unit and routinely scans its highways for asset management and many other purposes. This research project is also exploring ways in which the RAI can improve the efficiency of slope assessments, minimizing the need for dangerous and expensive fieldwork. The research team is also working with collaborators at GNS Science in New Zealand to analyze a similar data set of repeat laser scans of rockfall activity after the Canterbury Earthquake Sequence to yield insights into rockfall activity trends during and after major seismic events.

CHAPTER 2. THE ROCKFALL IMPACTS ON MOBILITY (RIM) DATABASE

A key project goal was to compile information from rockfall databases and supplement them with additional media information into a single database focused on rockfall impacts on mobility in transportation. The parameters that are the primary focus of the Rockfall Impacts on Mobility (RIM) database presented herein include date, number of events, event volume, associated event closure time, and associated event cost. We provide a description of existing databases in the Pacific Northwest, a description of the RIM database, and a series of relationships between key parameters in this chapter.

2.1. Existing Rockfall Databases

Several rockfall databases (table 2.1) have recently become available as state DOTs and other organizations have implemented or expanded their geotechnical asset management (GAM) programs. The level of detail and information varies significantly among these databases, depending on their purposes and priorities. This section summarizes several existing databases focused on the Pacific Northwest, including the ODOT's Unstable Slopes database, ODOT TripCheck mobility database, AKDOT&PF Geotechnical Asset Management (GAM) Rockslope database, AKDOT&PF Geotechnical Asset Management (GAM) Event Tracker, Washington State Department of Natural Resources (WADNR) Hazard Database, and the National Aeronautics and Space Administration (NASA) landslide database. Collectively, these databases contain a variety of information based on a variety of sources. DOT databases tend to be from maintenance reports and/or field investigations from engineers, geologists, and planners. The NASA database contains crowdsourced data from the public, particularly media reports on mass movements.

Table 2.1 Comparative table of fields available in different databases and summary info (e.g., number of rockfall records, duration of span)

Database	**Dates**	**Number of Rockfalls**	**Volumes**	**Closure Time**	**Cost**
ODOT Unstable Slopes	Oct. 2004 - Feb. 2020	1,758	Not Available	Not Available	Detailed repair costs per location
ODOT Trip Check	Jan. 2013 - Nov. 2020	15,167	Not Available	Seconds	Not Available
AKDO&PF GAM: Rock Slopes Data	Aug. 2010 - May 2019	1,017	Event Volume	None	Estimated Improvement Cost
AKDO&PF GAM: Event Tracker	Dec. 2003 - April 2020	4,549	Approximate	Approximate	Yes
Washington Department of Natural Resources (DNR)	Nov. 2015 - Jan. 2020	414	Not Available	Not Available	Not Available
NASA	April 2016 - Aug. 2020	904	Approximate (small - very large)	None	None

2.2. Database Objectives and Specifications

2.2.1. ODOT Unstable Slopes Database

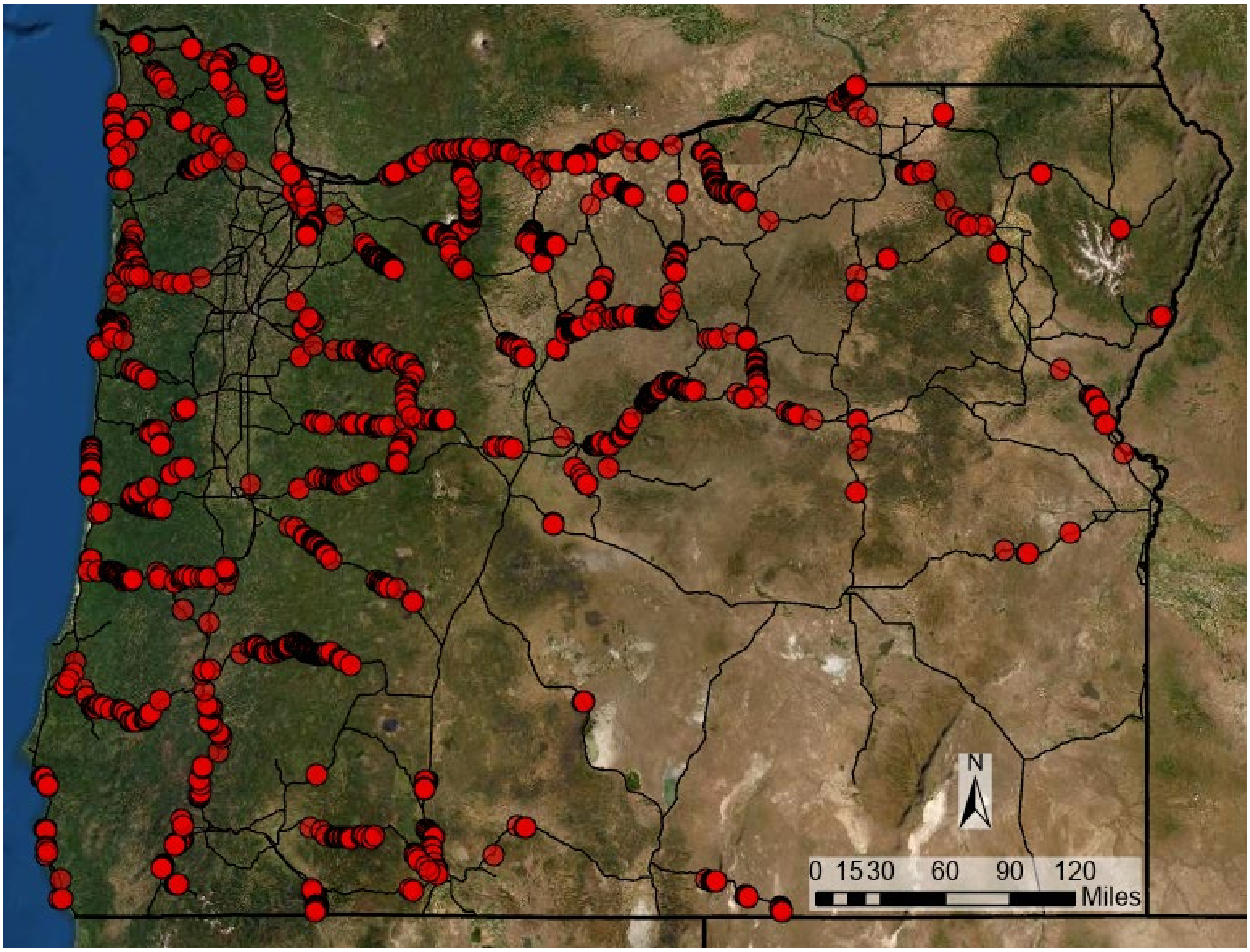

Figure 2.1 Map of the Unstable Slopes Database (Oregon Signed Routes Layer from Road Inventory and Classification Services Unit (RICS) and ODOT)

Oregon DOT manages a database of unstable slopes (landslides and rockfalls) that affect highways across the state (figure 2.1). This database contains detailed information related to the cost of repair of those sites to help in prioritizing mitigation. The database does not track the volumes of materials dislodged in a rockfall event but tracks volumes of materials hauled away or brought to the site for repairs. A basic design is completed for each slope to estimate the materials required to mitigate it. The database also contains ancillary traffic information such as average annual daily traffic (AADT) and accidents. A valuable component of this database is that it tracks rockfalls over time (figure 2.2), which shows the variability in recorded rockfalls and affected ODOT right-of-way per year. While some rockfalls may relate to changing environmental conditions, it is likely that the entire record is incomplete because of variability in resources to investigate and document rockfalls. However, it is possible, and even likely, that the peaks in these data owe to localized weather events (e.g., rapid snowmelt, localized storm systems), as no significant precipitation anomaly can be observed for the two peak years (2008, 2018) with recorded rockfalls. Nonetheless, the potential for large numbers of highway-relevant rockfall events demonstrates that record-keeping and planning for closure and cost is important for planning.

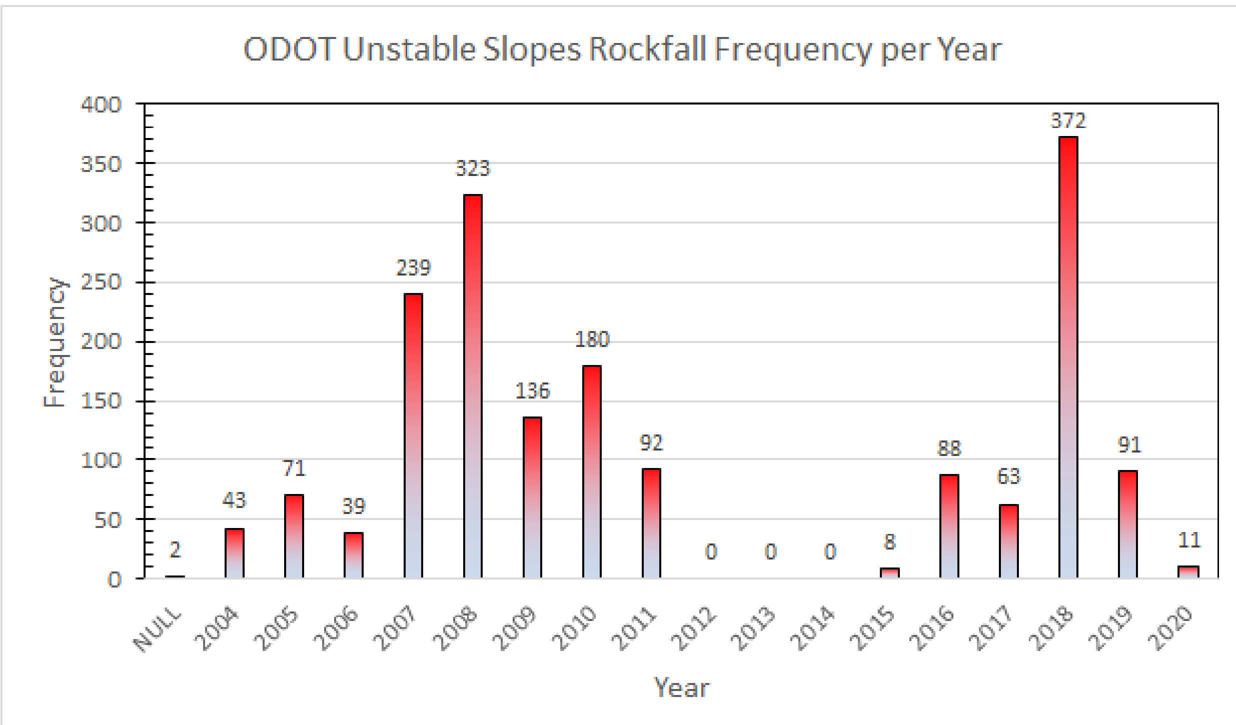

Figure 2.2 Rockfalls per year observed in Oregon from the ODOT Unstable Slopes database.

2.2.2. ODOT TripCheck

ODOT TripCheck (figure 2.3) provides incident reports that result in highway closures shown to the public in real time on its webGIS (figure 2.4). A detailed log identifying the hazard, precise location, and the resulting closure time is maintained in this database. However, it does not track volumes of failed materials or details about the rockfalls. The events in this database vary in severity and often result from a few rocks rolling onto the roadway from known hazard locations. This database rarely tracks large events, and many major rockfall occurrences were not tracked. There were also many rockfalls during the recent wildfires that were not reported to the dispatch centers because of low traffic impact (likely because the sections of the highways had already been closed). Out of the 16,493 events tracked in the database, over 90 percent were due to rockfall, 7 percent were landslides, and the remaining 3 percent were due to erosion.

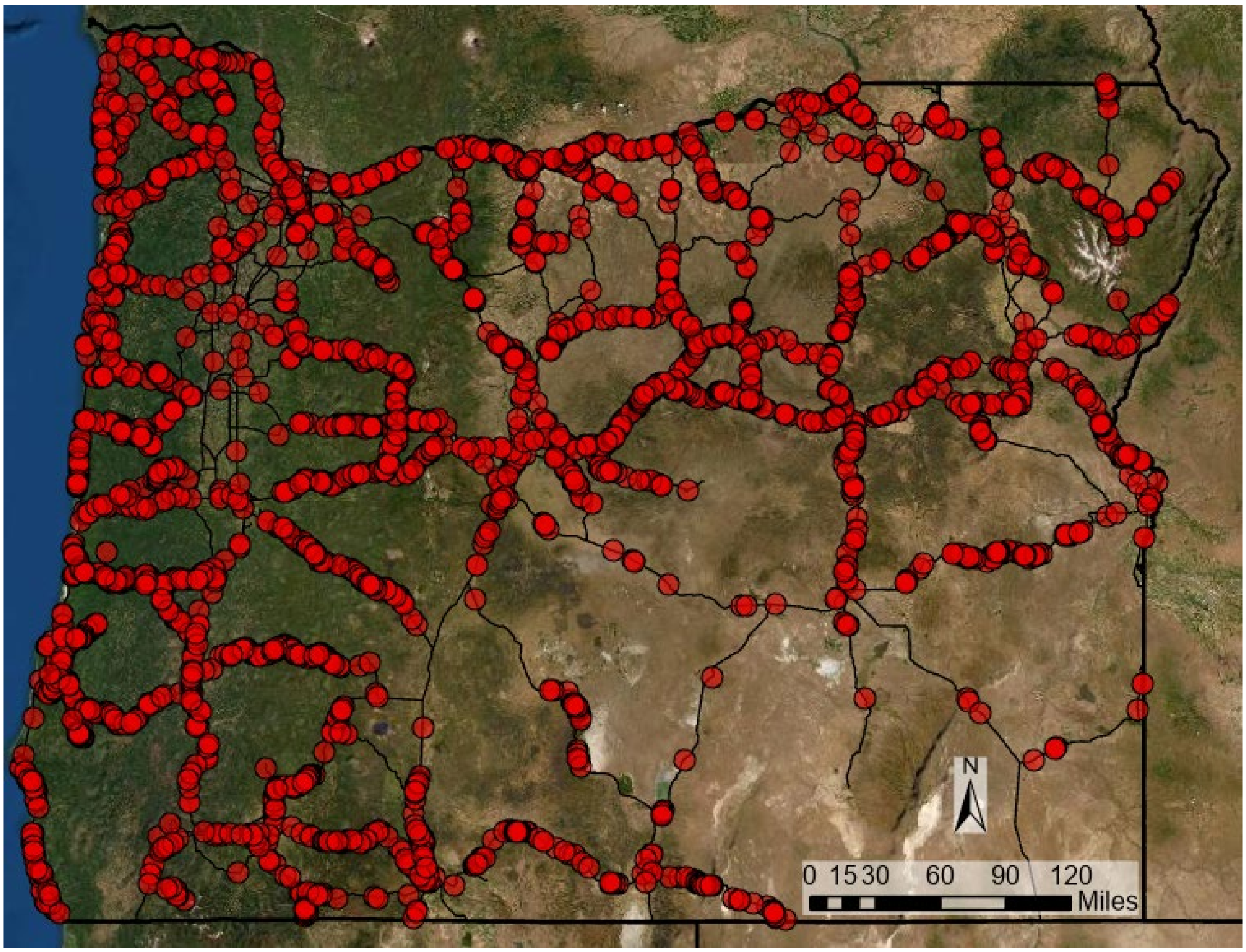

Figure 2.3 Map of the Rockslide TripCheck Database from 2015 on (Oregon Signed Routes Layer from Road Inventory and Classification Services Unit (RICS) and ODOT)

Figure 2.4 ODOT TripCheck database.

2.2.3. Alaska DOT GAM Program: Rockslopes

The Alaska Department of Transportation and Public Facilities has been expanding its Geotechnical Asset Management (GAM) Program over the last decade to document rock slopes, unstable slopes and embankments, retaining walls, and materials sites owned by the DOT (figure 2.6). The program's primary focus is on characteristics that can deteriorate over time and on creating deterioration models that can determine the life-cycle cost and return on investment. The AKDOT&PF GAM database contains detailed information on rockfall prone slopes, including rockfall hazard rating system scores, average annual daily traffic (AADT), speed limit, roadway width, sight distance, resources applied (e.g., maintenance), and accident information. It also includes basic slope geometry information such as the length and height, as well as the failure type (rock avalanche, block, planar, raveling/undermining, toppling, and wedge). This information is then aggregated into a condition index, condition state, and estimated improvement cost. This database is available in a webGIS format that is searchable and straightforward to analyze (figure 2.6). Like the ODOT Unstable Slopes database, the number of yearly rockfall events is variable, owing to potential variability in reporting or localized climatic events that result in clusters of rockfalls (figure 2.7). Nonetheless, many unstable rockslopes show repeat rockfall events (figure 2.8). This supports the need to track and catalog rockfall events as a means of prioritizing planning resources to increase the cost effectiveness of mitigation efforts.

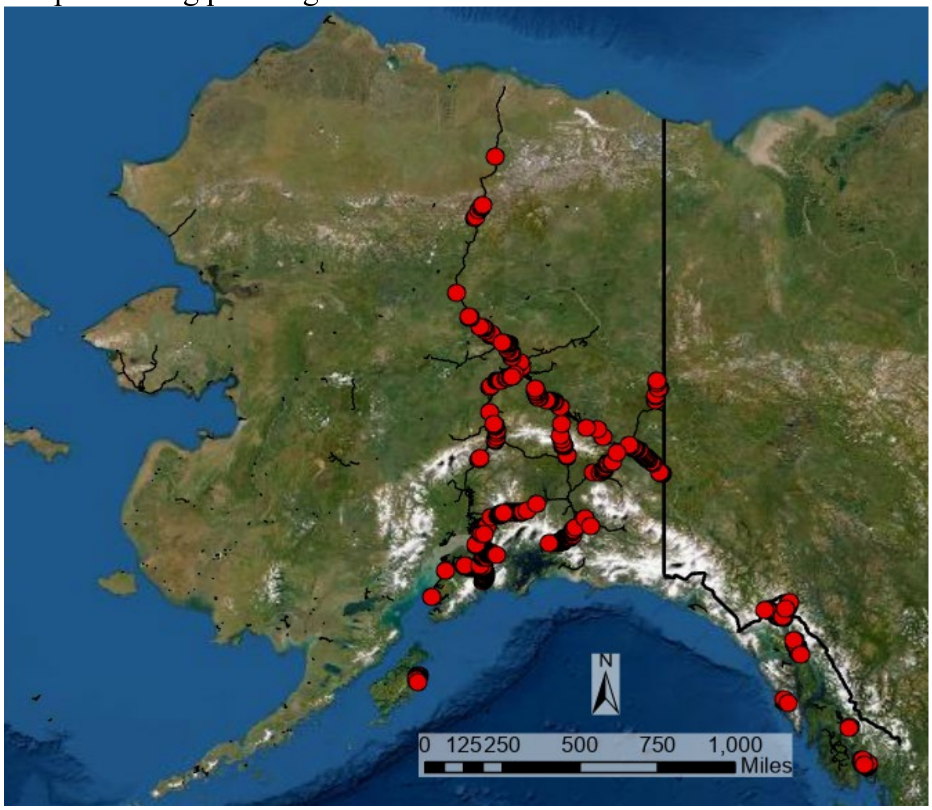

Figure 2.5 Map of AKDOT&PF rockslides (Roads from AKDOT&PF)

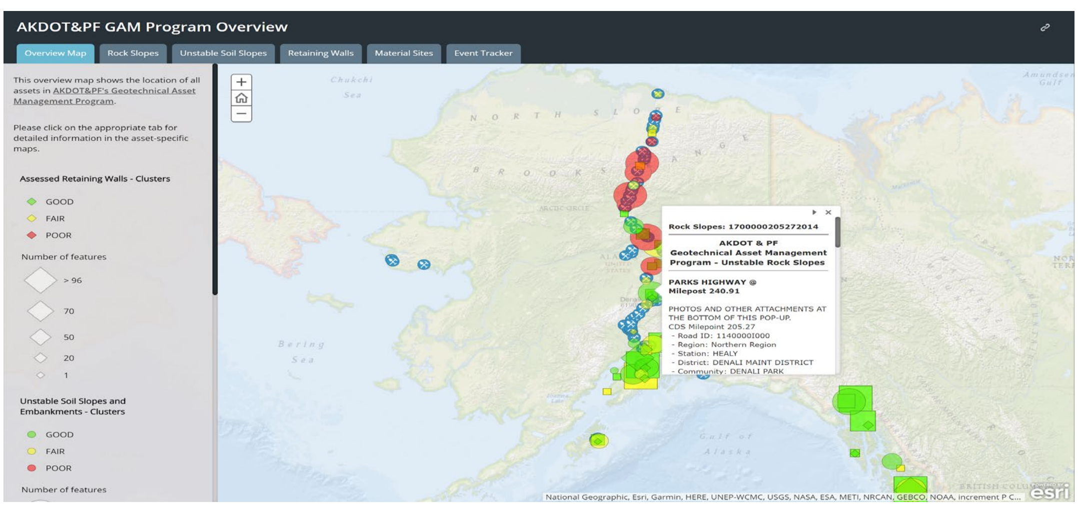

Figure 2.6 AKDOT GAM database web viewer.
https://akdot.maps.arcgis.com/apps/MapSeries/index.html?appid=0be74f9ba168424eac48983da02e0250

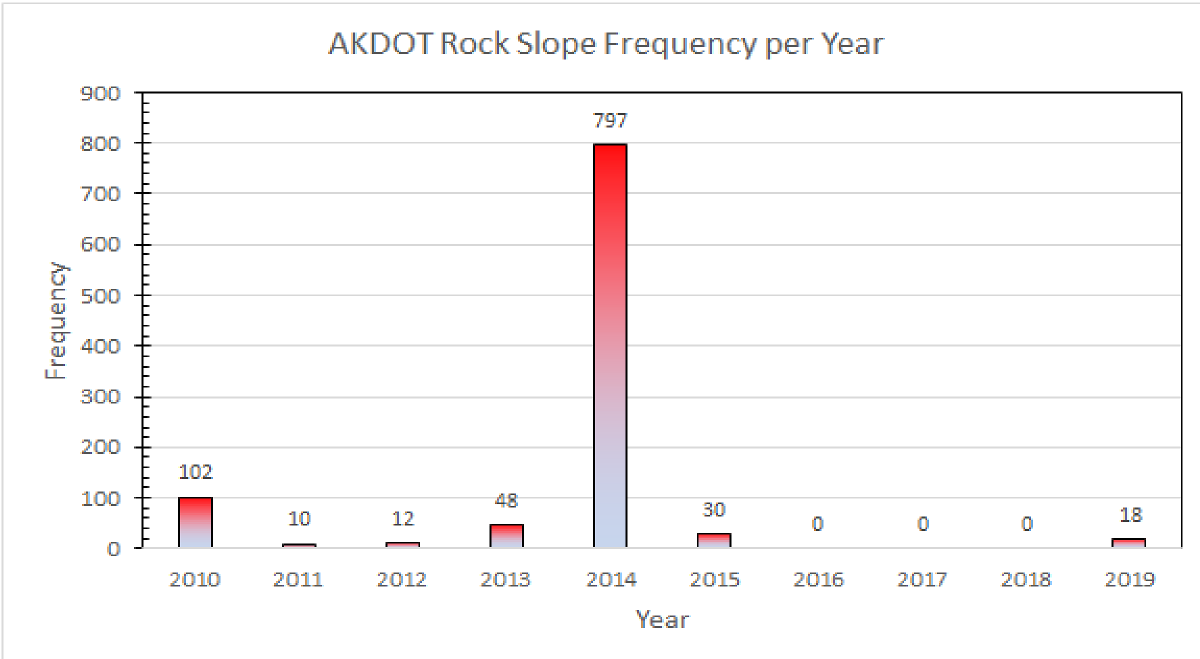

Figure 2.7 AKDOT rock slopes event frequency per year.

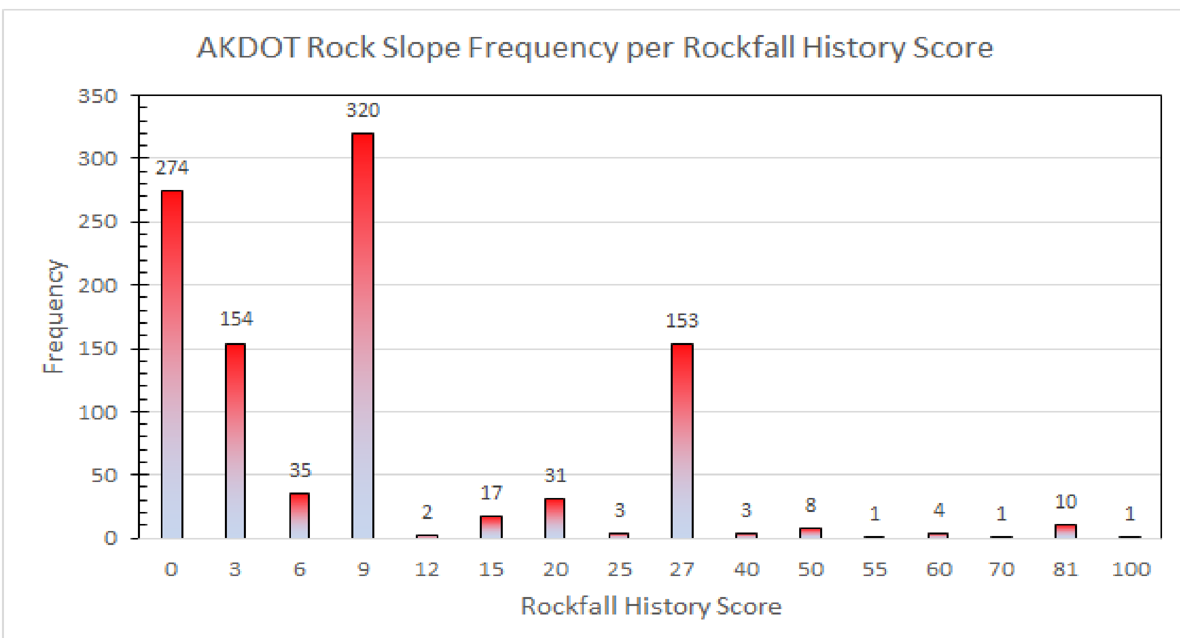

Figure 2.8 AKDOT rock slopes frequency per rockfall history score

2.2.4. AKDOT Geo-Event Tracker

The AKDOT&PF Event Tracker (figure 2.9) is part of their GAM program, which tracks events on the basis of maintenance logs. It displays both clustered events and individual incidences, containing fields that include event type, date, closure duration, resources applied, accidents, event size, cost, and roadway details (figure 2.10). These attributes are estimations of closure with ranges of time (less than an hour, between 1 and 6 hours, between 1 week and 1 month, etc.) and size (routine-minor, moderate, major, or catastrophic). The high quality tracking shows that rockfalls are a perennial issue in Alaska (figure 2.11) but still variable with time, as shown in other databases. The attribute codes for event type, closure duration, and event size, are listed in table 2.2, as well as counts of records corresponding to each code.

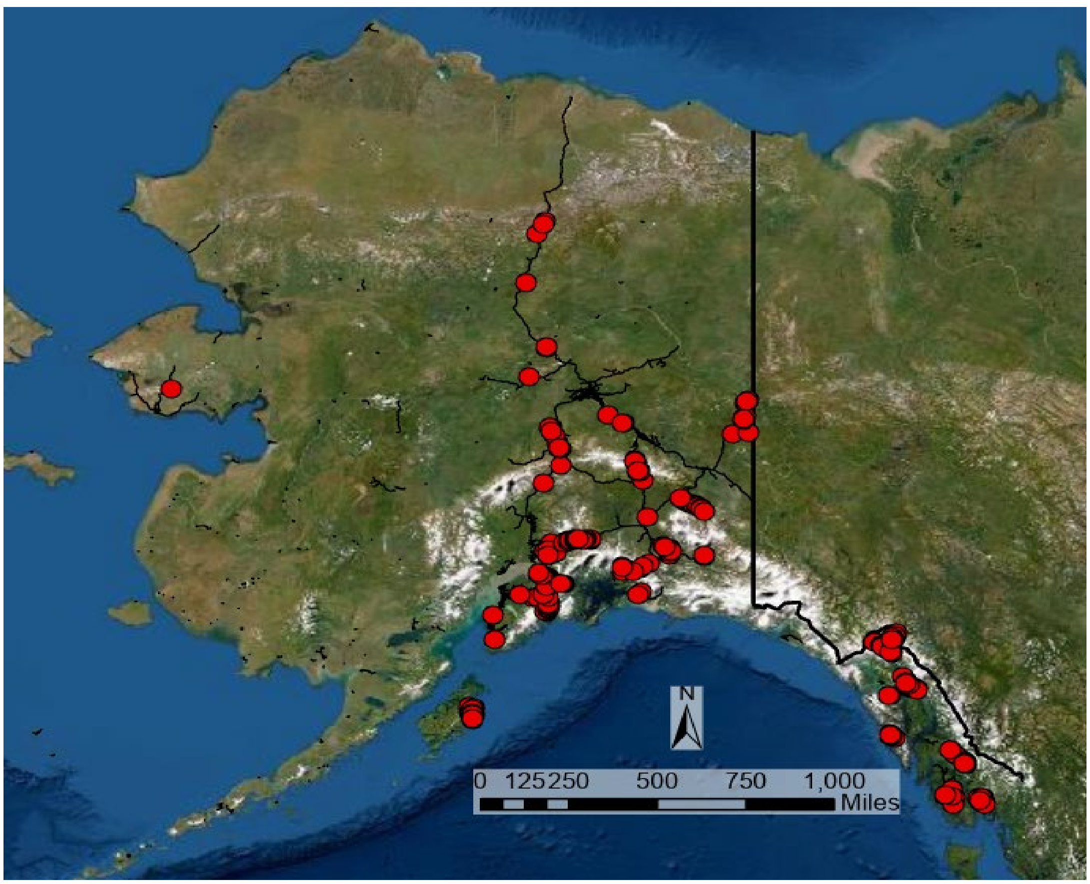

Figure 2.9 Map of the AKDOT&PF Geo-Event Tracker (Roads from AKDOT)

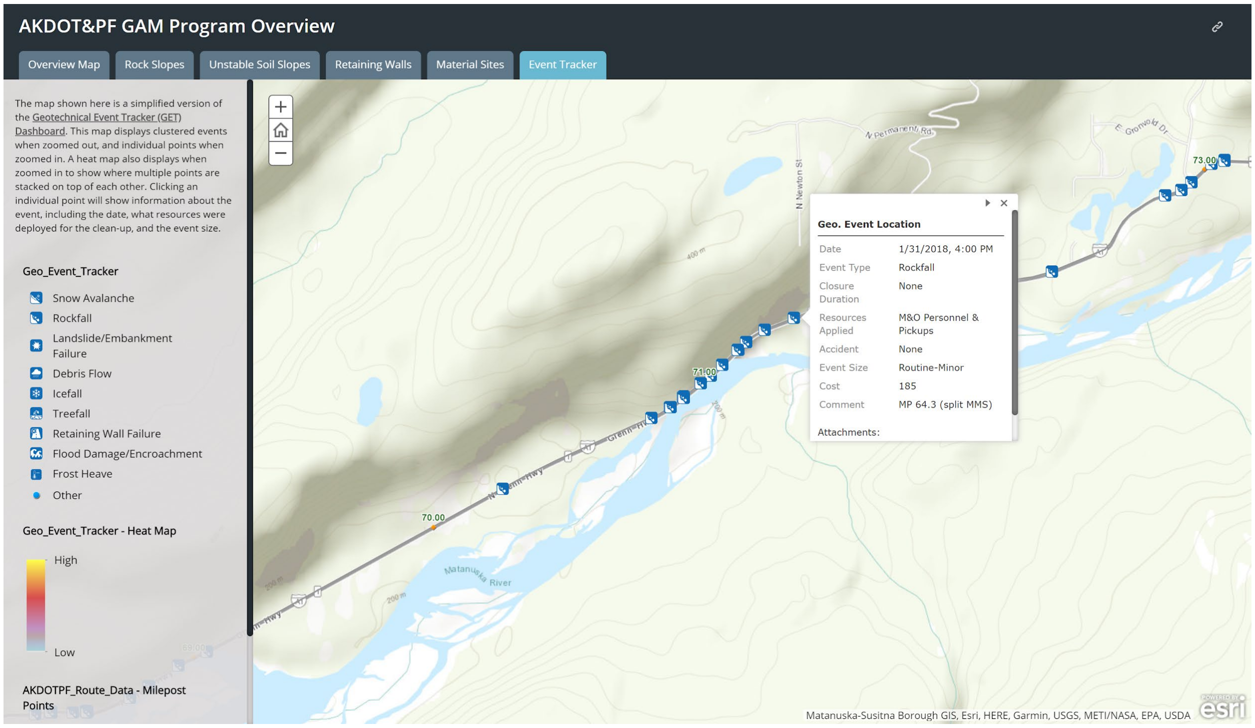

Figure 2.10 AKDOT GAM data viewer

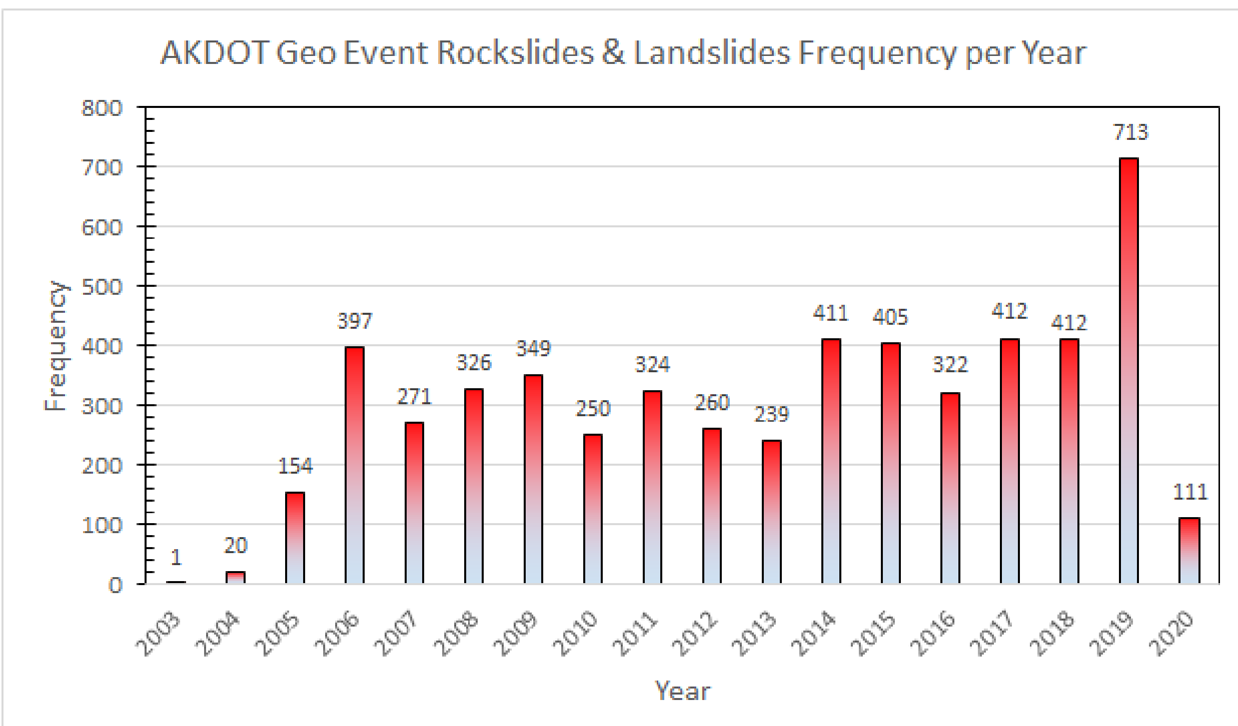

Figure 2.11 Rockfall frequency by year in Alaska

Table 2.2 Event type in the AKDOT&PF GAM database

Code	Event Type	Count		Closure	Count		Size	Count
0	Rockfall	4549		None	11160		Routine-Minor	7070
1	Landslide/Embankment Failure	827		Temp Slowdown <30 minutes	11		Moderate	2188
2	Debris Flow	374		Temp Slow 30 min - 2 hr	13		Major	1380
3	Frost Heave	0		Temp Slow >2 hr	11		Catastrophic	599
4	Snow Avalanche	5479		Closure < 1hr	4		-	
5	Icefall	2		Closure 1 - 6 hr	25		-	
6	Retaining Wall Failure	1		Closure 6-24 hr	7		-	
7	Treefall	2		Closure 24-72 hr	5		-	
8	Flood Damage	0		Closure 72 hr - 1 week	1		-	
9	Other	3		Closure 1 week - 1 month	0		-	
10	-			Closure > 1 month	1		-	

2.2.5. *Washington Department of Natural Resources Database*

The Washington State Department of Natural Resources (WADNR) maintains a database of recent landslides (figure 2.12) based on information from the media as well as city, county, and state sources (figure 2.13). It contains basic closure information and relatively precise locations. In the fall, winter, and spring, staff members check media websites and WSDOT's road closure page daily. Typically, they search for "landslide Washington" and restrict the time frame to within the past 24 hours. During storm events, staff sometimes check WSDOT's page hourly to keep updated. WSDOT does not save information associated with the events after the rockfalls have been cleaned up; therefore, constant observation of the website is necessary to document all of the events. A review of the data showed that some of the events in the database were repeated, sometimes with conflicting information. Because the number of these repeat events was not known, it was unclear how reliable the numbers were in terms of occurrences.

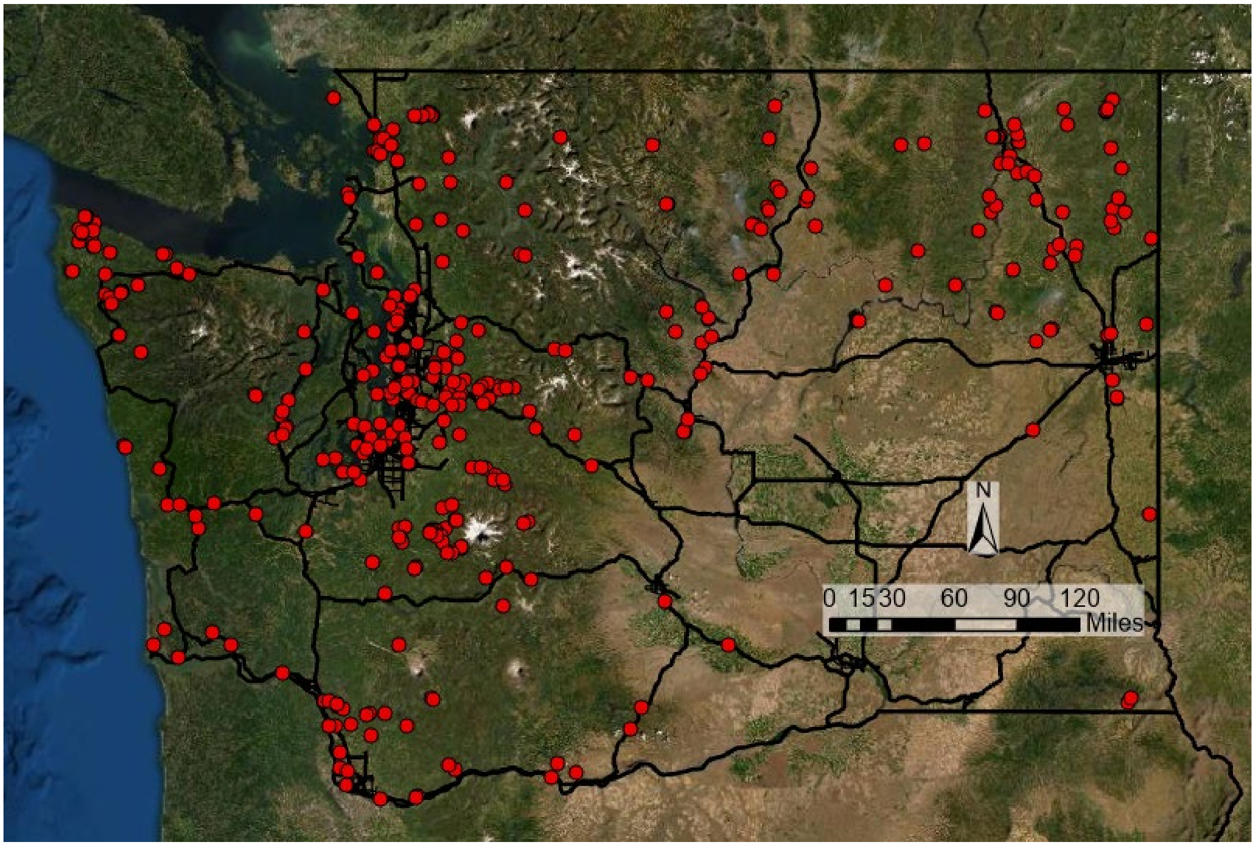

Figure 2.12 Map of the WADNR landslides database (Roads from WSDOT)

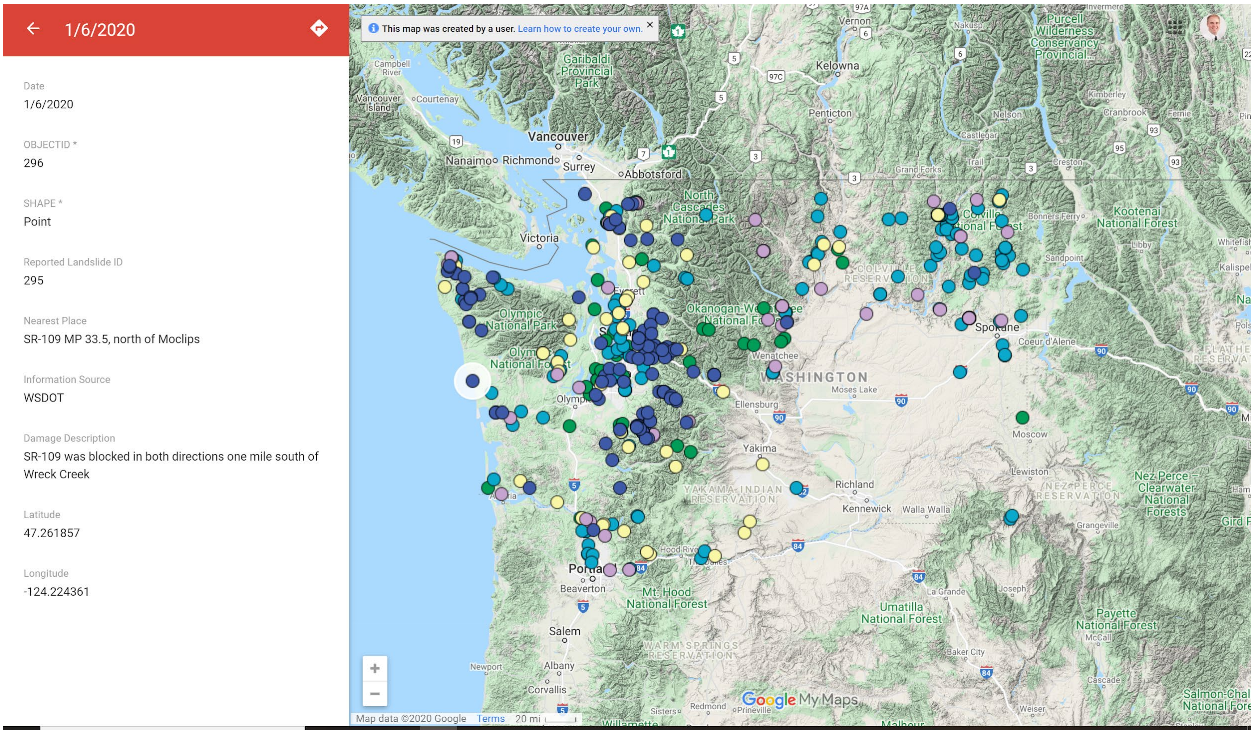

Figure 2.13 WADNR landslide database interface.

2.2.6. NASA Landslide Viewer

The National Aeronautics and Space Administration (NASA) has created a landslide database called the Cooperative Open Online Landslide Repository (COOLR), which is the biggest open global landslide catalog. The COOLR currently includes NASA's Global Landslide Catalog (GLC), Landslide Reporter Catalog (LRC), and collated landslide inventories from other institutions. NASA started cataloging landslides globally in 2007 in the GLC but later added the LRC to allow citizen scientists to add reports as well. The addition of citizen science sources helped in collecting recent landslides and aided NASA in the time-consuming process of maintaining a global database. The database contains information on the media source, date, location, a brief description, the general size (small, medium, large, etc.), injuries, and cause if known (figures 2.13 through 2.15).

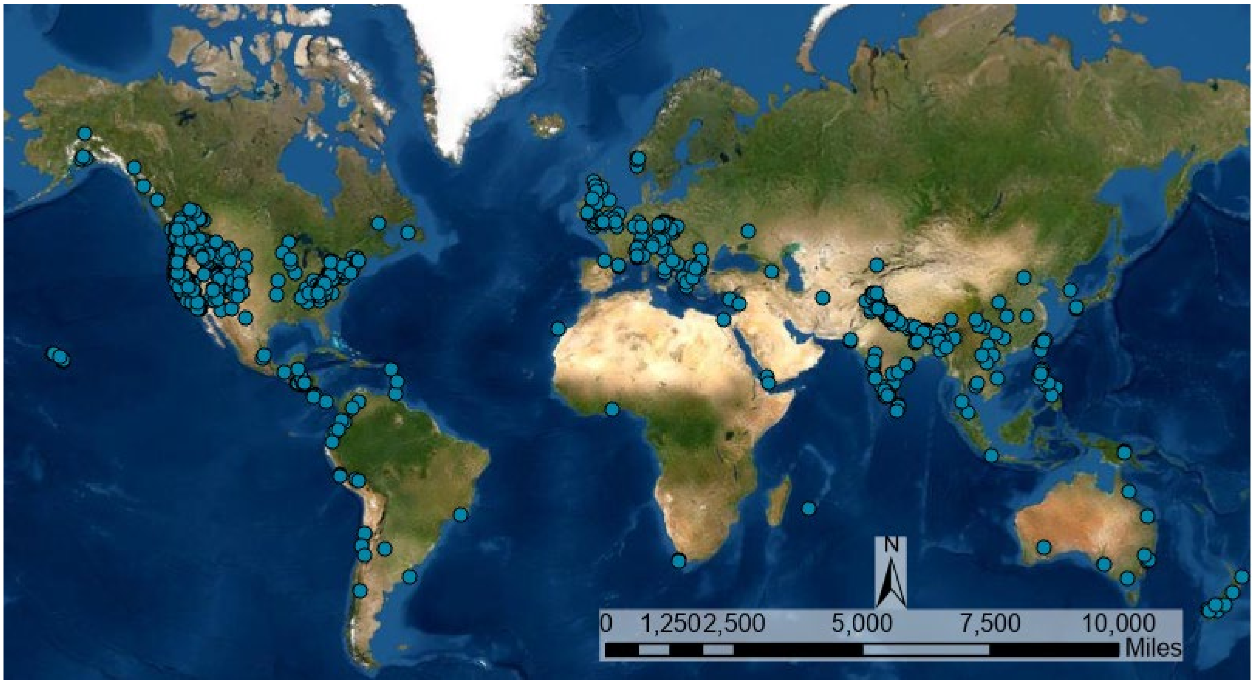

Figure 2.14 Map of NASA landslides.
https://maps.nccs.nasa.gov/arcgis/apps/webappviewer/index.html?id=824ea5864ec8423fb985b33ee6bc05b7

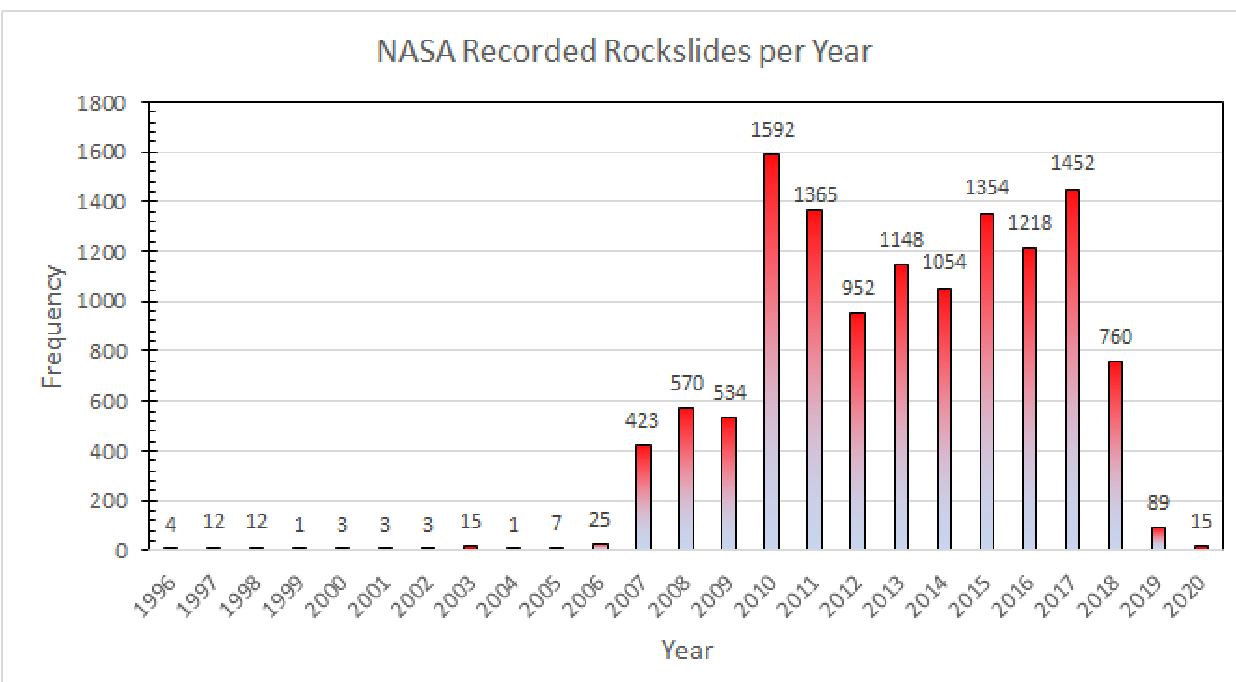

Figure 2.15 NASA landslide database rockfall/rockslide event frequency by year.

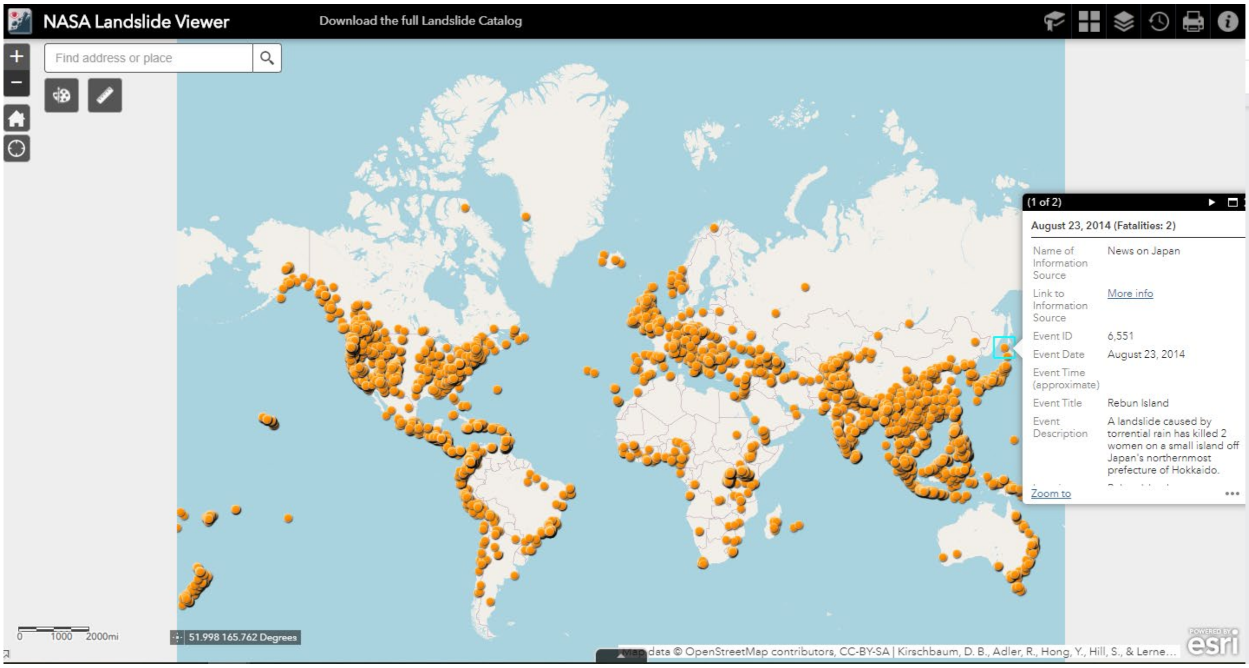

Figure 2.16 NASA Landslide Viewer

2.3. Database Management

In this project's initial stages, the only databases to which we had access were the ODOT Unstable Slopes and the AKDOT&PF Geo-Event Tracker. We worked with python code to combine the two into one comprehensive database. The idea behind this code was that we could easily update our comprehensive database when either source database was updated. The code first transferred the AKDOT&PF database into the Microsoft Access Database that the ODOT database was in. From there both databases were formatted to prepare them for the final combined database. This included renaming shared fields to match, adding new fields to either table for fields that did not match, and translating AKDOT&PF data codes into values. This process was very difficult because there were not many shared fields, and fields that were shared were often in different units or scales. Most of the shared fields were about location and highway details. The fields in which we were really interested were volumes, costs, and closure durations. However, ODOT contained costs and closure durations but not volumes, and AKDOT&PF contained volumes and costs but not closures. So while the cost fields could be compared, without additional shared fields, the trends in which we were interested were unattainable with our comprehensive database. This led to the development of our own RIM database, which consistently contains closure and volume data for each event. This database is discussed in further detail later in this report.

Code that could automatically combine these different databases would be ideal but proved difficult to implement as we found more databases to combine. When we originally reached out to Alaska, Washington, Oregon, and California DOTs about their rockslide databases, we received information only about the ODOT Unstable Slopes and AKDOT&PF Geo-Event Tracker. However, we eventually also found the WADNR, ODOT TripCheck, NASA, and AKDOT&PF Rockslide databases. As we developed the RIM database, we created a general template for what a final combined database could look like, and in the future we will develop code to automatically combine the databases we found.

2.4. The RIM Database

While the aforementioned databases contain a substantial amount of valuable information (figure 2.17), accurate data about closure times and volumes of failed material were generally not available within a single database. As a result, the research team conducted data mining of media to find articles about recent closures due to rockfalls (figure 2.18). When possible, these were then correlated with information available in the other databases to extract the most accurate data possible for each site. The information provided, as well as the actual data quality, varied substantially among articles and reporting venues. This is tracked in the database via confidence scores. As a result, as the RIM database continues to expand, and users can set thresholds for records on the basis of the fields needed for their analysis. Figure 2.19 plots the number of rockfalls per year recorded in the database.

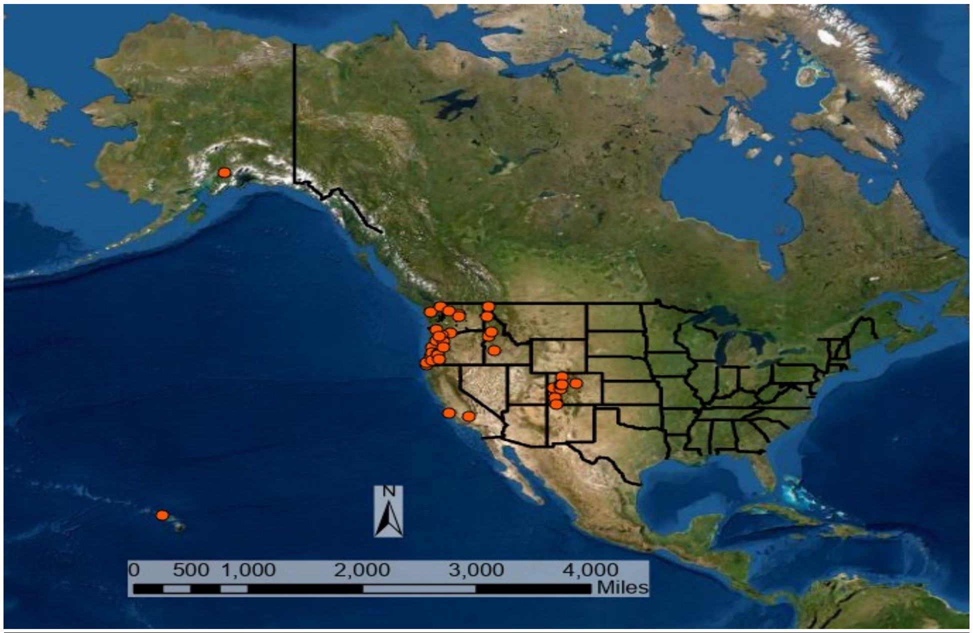

Figure 2.17 RIM database rockfall locations

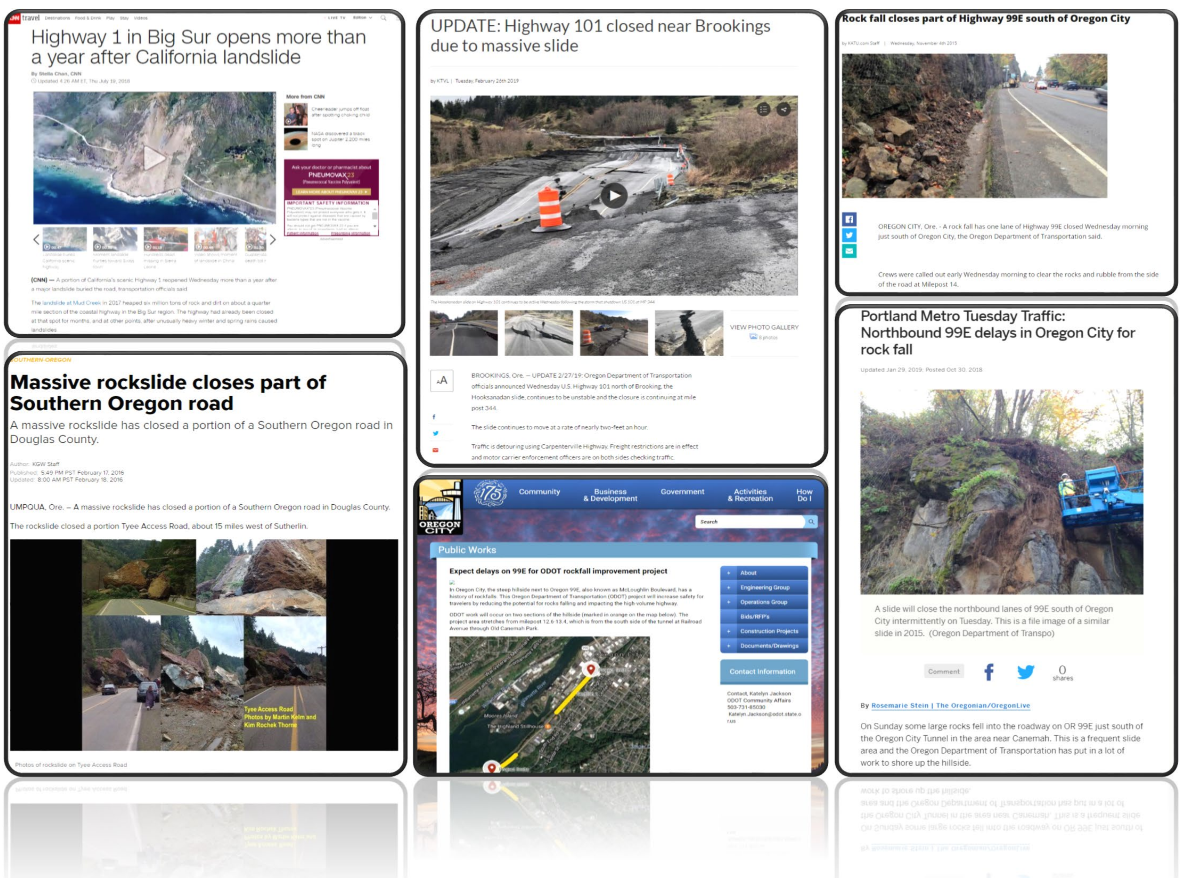

Figure 2.18 Example media articles of highway closures due to rockfalls.

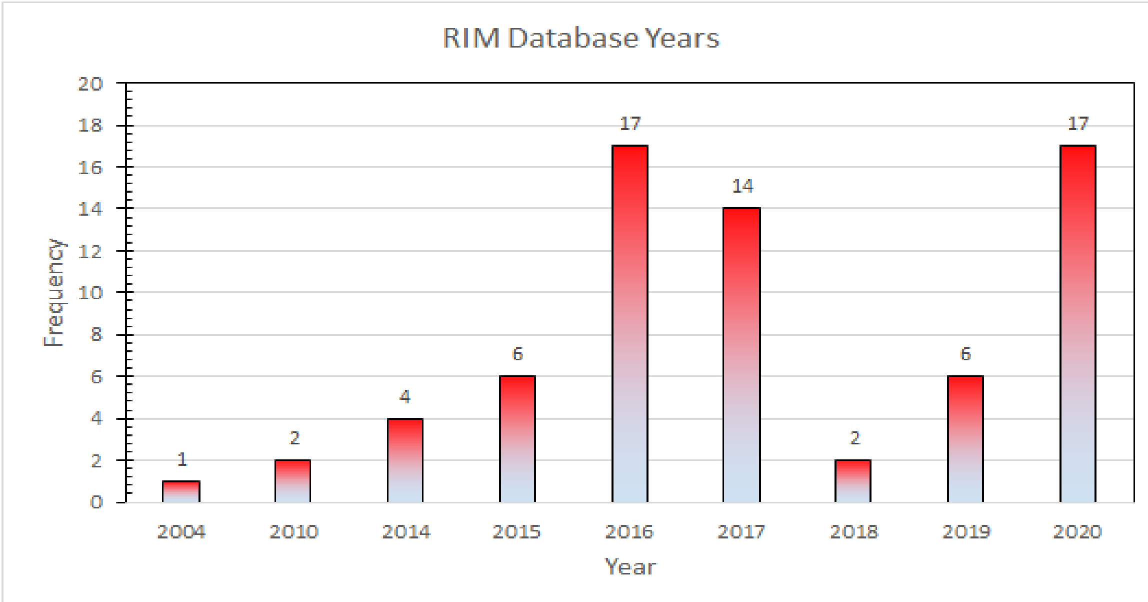

Figure 2.19 Histogram of dates of rockslides in the RIM database.

2.4.1. Database Structure

Owing to the variability in reported data in media articles, the research team created a consistent workflow to extract relevant volume and closure data from each catalogued event. Overall, the database we created has a total of 70 entries. All entries have closure times and volume estimates, but only a handful have cost information. The database also includes assigned confidence scores, which help in evaluating the relationships between event size and impact. Table 2.3 shows an example using the recent Big Sur Landslide, a high profile landslide that closed Highway 101 for over a year.

Table 2.3 Example fields of information in the RIMS database.

Field	Value	Units	Confidence Score
ID	0	-	-
DATE	5/24/2017	-	100
Location	Big Sur, California	-	100
LengthDebris	0.25	miles	100
ClosureDuration	400	days	100
Mass	1E+06	tons	75
RepairMaterial	6E+06	tons	100
RepairCost	54000	thousand $	100
Cause	Heavy Rainfall	-	100
Fatalities	0	people	100
Hyperlink	https://www.cnn.com/2018/07/18/us/california-scenic-highway-reopens-after-landslide/index.html		

Note that in some cases volumes were not directly available in the media article; however, they could be reasonably estimated with some judgment from a photograph provided with the article. In addition, the following conversion was applied when the news article reported weights rather than volumes of failed material, which also accounts for bulking effects.

1. Mass Density of Rock

$\rho_w := 1000 \frac{kg}{m^3}$ Mass Density of Water

$G_s := 2.7$ Specific Gravity

$\rho_r := G_s \cdot \rho_w = 2700 \frac{kg}{m^3}$ Mass Density of Rock

2. Failed Mass Density of Rock

$Bulk := 1.25$ Bulking Factor which means that the volume expands by 25% when it fails (mass stays the same) Hungr O. & Evans, E.G. (2004)

$\rho_{fail\_r} := \frac{\rho_r}{Bulk} = 2160 \frac{kg}{m^3}$ Failed Mass Density of Rock

3. Convert to Volume

The failed mass density of rock can now be used to convert mass (or weight) to volume.

1 ton = 907 kg

$\rho_{fail\_r} = 2.381 \frac{ton}{m^3}$

4. Convert cubic meters to cubic yards $1\ yd^3 = 0.765\ m^3$

$\rho_{fail\_r} = 1.82 \frac{ton}{yd^3}$

5. Convert weight/mass of failed material to volume

$W_{failed\_material} := 1\ ton$

$V_{failed\_material} := \frac{W_{failed\_material}}{\rho_{fail\_r}} = 0.549\ yd^3$

2.4.2. Challenges

There were quite a few challenges with gathering this information. The key issues were finding events and finding closure times. Initially, events were gathered by googling key terms such as closure, rockfall, state, reopening, year, month, etc. Using these terms, we searched for rockfall events in Washington, Oregon, Alaska, Idaho, California, and Colorado. This methodology proved to be time consuming and ineffective. It was very difficult, even by changing searches, to find events that had not already been recorded. To overcome this issue, we used the NASA Landslides database and the WADNR Landslides database to find more events. These databases contained only brief descriptions of rockfall events but provided us with sources to pursue. Most of the time it was easy to find images from which to estimate volumes, but then we ran into the issue of closure times.

Typically, news sources in Oregon and Washington had multiple articles about one event, but the information in all of them would be taken from the ODOT or WSDOT websites, leaving us with no new information. To overcome this issue in Oregon, we used the TripCheck database to search for recorded closure times. However, that database records only the estimated location, date, and closure duration without any additional descriptions or links, which meant that finding the right event proved to be difficult when multiple rockslides occurred on the same road within the same day. This resource was used fewer than ten times. For both Oregon and Washington, past Tripcheck reports were not available, and therefore closure times were often found from social media posts on road openings. In order for WADNR to keep up with its database, it has to check WSDOT Tripcheck updates daily, so searching for non-current events through WSDOT was not always successful.

In Alaska, California, Colorado, and Idaho, there were fewer social media posts to refer to for closure times, and seemingly fewer news articles about rockfall occurrences. Therefore, an overwhelming amount of our events were found in Oregon and Washington. For Alaska, we tried to use the Rockfall Database in the same way we used the NASA and WADNR databases but were not successful. AKDOT's database did not contain links, and the dates and locations of the rockfall events were not enough information to find the events through a Web search. There were seemingly fewer media articles about Alaska rockfall events.

The development of our small database clarified why WADNR and NASA have staff searching the Web for events around the clock in order to keep their databases current.

2.5. Analysis Results

Relationships between rockfall magnitude and impact were evaluated to provide relevant information to transportation planners regarding the prioritization of mitigation and evaluation of rockfall risk. Several relationships were explored in this research. Only the strongest and most relevant relationships are presented herein for closure times, costs, and both combined.

2.5.1. Closure Times

The magnitude of rockfall volume (in cubic yards) and closure time (hours) is expected to follow a power-law relationship because of the wide range of magnitudes observed in rockfall sizes. Figure 2.20 shows data for estimated rockfall volumes versus closure times from data catalogued in the RIM database. As seen, the data showed significant scatter, given the uncertainty in measuring and reporting volumes, but some correlation was observed. The variability in the data likely owed to the potential lack of equivalent impact among rockfall events. That is, in some cases, a large rockfall event may have occurred but impinged only slightly on existing right-of-way. However, in some cases, more modest events in narrow right-of-way may have closed a highway for a considerable period. While limited data were available on the spatial collocation of rockfalls and adjacent right-of-way, it was evident that larger rockfall events resulted in longer closure times—in some cases, those closure times were in the order of days to weeks. A power-law regression is presented for application by transportation planners.

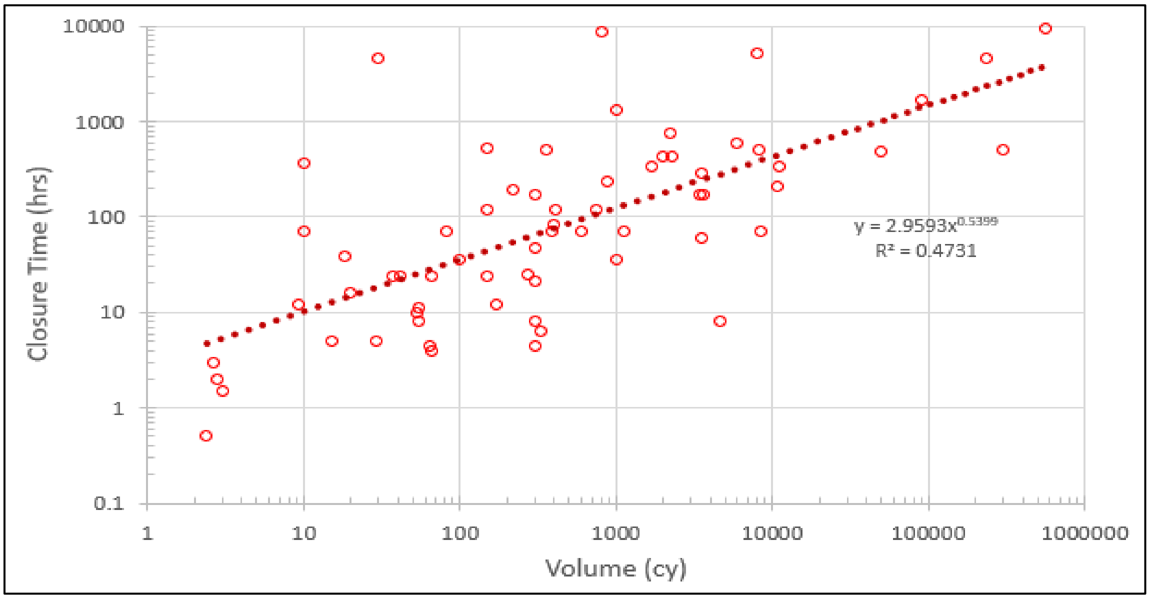

Figure 2.20 Estimated rockfall volumes versus associated closure times catalogued in the RIM database. An associated power-law regression line is shown.

Figure 2.21 shows closure times regressed to both estimated and reported rockfall volumes to identify whether there was significant bias in estimating the volumes from the photographs. Both relationships demonstrated trends similar to those previously described—larger rockfall volumes tended to result in longer closure times. The trends were similar, demonstrating that the procedure for estimating rockfall volumes was relatively consistent with data from reports. This supports the concept that images and estimates from news reports may be used to supplement the data in the RIM database when the information has not been recorded. A power-law regression is presented for both relationships for comparison.

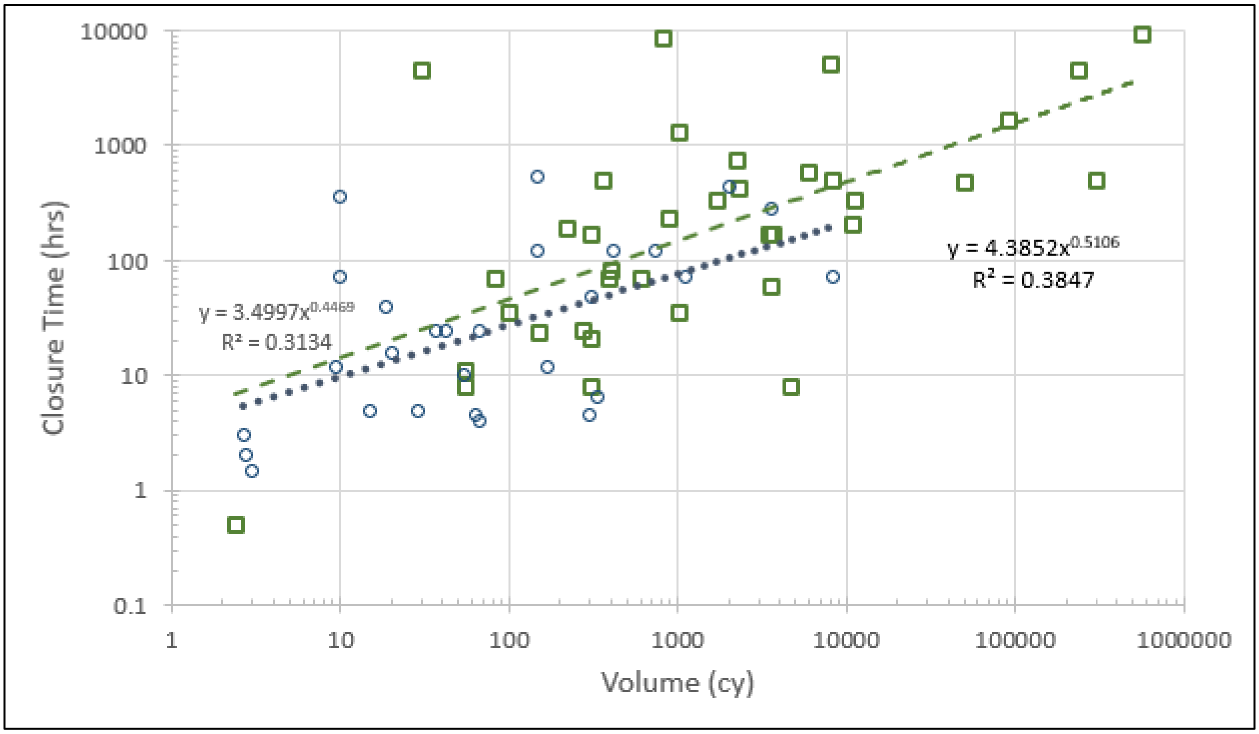

Figure 2.21 Estimated rockfall volumes versus associated closure times catalogued in the RIM database distinguished by reported rockfall volumes (green squares) and estimated rockfall volumes (blue circles). An associated power-law regression line for each is shown.

Note that the numerous variables that can influence the relationship between rockfall volumes and closure times were not readily captured in the catalogued data used in this analysis. One primary factor was a lack of information regarding the source location of a rockfall (e.g., height on the slope where debris originated, clearance from the highway), which would directly influence the likelihood of debris to reach the right-of-way. Furthermore, geological factors such as rock type, bedding, and joint attitude affect the size and initial trajectory of rockfalls. The strength and hardness of the both the rockfall and rockslope may also influence this relationship, as rockfall may fracture and disintegrate during impact with the underlying rockslope and/or the geometry of the rockslope and rockfall may alter the trajectory of a rockfall upon impact. Lastly, there was limited information regarding the highway clearance from a rockslope, rockslope height, and travel lanes, which may influence closure times. For example, if a large rockfall occurs but only partially reaches the highway, then no closure may be required. Alternatively, a road that has a rockfall may require only a lane closure but not complete closure of a road. Further cataloguing of rockfall impacts on highway closure should place particular focus on rockslope clearance from the highway, rockfall materials, rockslope attitude, and highway features (lanes, shoulder width, etc.).

The AKDOT GAM database provides an index for event size (table 2.2) along with an index for closure duration (figure 2.22). These dimensionless indices reflected a trend, albeit weak, in which closure duration score increased with event size. The variability in results and the relatively small number of bins muddled the results, but variability was expected, as data on the spatial collocation of rockfall events with right-of-way were often unavailable. Nonetheless, a trend was observed, and the observed data provided an upper and lower bound for potential rockfall impacts on infrastructure.

Figure 2.23 shows the impacts of event size on closure duration from the information solely provided in the AKDOT Event Tracker. No distinguishable trend was observed, likely a result of the data being recorded in generalized categories rather than actual volumes and durations, as shown in figure 2.20 in the RIM database.

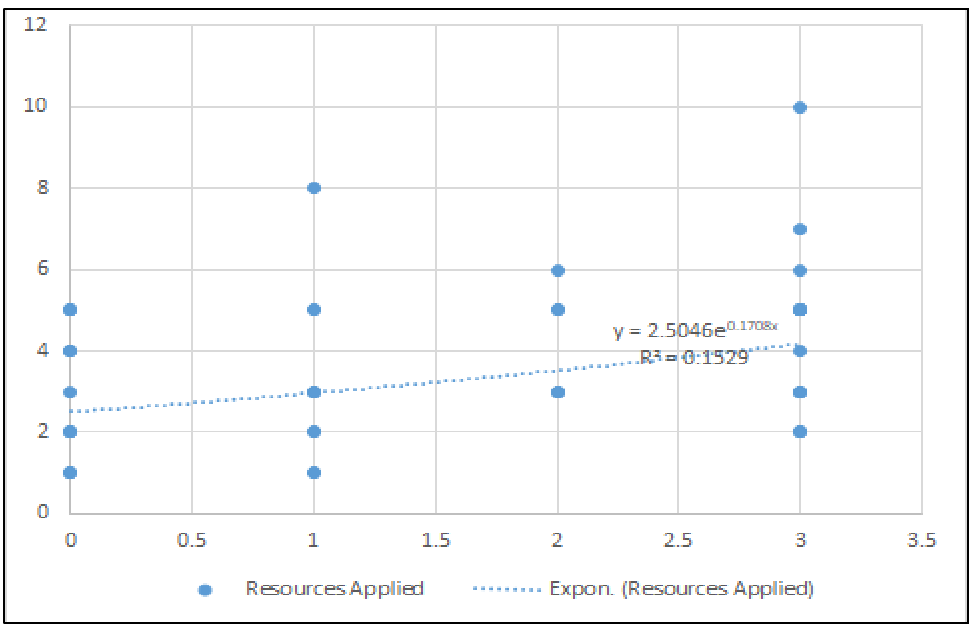

Figure 2.22 Plot of event size versus closure time. See Table 2 for interpretation of the codes. In order to apply different regression modes, all 0's were modified to be 0.0000001.

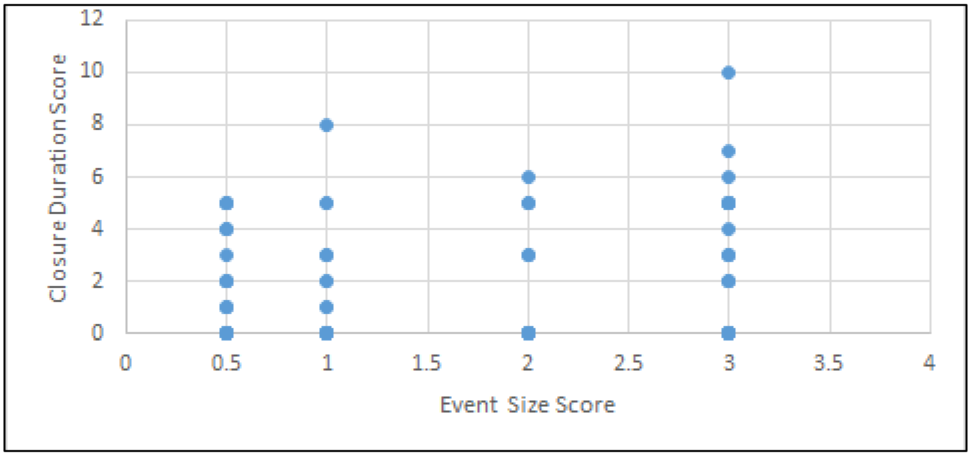

Figure 2.23 AKDOT Geo Event Tracker event size score vs. closure duration score. See Table 2 for definitions of the codes.

2.5.2. Costs

Rockfall event sizes were compared to repair costs from the AKDOT GAM (figure 2.24). While there was data scatter in each event bin, there was also a statistically significant relationship between event size and cost. As expected, smaller events resulted in smaller costs, likely stemming from debris removal and minor pavement repair. However, as event size increased, the cost became notably more significant, suggesting that significant repaving and more intensive debris removal techniques (crushing, hauling) were required. The range in costs for each bin again likely owed to the proximity of rockslopes (and associated rockfall events) to the right-of-way, as large rockfall events that do not extensively affect right-of-way require less clean-up and removal. A regression between event size and cost was created for simple application by highway planners.

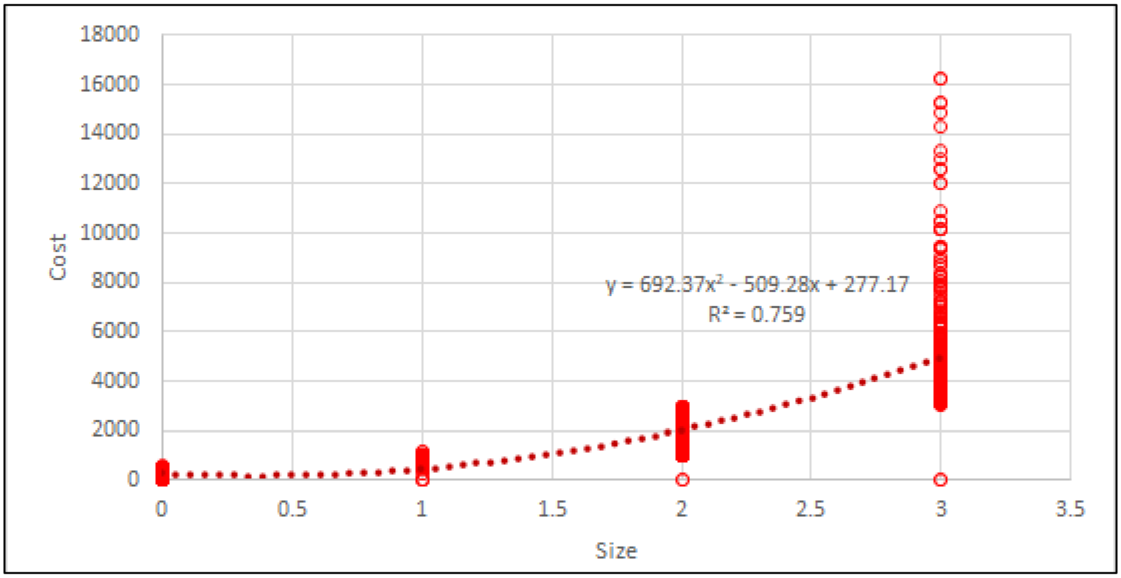

Size Code: 0 = Routine-minor, 1 = moderate, 2 = major, 3 = catastrophic

Figure 2.24. AKDOT rock event size versus cost.

2.5.3. Closure Times and Costs

2.5.3.1 ODOT Estimated Closure Time versus Repair Cost

Rockfall event closure times were compared to repair costs from the ODOT Unstable Slopes database (figure 2.25). The data showed significant scatter, likely owing to rockfall events not directly creating road closures, but to ODOT taking preventative mitigation measures to ensure that future rockfall events would not affect closures or driver safety. For large estimated closure times with small repair costs, it is hypothesized that either (1) data gaps existed or (2) large rockfall events resulted in significant closure times but costs were relatively small for debris removal. The costs presented did not include lost time, commerce, or rerouting expenses that would likely have been very significant with the associated closure times. These data also suggested that smaller events likely dominated costs, as they occurred notably more frequently than large events.

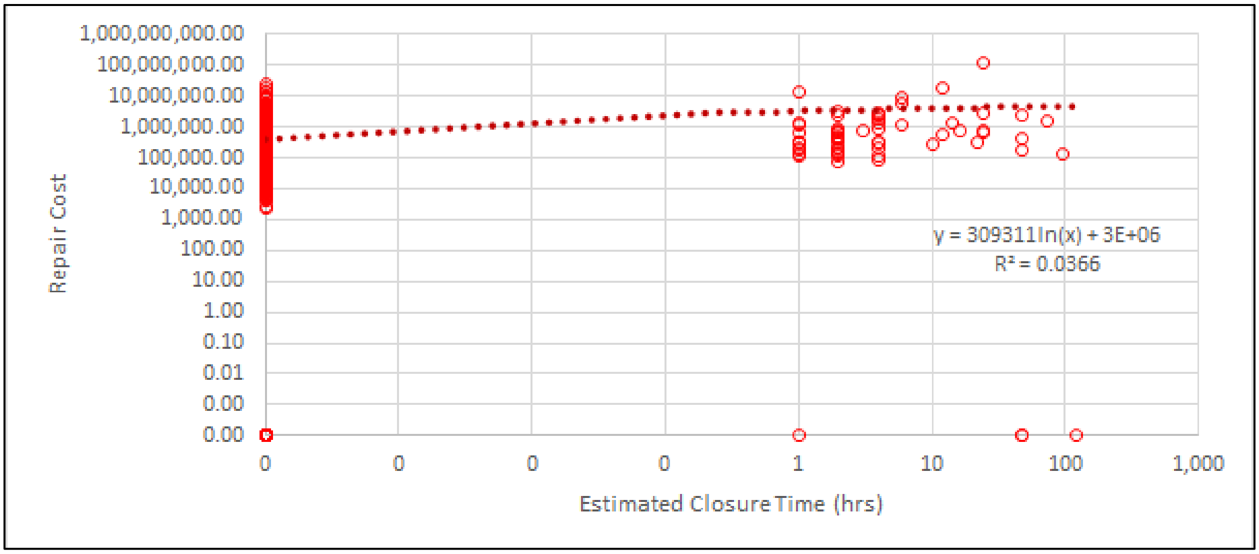

Figure 2.25. Estimated repair costs versus closure times attained from the ODOT Unstable Slopes database.

2.5.3.2 AKDOT Geo Event Tracker Closure Duration versus Cost

Rockfall event closure time scores were compared to repair costs from the AKDOT database (figure 2.26). The data showed significant scatter, likely owing to rockfall events not directly creating road closures but to AKDOT taking preventative mitigation measures to ensure that future rockfall events would not affect closures or driver safety. For large estimated closure time scores with small repair costs, it was hypothesized that either (1) data gaps existed or (2) large rockfall events resulted in significant closure times but costs were relatively small for the debris removal. The costs presented did not include lost time, commerce, or rerouting expenses that would likely have been very significant with the associated closure times. These data also suggested that smaller events likely dominated costs, as these events occurred notably more frequently than large events.

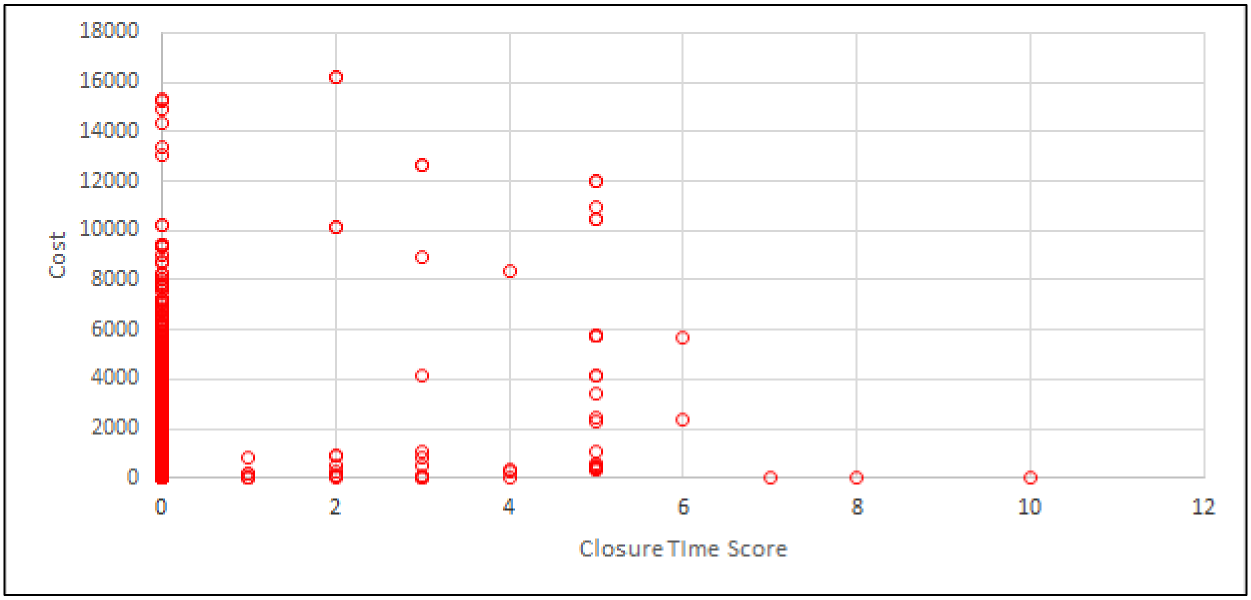

Figure 2.26. Closure times and costs from the AKDOT Geo Event Rockslide and Landslide database.

2.5.3.3 ODOT Repair Costs in Relation to Annual Maintenance Costs

Rockfall event annual maintenance costs (figure 2.27) and closure times (figure 2.28) were both compared to repair costs from the ODOT Unstable Slopes database. Very low correlation was observed between these parameters and repair costs.

Figure 2.27. Plot of repair costs versus annual maintenance costs. Entries with 0's have been removed.

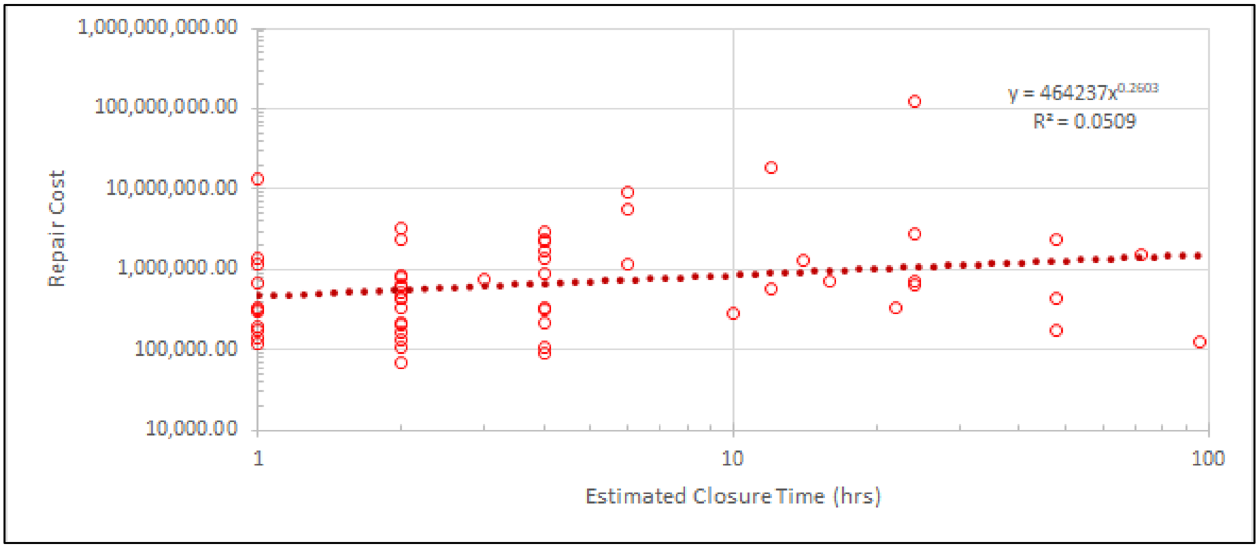

Figure 2.28 Plot of estimated closure times and repair costs. Entries with 0's have been removed.

2.6. Conclusions

A series of databases were analyzed, or created, to reflect the potential impacts of rockfall events. A variety of relationships were established, and they suggested that larger rockfall events may have greater impacts, but more frequent, smaller rockfall events are often the source of many closures. The regressions presented provide an index for the potential impacts of rockfall events in terms of closure times and costs. While data gaps existed in all the databases because of nuanced differences in their purposes, they clearly showed that variability in rockfall impacts existed in all states in the Pacific Northwest. Despite this variability, basic relationships that would support simple cost-benefit analyses were developed. Overall, we found that larger rockfall events had a bigger impact, however, although those events were less frequent. This suggests that there is potential to optimize mitigation efforts on the basis of rockfall frequency and impact, which may be determined by transportation planners by using some of the regressions presented. Much of the variability described here owed to incomplete data sets and a lack of data on the spatial correspondence of rockslopes with proximity to adjacent highways. It would be beneficial to improve this data set in the future to improve cost-benefit analyses and evaluations of risk and impact.

A second challenge was that the use of codes rather than actual values made it difficult to combine different databases. Use of either a consistent code or preferably the actual values or estimates with uncertainty would generally be preferable to make the database more usable for more rigorous analyses.

CHAPTER 3. STUDY SITE AND DATA

This research built on five years of slope stability research in Alaska at Long Lake and Glitter Gulch. A baseline of terrestrial laser scan (TLS) data had been established to develop landslide forecast models and for the emerging geotechnical discipline of change detection. The two research sites were along critical transportation corridors linking Alaska's interior to Anchorage, its most populous city. The Long Lake site is on the Glenn Highway between Palmer and Glennallen, between mileposts 78 and 89. The Glitter Gulch site is near the Denali National Park entrance, between mile posts 239 and 247 of the Parks Highway. Numerous unstable rock slopes throughout Sites A and B (figure 3.1) were surveyed along the Glenn Highway in Alaska with both TLS and SfM techniques. In previous surveys, we used a total station to create a control network with survey targets that were then used to geo-reference both the TLS and SfM data sets.

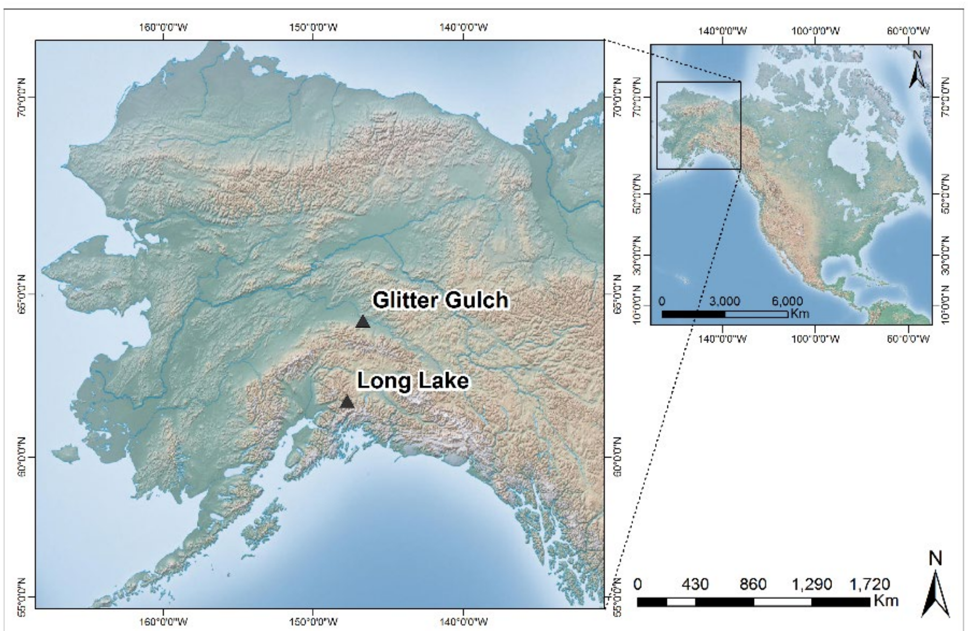

Figure 3.1 Location of the study sites in Alaska

The Long Lake region primarily comprises sedimentary rocks of the Matanuska and Chickaloon Formations. The Matanuska Formation is a marine sedimentary deposit formed during the orogenic rise of the Talkeetna Mountains. The Chickaloon Formation was deposited as propagating alluvial fans on top of the Matanuska Formation that formed as the Talkeetna

Mountains were uplifted and sequentially eroded [O'Banion et al. 2018]. The highway follows the glacial cut into the Chickaloon Formation; however, no other glacial evidence may be found in the area [Trop et al., 2015]. Regions of the Matanuska Formation exposed in road cuts along the Glenn Highway largely consist of dark mudstones, and Chickaloon Formation outcrops mainly consist of carbonaceous siltstone, coal, and sandstone [Trop et al., 2015].

At Glitter Gulch, outside the Denali National Park entrance, is an unstable highway slope where the research team collected several data sets in previous Pactrans projects and other endeavors. The collection of various types of remote sensing data at this location are being organized and cataloged to generate a remote sensing "super site" for the long- term analysis of the geology and infrastructure. The super site data now include six campaigns of static terrestrial data to model the unstable slopes and historic airborne imagery dating to the construction of the road.

3.1. Data Collection

In August 2018 and 2019, TLS surveys were completed by using a Maptek XR3 laser scanner for multiple sites, including sites LL71, LL75.8, LL75.9, LL85.5, LL86.9, LL87, GG(MP239-240), GG241S, and GG241N, which had been captured in previous years. In addition, in 2019 a new site, LL89, was surveyed. Also, in 2018, a Riegl VZ-400i was used to supplement the Maptek scans. For georeferencing, a Leica GS18 Global Navigation Satellite System (GNSS) receiver was set up as a base for each site, and it logged static data (a minimum of one hour, but length depended on the time required to complete the scans at each site). A second Leica GS18 was mounted above the scanner, and it logged approximately 15 minutes of static GNSS data per scan location. A digital compass inside the scanner recorded the orientation of the scanner.

Data were post-processed with the following workflow. First, the raw GNSS observations from the base station were processed with OPUS, which is an online GNSS post-processing service provided by the National Geodetic Survey. Next, baseline GNSS processing between the rover at the scan positions and the base was completed with the Leica Infinity software. Then the georeferencing methods described in Olsen et al. (2009, 2011) were implemented. The GNSS coordinates were applied to the scanner origin (accounting for the height difference), leveling information was applied, and the azimuth orientation of the scanner was found through a global registration process evaluating correspondence between neighboring scans after initial estimates from the digital compass had been used.

After registration, the data were cropped in Maptek Point Studio 8.0 and/or CloudCompare software by using a polygon around the extents of the exposed rock developed for previous surveys such that the analysis extents would remain the same. Then large pockets of vegetation were manually removed from the data. After these manual edits, RAMBO software (Olsen et al. 2020, In Press) was utilized to undertake ground filtering to remove remaining vegetation, generate surface models, perform change detection and analysis, and conduct the RAI morphological analysis for each site.

A key project goal was to compile information from rockfall databases and supplement it with additional media information into a single database focused on rockfall impacts on mobility in transportation. The parameters that are the primary focus of the RIM database presented herein includes date, number of events, event volume, associated event closure time, and associated event cost.

CHAPTER 4. MITIGATION ASSESSMENT[1]

4.1. Introduction

Tens of millions of dollars are spent annually by state DOTs in the U.S. to protect and maintain roads that intersect geologically unstable slopes (Pierson and Turner, 2012). This money is allocated not only to protect traveling citizens but to ensure reliable transportation routes for industry and to safeguard investment in the infrastructure itself. Today, many factors, including the environment, rock or soil quality and properties, hydraulic conditions, and construction plans, are considered when roads are built, with the cost-efficient longevity of the asset considered (Stead and Wolter, 2015). Historically, however, the future effect of action on a slope has not necessarily been considered, and the location of the roadway and the excavation methods used may have been less than ideal (Basahel and Mitri 2017). The rapid pace of past construction has left many transportation corridors vulnerable to geologically driven hazards and in need of defense (Pierson, 2012).

The most common methods of safeguarding against slope failure fall into two basic categories: stabilization action on the slope and passive protection of the roadway (Pierson and Vierling, 2012). For a soil-mantled slope, the action approach involves keeping the slope below its angle of repose as determined by its factor of safety, and the protection approach involves using retaining structures to hold back the fallen, loose material that is beyond the angle of repose (Wyllie, 2017). Similarly, rock-dominated slopes can be actively maintained through controlled removal of loose material by blasting or mechanical excavation, as well as by anchoring loose material with bolts and/or a concrete coating, and the roads can be passively protected by installing ditches and creating barriers or using metal mesh to catch and keep falling rock near the slope (Andrew and Pierson, 2012).

Although the choice for a rock-dominated slope is often stabilization by further excavation, usually by scaling and/or trim blasting, as this appears to be the most economical and least intensive option, it can be a very temporary fix (two to ten years) that requires continued, if not increased, removal (Andrew and Pierson, 2012; Pierson and Vierling, 2012). Scaling is a

---

[1] *Portions of his chapter were published by Kristen Marohl as a Report (MESSAGe Technical Report Number: 079) in fulfillment of the degree Master of Science in the Department of Earth and Space Sciences at the University of Washington in May 2019.*

procedure that involves removal of the "scales" or weathering rind of the rock face, i.e., the loose rock that is predicted to fall in the near future; by its nature, weathering will begin working on the fresh rock, and the process will need to be repeated (Andrew and Pierson, 2012). Scaling may be completed by workers suspended on ropes using pry bars, expansive concrete products, and air bags or by heavy machines such as hydraulic hammers, excavators, and bobcats; strategic blasting may also be used (Andrew and Pierson, 2012; Pierson and Vierling, 2012). Removal of rock on a slope may lead to unplanned increases in rockfall because of the destabilization of the slope, over-break on discontinuities, or elastic rebound, as well as because of stress relaxation (Andrew and Pierson, 2012; Wyllie 2017). To properly address each of the hazardous slopes within a transportation agency's domain, efficiency in slope monitoring and maintenance must be increased while the safety of the field crew is maintained or improved (Gigli et al., 2014; Pierson and Turner, 2012; Wyllie 2017).

Historically, it was thought that a thorough site assessment would facilitate a more streamlined maintenance protocol, as site assessments enable the geologist or engineer to empirically understand the processes that lead to failure at a given location (Lato et al., 2012; Basahel and Mitri 2017; Pierson and Turner, 2012). While this is accurate, an agency that has thousands of slopes intersecting hundreds of assets must have criteria for discerning the relative urgency of attention to a site; the use of a classification scheme can resolve that issue (Pierson, 2012; Pierson and Turner, 2012; Wyllie, 2017). Classification schemes such as the Rockfall Hazard Rating System (RHRS) serve as an efficient communication tool between field staff and designers, as well as facilitate a more judicial evaluation of the rock mass properties and hazards, even when the geology varies (Pierson, 2012).

Still, classification systems are not without their flaws. The heterogeneous and anisotropic nature of a rock mass means that classification systems can be susceptible to varying interpretations that are biased by the assessor and can be dangerous or impossible to obtain on very high or active slopes (Lato et al., 2012; Gigli et al., 2014; Kromer et al., 2015). Because of budgetary responsibilities, a site is often visited only once, with documentation in the form of field sketches and site photos from ground level (Wyllie, 2017). Some agencies use a drone, but this requires submission of flight plans in advance, and post-field assessments are open to communication issues (Pierson, 2012). Additionally, most hazard rating systems don't consider the potential external triggers (Basahel and Mitri 2017) or identify the potential failure locations on the slope (Kromer et al., 2015).

To correct for the issues mentioned above of subjectivity, access, and the possibility of further assessment after leaving the field, many researchers (Gigli et al., 2014; Lato et al., 2012) have attempted to improve methodologies for obtaining discontinuity information and rock block size from TLS (terrestrial lidar scans), and most commercial software for processing TLS point cloud outputs has been set up to aid in the identification of those features (Kromer et al., 2015). These technological advancements have enabled the determination of potential rockfall trajectories and provided the ability to map and quantify rock falls with successive scans over time (Kromer et al., 2015; Gigli et al., 2015; Lato et al., 2012; Stead and Wolter, 2015). Additionally, Matasci et al. (2018) used TLS processing software to create a slope susceptibility index of specific failure mechanisms based on morphology, discontinuity assessments, and long-term monitoring. The main weakness of this line of research, however, is that discontinuity surveys do not provide reliable information on slopes comprising poor quality rock or complex and varying morphology (Gigli et al., 2014; Olsen et al., 2015). Recently, a classification scheme called the Rockfall Activity Index (RAI) has strived to answer for complications in morphology by considering the roughness of the slope in place of mapping the major discontinuities alone (Dunham, et al., 2017).

It is assumed that these advancements are effective, but little work has been done to test their levels of improvement on the efficiency and safety of slope maintenance and monitoring. By identifying likely areas of future failure, between successive years of data, can we quantify effectiveness in terms of risk depreciation and of rock slope scaling over annual timescales? If we can accurately quantify the effects of scaling, transportation agencies can make maintenance and mitigation decisions more efficiently. Using the RAI for the study, we may also determine its efficacy by noting whether the model identifies the same high hazard areas as engineers.

This research examined TLS data on a road cut in Alaska, immediately preceding and following a slope stabilization project, noting any changes in rockfall and comparing the work done during excavation to the hazardous areas identified through the RAI model.

4.2. Background

4.2.1. Regional Geology

The state of Alaska is largely a syntaxis of accreted terranes identifiable as the bounding of the Gulf of Alaska by the southern reaches of the state that border British Columbia on one flank and the barrier islands to the Bering Sea on the other (Falkowski et al., 2016). The oldest of these, the Precambrian Yukon-Tanana Terrane, is exposed immediately to the north of the continental divide in the Alaska Range (figure 4.1). The rocks are metasedimentary oceanic basin rocks and metavolcanics that were first metamorphosed during the Cretaceous collision with the North American Plate and have since experienced localized contact metamorphism via basaltic and granitic intrusion.

Alaska is an extremely active state, with dozens of fault systems (figure 4.1) that aid subduction processes in creating active volcanos and large mountains, such as Denali, that have the greatest relief on the North American Continent. Currently, the Pacific Plate and the Yakutat Microplate are subducting in a north-northwest direction, translating motion eastward, onto several faults including the Chugach, Border Ranges, and Denali faults (Eberhart-Phillips et al., 2006). Near the study site, where a strand of the Denali fault, the east-west trending Hines Creek Fault, intersects the northward draining Tanana River, the basement rocks of the Yukon-Tanana Terrane are exposed on hillslopes and in roadcuts.

4.2.2. Local Geology

The dominant unit of the Yukon-Tanana Terrane is the Birch Creek Schist, a meta-sedimentary schist of marine shale and sandstone origin whose original structures have been erased during metamorphism. Its greater than 10,000-ft thickness is not a true stratigraphic thickness, as it is measured perpendicular to the axial plane cleavage (Wahrhaftig, 1968). Wahrhaftig (1968) classified the Birch Creek Schist as mostly quartz with sericite (mica), calcite, and trace albite and microcline (feldspars). Near Denali Park, the Healy Schist, a local sub-unit of the Birch Creek Schist, is a quartz-sericite schist or phyllite with interbedded quartzite that is locally carbonaceous with perfect cubic pyrite up to ¼ inch in diameter, very fine-grained, and highly anisotropic, with strong foliation defined by micas (Wahrhaftig and Black, 1958). Near-vertical and irregular joints trend north-south; some have basaltic intrusions (Wahrhaftig and Black, 1958).

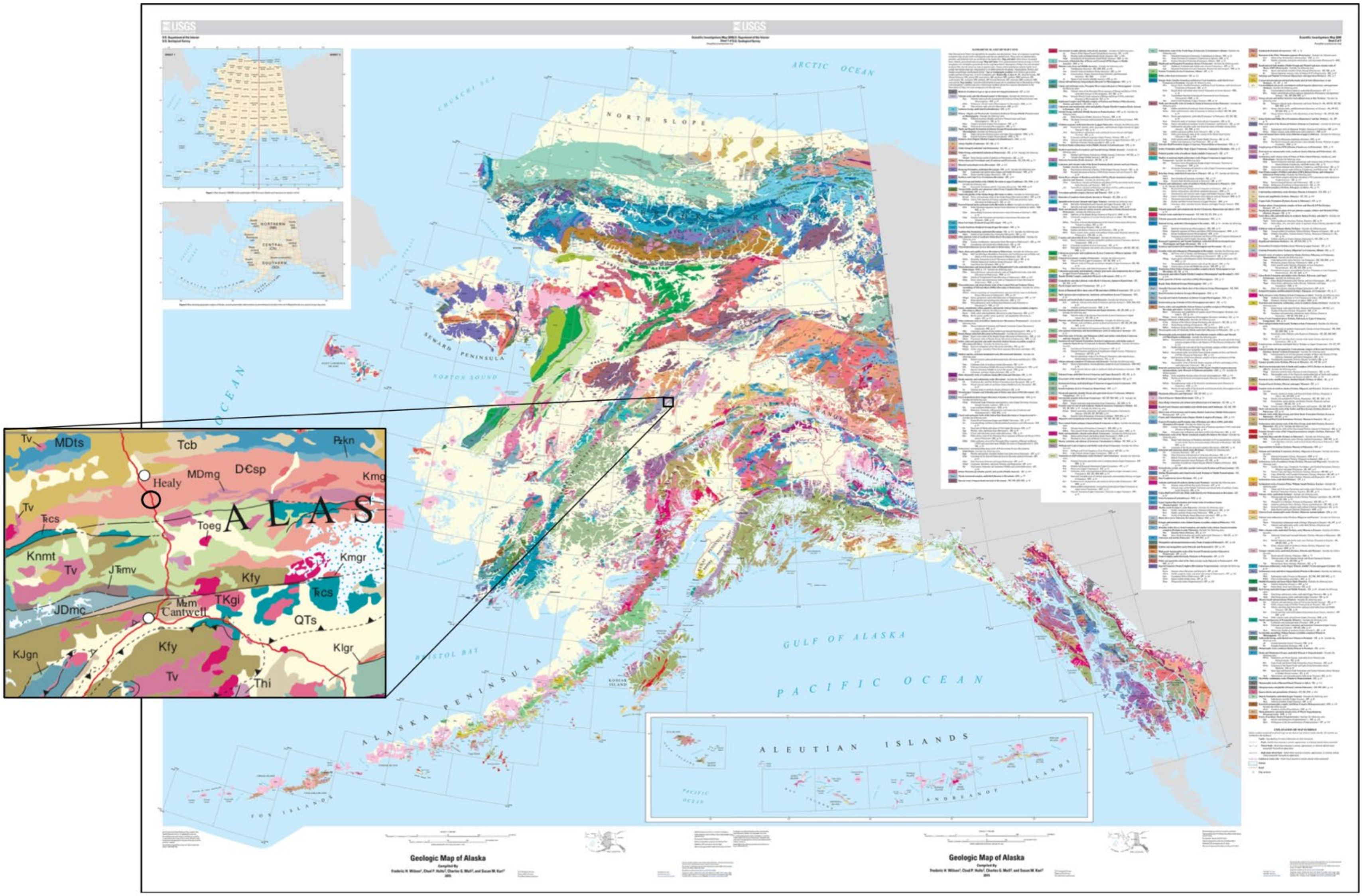

Figure 4.1 Geologic map of Alaska with an inset of 1:250,000. The Healy Quadrangle encompassing the study area is circled in black (Wilson et al. 2005).

Slope failures in the unit have been well documented in studies done for the adjacent railroad; they are typically related to freeze-thaw cycles or high pore-water pressure along foliations; although, some slide planes hundreds of feet deep have been identified where schist, that has decomposed into clays, retains water in the slope (Wahrhaftig and Black, 1958). This, combined with the high quartzite content of the schist, can lead to catastrophic failures (Stead and Wolter 2015). Additional failures can include remobilization of the loose philitic material that resides on the slope because of less severe failures (Stead and Wolter 2015). Most of this rockfall is evident in the spring, when high precipitation on elevated water tables invades weathered regions on slopes and discontinuities that have been jacked open by frost heave are released (Wyllie, 2015).

4.2.3. Study Site

"Glitter Gulch" is located along the George Parks Highway (AK-3) from milepost 239 to 241, in the Nenana River Valley, near Healy in the Alaska Range (figure 4.2). It is a precarious stretch of rock slopes outside of Denali National Park in Alaska. Originally constructed in 1971 on cut and filled glacial debris (Wahrhaftig and Black, 1958), this stretch of the highway is reported to have had over 300,000 yd^3 of debris removed by 2008, which has included slabs of up to 1,000 tons (Cole, 2016). Because the George Parks Highway is the main route between Anchorage and Fairbanks, in addition to serving all tourists to Denali National Park, the ADOT&FS staffs four or more full-time road maintenance personal for mileposts 231 to 276 alone (Jeff Curry, personal communication, 2018). The slope considered in this report is the 800-ft wide and 90-ft tall outcrop immediately north of Fox Creek near milepost 241, within Glitter Gulch (figure 4.3).

In 2016, the ADOT&FS began a year-long project at Glitter Gulch. This work was prompted during a re-grading project when an engineer identified a larger than acceptable risk of rockfall during construction activities (Jeff Curry, personal communication, 2018). A scaling crew, Landslide Technology, was hired to remove loose material from the five most hazardous of the eleven slopes along the stretch by scaling and trim blasting, as well as by installing extensive barriers between the catchment ditches and the George Parks Highway where the ditch was determined to be insufficient to protect the roadway.

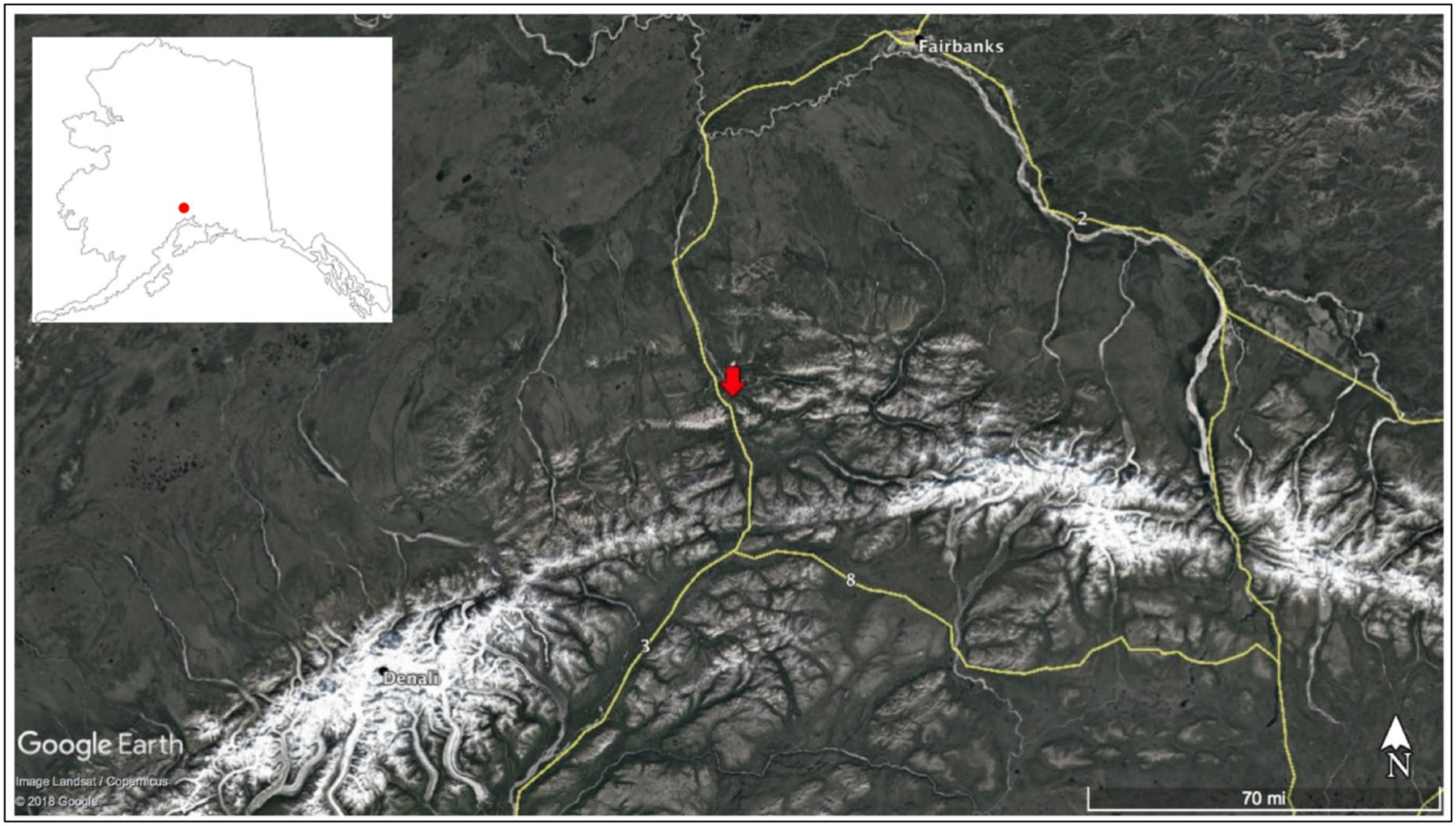

Figure 4.2 Location map obtained from Google Earth of the Glitter Gulch study site outside of Denali National Park in Alaska. State Route 3, also known as AK Interstate 4, more commonly referred to as the George Parks Highway, is the affected transportation route. This route borders the Nenana River, a tributary to the Tanana River that drains the northern slopes of Denali.

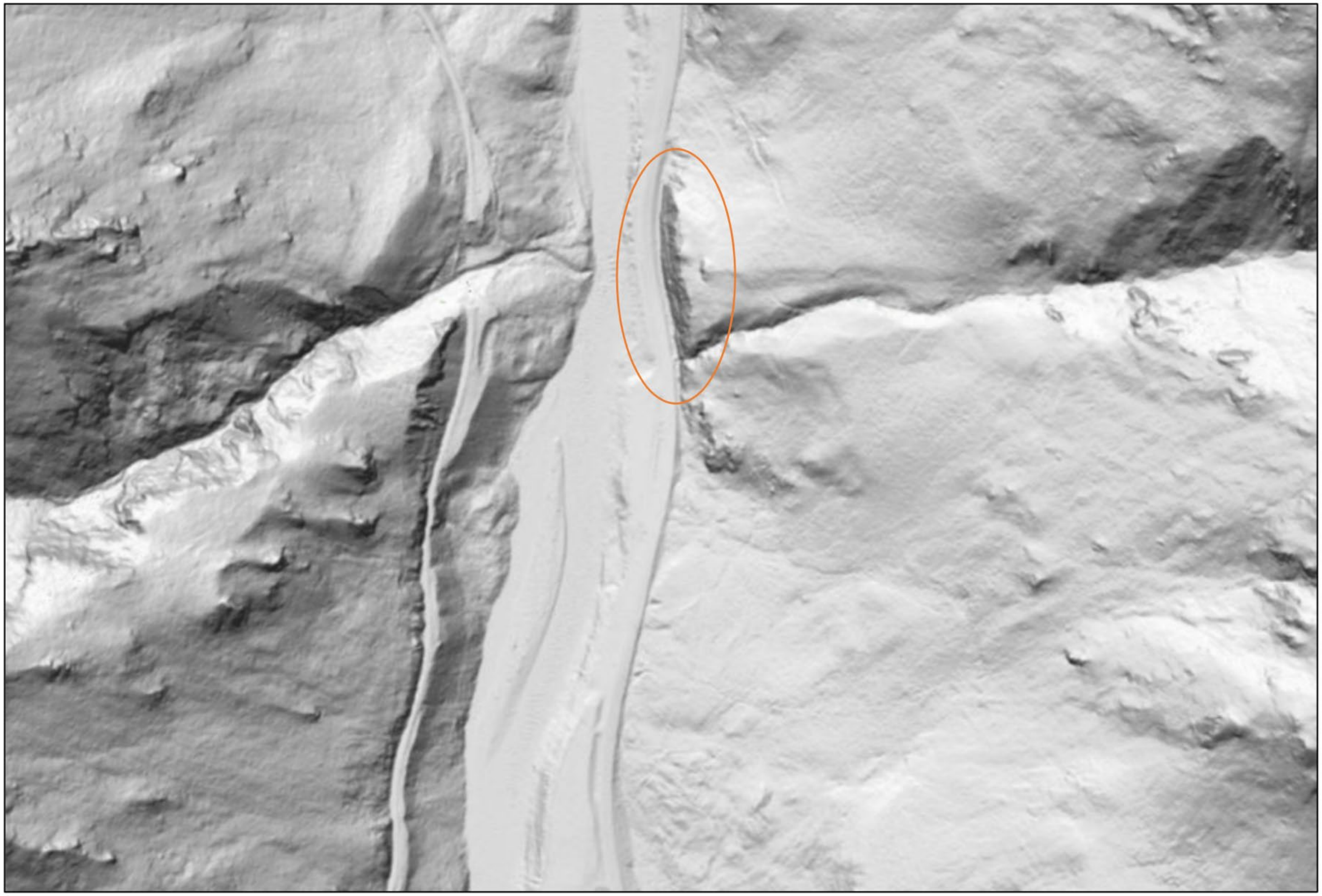

Figure 4.3 Aerial lidar DEM of the study area (circled in orange) obtained from the state of Alaska's Department of Geological and Geophysical Surveys on 8/20/18.

4.2.4. Data Acquisition

Since 2012, laser scanners have been used to capture 3-D imagery of the Glitter Gulch study site. These scanners determine 3-D relief by sending electromagnetic pulses toward the object(s) and recording the relative speed of return after reflection. The 2012 data set was captured by the consulting firm David Evans and Associates with a TITAN Mobile Laser Scan system. The 2013, 2014, 2015, 2017, and 2018 data sets were captured by a joint University of Oregon-University of Washington research team using various terrestrial laser scanners and related equipment, as represented in fable 4.1. The procedures involved setting scan positions, on the shoulder of the opposite side of the highway, approximately 60 m apart, with the scanner set to capture a field of view of at least 180 degrees horizontally by 100 degrees vertically (+70 degrees to -30 degrees from horizontal) for at least 20 minutes to maximize recording time and point density in the allotted field time.

Table 4.1 Data acquisition equipment used by the PacTrans research team. The 2012 data are excluded, as they were captured by David Evans and Associates using a proprietary mobile system, the TITAN Mobile Laser Scanner.

Year	Scanner	Coloring	GPS
2013	Riegl VZ-400	Nikon D700	Trimble R8 GNSS
2014	Riegl VZ-400	Nikon D700	Trimble R8 GNSS
2015	Riegl VZ-400	Nikon D700	Trimble R8 GNSS
2017	Leica ScanStation P40	In-scanner	Trimble R8 GNSS
2018		In-scanner	Trimble R8 GNSS

*Survey was not conducted in 2016, due to a significant slope maintenance project where scaling and trim-blasting was done on the slope in conjunction with re-paving of the highway.

4.2.5. Data Processing

As described by Olsen et al. (2015), each scan was logged individually in the field, which necessitated a preliminary transformation to a common coordinate system. The Alaska State Plane Coordinate System Zone 4, North American Datum 1983 (2011) Epoch 2010.00, Geoid 12A was the chosen system.

The scans were then manually cropped to represent only the slope and were cleaned of noisy data, such as significant vegetation with the Maptek software I-Site Studio. This was done by manipulating thinly sliced (1- to 5-m) cross-sections of the scan (in each of the three planes) to enable a polygon to be drawn around only the vegetation whose contained points were then deleted from the data set. Care had to be taken during this step, as it was crucial for difference analysis that the growth or removal of vegetation not be mistaken for a rock fall or accumulation event.

To prepare the data for a cloud to cloud differencing using the RAI software, the successive point clouds were registered together to minimize error from misalignment. Following methodologies written by the RAI software creators, the prepared scans were imported to an open-source point cloud manipulating software, CloudCompare, and finely registered in change epoch year pairs: 2012-2013, 2013-2014, 2014-2015, 2015-2017, 2017-2018. Before using the Finely Register tool, the clouds were manually oriented as close as possible with the Bounding Box Align tool and the Translate/Rotate tool to expedite the processing time. Keeping to the prescribed methodologies, the number of points that each cloud contained was noted, and a random sampling unit of 1/20th of the largest of the two clouds for the Finely Register tool was selected; the root mean square (RMS) difference was also lowered to 1.0e-7, and the option to remove the farthest points was chosen. These jointly registered clouds were then exported as text files to best facilitate file conversion.

4.3. Observations

4.3.1. Site Characteristics

The study slope presented as a competent, near-vertical mass of rock protruding from the hillside, necessitating a strong bend in the highway that leads to a slight blind corner for the northbound traveling traffic (figure 4.4). An arcuate feature with significant drainage to the south and a lower, talus slope to the north, this portion of the eastern flank of Mount Healy was amputated by the Nenana River. The rock had an unconfined compressive strength (UCS) of weak to very weak (<25mPa) where schist dominated, and of strong to extremely strong (>25mPa) where quartzite veining dominated. Micaceous talus clung to the slope above ledges, and oxidization stained approximately 75 percent of the face. The schistosity was parallel/sub-parallel to the slope, and there were a few, widely spaced, intersecting joint sets with very high persistence.

Figure 4.4 Oblique photograph taken in August 2018 of the study slope at MP 241 on the George Parks Highway near Glitter Gulch, Alaska. The image was captured with a DJI Phantom 4 drone flown by Jake Dafne. Sugar Loaf Mountain is in the distance, and the Nenana River is in the foreground.

The Rockfall Hazard Rating System (RMHR) score was between 190 and 304; the dominant controllers of the score were the overall height of the slope and the very high persistence joints. At the time of the site visit, the minimal rock fall present was well within the ditch. However, visible track marks from heavy machinery indicated that the ditch had recently been cleaned. This made it difficult to classify the typical rock fall behavior. Yet another of the high-hazard mitigated slopes, which was not included in this study, had visible track marks as well as rock fall debris on the roadway so sufficient time may have passed since the ditch/road cleaning.

4.3.2. Data Acquisition and Preparation

During the preparation of the data, significant differences in the metadata emerged (table 4.2). Abilities of the scanners as well as differences in the spacing of successive scans and the length of each scan led to varying point cloud densities that might represent the slope with more or less accuracy. Alignment accuracy also varied over each change epoch. Each epoch had a lower RMS error than the preceding epoch, leading to more accurate change detection potential.

Table 4.2 Point cloud statistics for each of the six scans, as well as successive cloud registrations.

Survey Year	Final Cloud Density (n points)	Alignment Error (m RMS)
2012	1,771,314	
		0.045
2013	23,091,227	
		0.034
2014	51,332,016	
		0.032
2015	69,689,364	
		0.029
2017	69,311,656	
		0.017
2018	116,969,737	

*Survey was not conducted in 2016, due to a significant slope maintenance project where scaling and trim-blasting was done on the slope in conjunction with re-paving of the highway.

4.4. Findings

4.4.1. Hazard Data

4.4.1.1 2012 RAI Outputs

The poorer resolution of the point cloud, especially at higher points in the slope, the RAI maps for 2012 were limited (figure 4.5).

The portions of the slope that were mapped represented the morphology well (figure 4.5: A). The lower third of the slope was nearly sufficiently captured, and overhangs along discontinuities were accurately identified. The middle, approximately third of the slope was less than 15 percent mapped, but significant hazards such as the large wedge on the upper-left were, at least in part, identified. The upper third of the slope was virtually non-existent except for small spots on the large knob in the upper-center of the slope.

With the caveat of the poor resolution, hazardous areas such as overhangs and small blocky sections around discontinuities were accurately flagged (figure 4.5: B). Improved resolution was needed to analyze further.

4.4.1.2 2013 RAI Outputs

With 13 times the point density of the 2012 scans (table 4.2), the 2013 maps provided better resolution (figure 4.6).

The morphology was moderately well identified by the RAI classification scheme in the 2013 map (figure 4.6: A). Very persistent discontinuities were highlighted by a lineation of rock mapped as widely spaced discontinuous, although those with less persistence were more challenging to identify. Even small ledges were mapped well by the presence of talus on the face of the slope. Overhangs were well mapped, but the extent of the block that was related to the overhang was more difficult to identify without the presence of significant discontinuities flanking the overhang. Mapping of large protrusions was almost non-existent.

Mapped hazards were well highlighted but poorly scored (figure 4.6: B). Large protrusions high on the slope were only mapped as having a moderate hazard even though there were unfavorable discontinuities with the potential to create blocks of up to 30 ft in diameter, over 50 ft high on the slope. Small block (<2 ft) potential failures from atop ledges at the same elevation were given the same kJ rating.

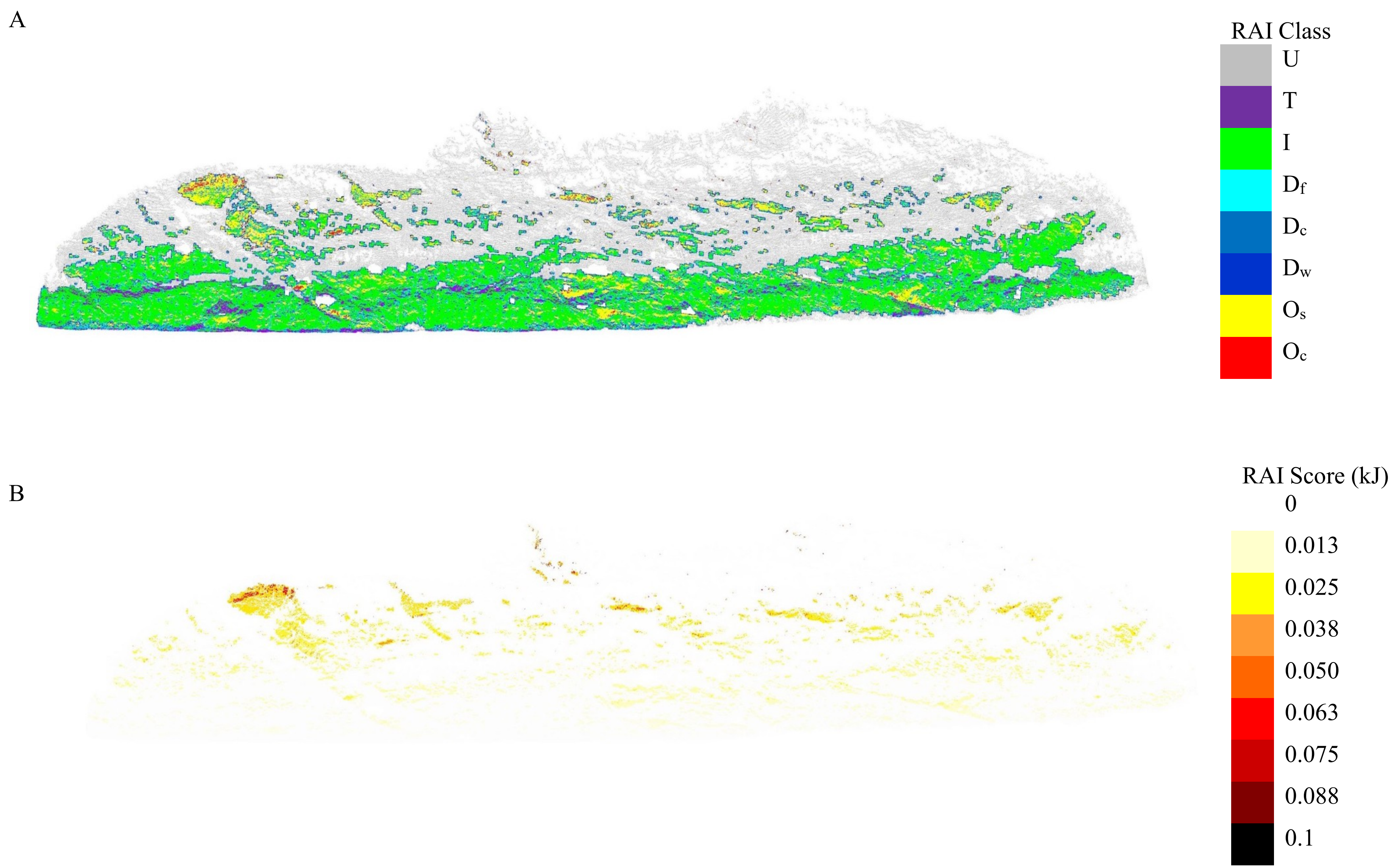

Figure 4.5 RAI classes (A) and RAI scores (B) for the 2012 scan of the study slope at MP 241 on the George Parks Highway near Glitter Gulch, Alaska.

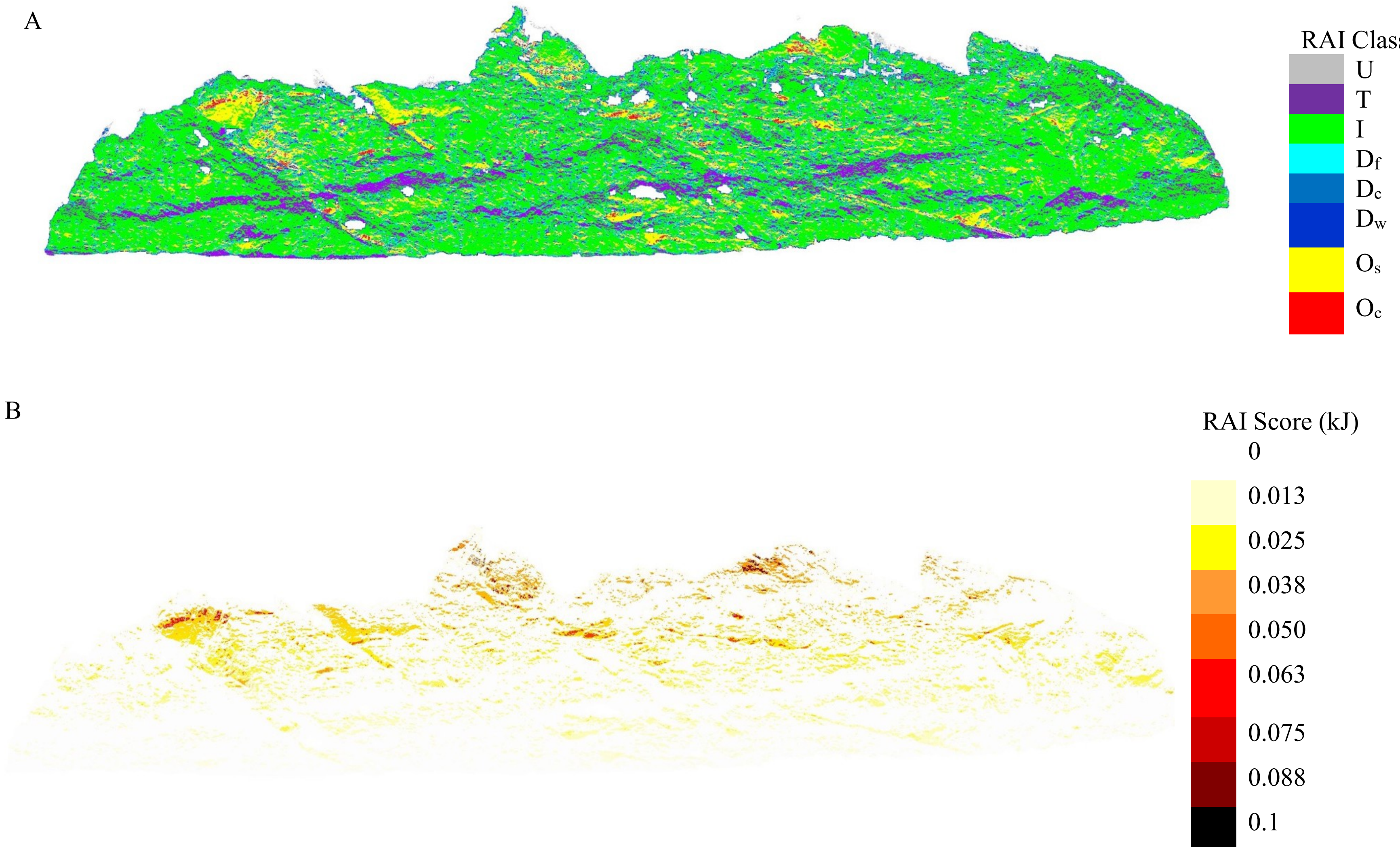

Figure 4.6 RAI classes (A) and RAI scores (B) for the 2013 scan of the study slope at MP 241 on the George Parks Highway near Glitter Gulch, Alaska.

4.4.1.3 2014 RAI Outputs

The point cloud density doubled between 2013 and 2014 (table 4.2), leading to finer resolution of the slope (figure 4.7).

Morphology mapping patterns followed the results listed for 2013 except for an increase in overall area and a decrease in intact rock (figure 4.7: A). Data gap areas were much smaller than the previous year, and the furthest extent of mapping increased. While the increased area increased the volume of rock identified as intact, finer resolution reclassified some intact areas as talus or as discontinuous rock. Rock classified as overhanging did not appear to have a significant volume change.

Mapped hazards gained significant resolution from the previous year (figure 4.7: B). While the total RAI score for the slope likely did not increase, a larger portion of the slope was identified as at least a small hazard. The increase in hazard followed areas that changed from those classified as intact to those that were discontinuous, while decreases in hazard followed small discontinuities created by the roughness classification.

4.4.1.4 2015 RAI Outputs

With a 35 percent increase in point cloud density from 2014 (table 4.2), the pattern of increasing resolution of the slope maps continued (figure 4.8).

The morphology and hazard mapping patterns followed those listed for 2013 and 2014. Volumes of rock classified as intact decreased while discontinuous and talus classified rock volumes increased (figure 4.8: A). More of the slope was mapped as having some hazard, while areas mapped as significant hazard were further bisected (figure 4.8: B).

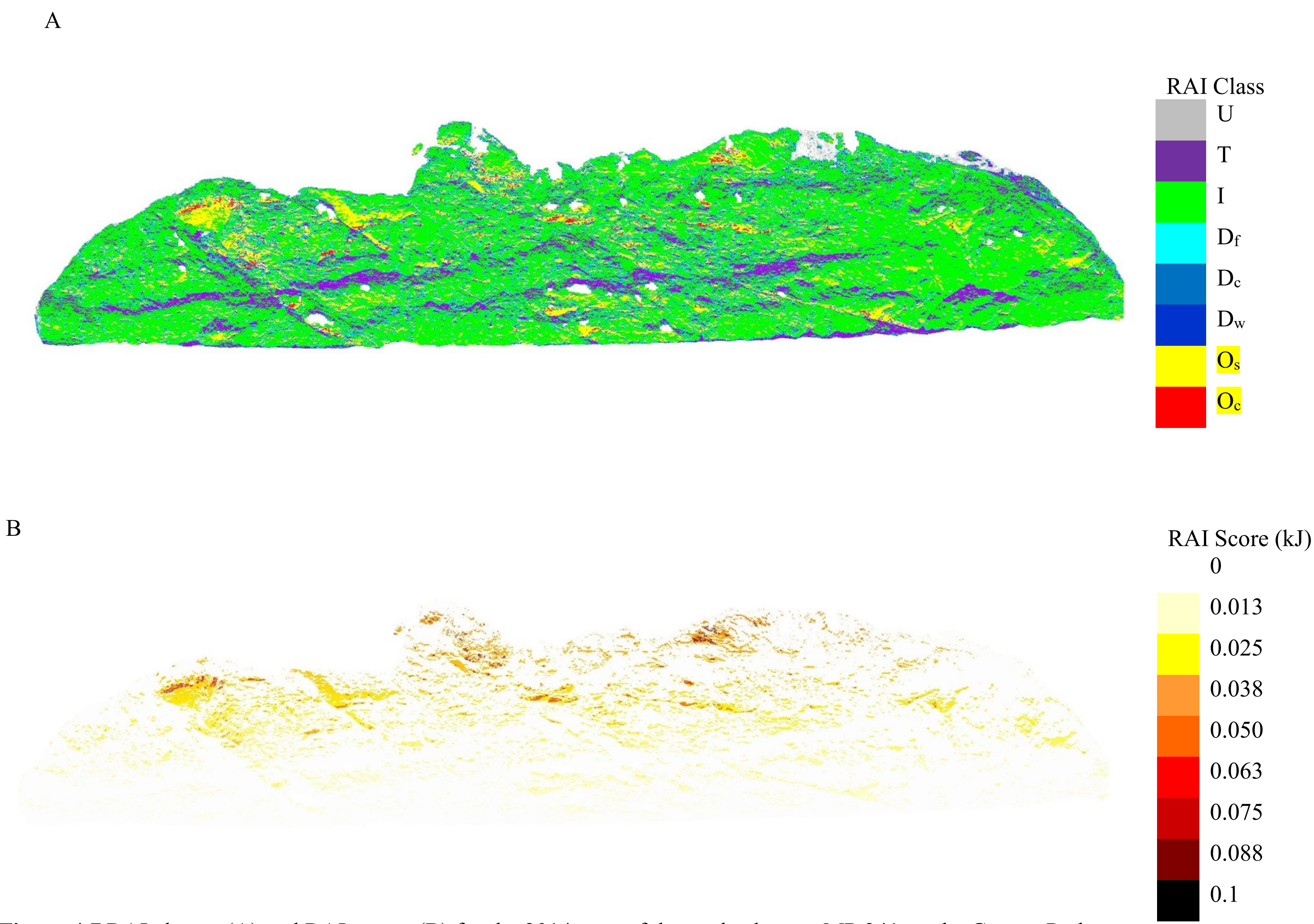

Figure 4.7 RAI classes (A) and RAI scores (B) for the 2014 scan of the study slope at MP 241 on the George Parks Highway near Glitter Gulch, Alaska.

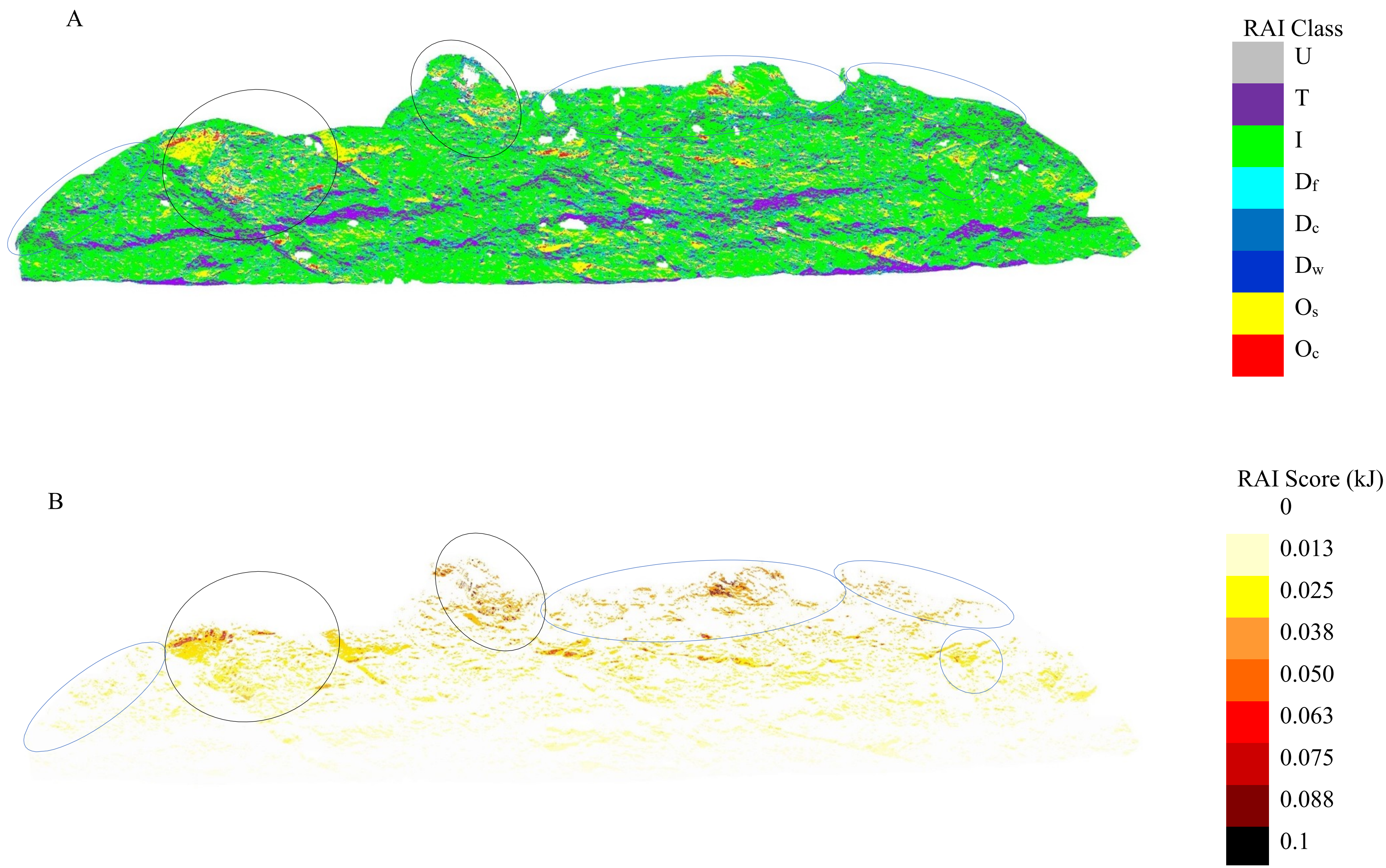

Figure 4.8 RAI classes (A) and RAI scores (B) for the 2015 scan of the study slope at MP 241 on the George Parks Highway near Glitter Gulch, Alaska. Planned mitigation areas are circled in blue for scaling and black for trim blasting.

4.4.1.5 2017 RAI Outputs

Point cloud density remained nearly constant between 2015 and 2017 (table 4.2). However, a large maintenance project in 2016 removed significant volumes of rock (predicted to be ~75,000 tons) and reshaped large portions of the slope (figures 4.8 and 4.9).

Morphology identification patterns followed those of 2013, and changes in overall volumes of each morphology type were fairly constant while local morphology re-classifications between 2015 and 2017 were significant (figure 4.9: A). The upper left region of the slope where the ~70-foot-wide wedge was removed was re-classified as mostly intact (from discontinuous and overhanging), with an underlying ledge of significant talus accumulation (from intact). The upper left region of the slope where the two significant protrusions were minimized and vegetation was removed increased in the extent of the mappable area, while data holes increased and significant portions of rock classified as intact were re-classified as discontinuous or talus. Over the remainder of the slope, volumes of rock classified as talus and intact decreased, while discontinuous and overhanging classification volumes increased significantly.

The hazard mapping identification patterns followed those indicated in 2013 and 2014, while the patterns of hazard changes followed that of the morphology changes (figure 4.9: B). The left third of the slope was downgraded in maximum hazard from 2015 significantly, but a larger percentage of the region was re-mapped as having some hazard potential. The remainder of the slope increased in overall hazard, with many new, small blocks (<2 ft) being mapped as high hazard, and the upper third of the slope nearly doubling in volume mapped as a moderate hazard (from zero).

4.4.1 6 2018 RAI Outputs

The point cloud density nearly doubled from 2016/2017 to 2018; 4 times the points of the first complete year, 2013 (table 4.2). The resolution did not appear to be significantly improved, however (figure 4.10).

Morphology identification patterns continued to follow those of 2013, while there did not appear to be a significant change in morphology classification (figure 4.10: A). The only notable changes in the morphology map were the sizes of data holes; some increased while others decreased. Also, the amount of rock classified as talus, downslope of the large wedge removed in 2016, increased while intact rock decreased.

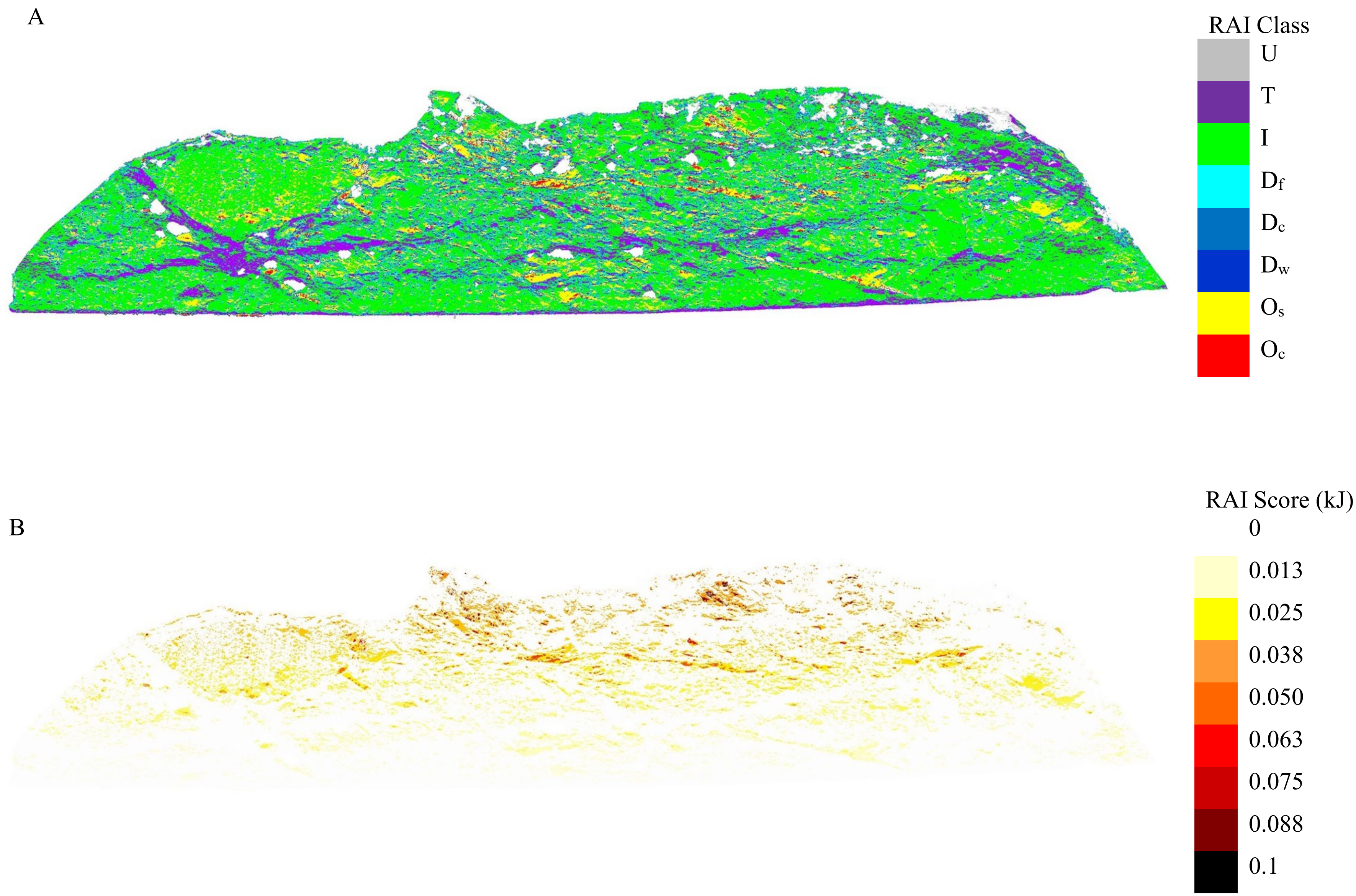

Figure 4.9 RAI classes (A) and RAI scores (B) for the 2017 scan of the study slope at MP 241 on the George Parks Highway near Glitter Gulch, Alaska.

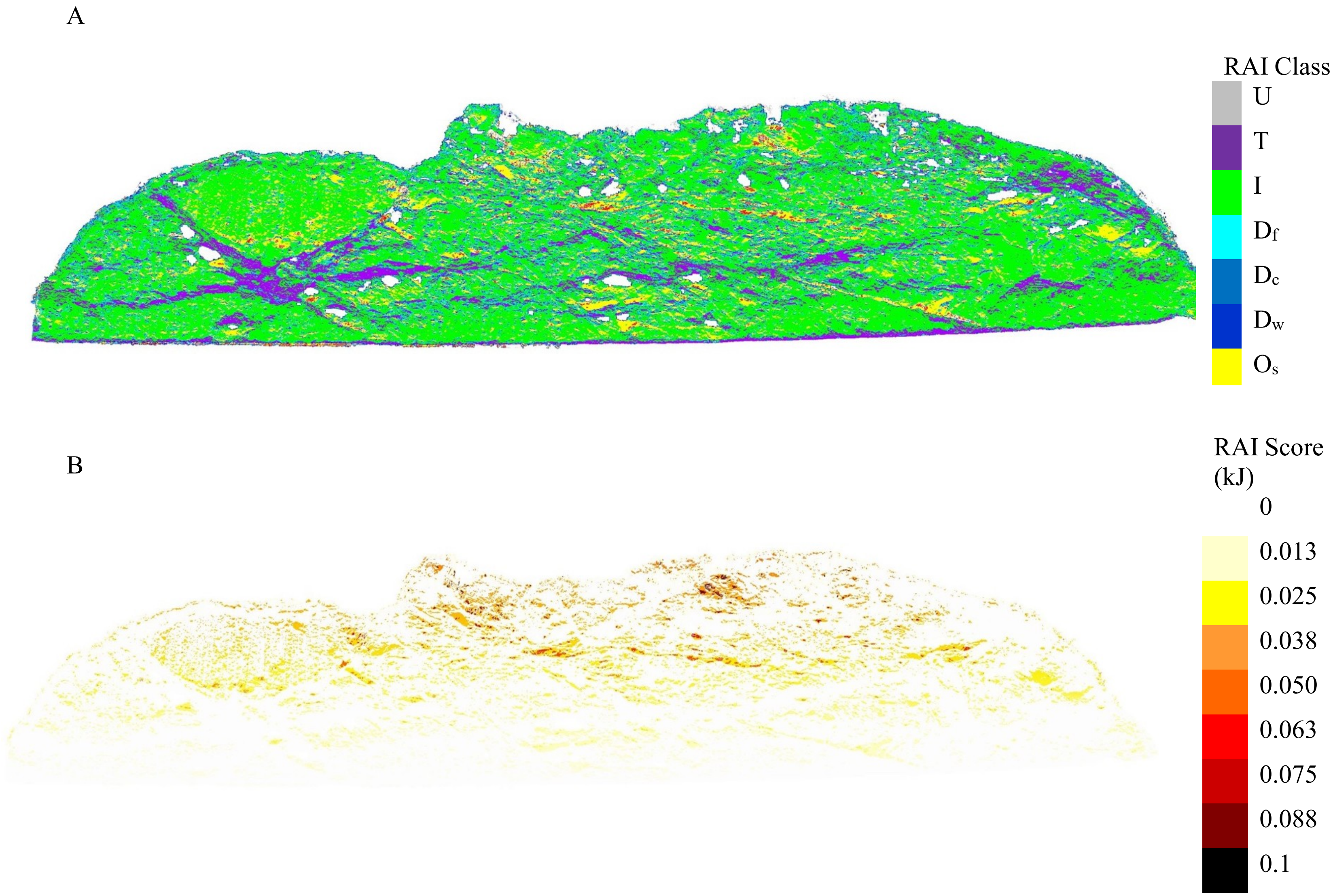

Figure 4.10 RAI classes (A) and RAI scores (B) for the 2018 scan of the study slope at MP 241 on the George Parks Highway near Glitter Gulch, Alaska.

The overall hazard as indicated by the RAI score appeared to remain fairly constant as well (figure 4.10: B). The only notable changes were an increase in rock mapped as moderate hazard near the knob at the upper-middle region of the slope.

4.4.2. Change Data

4.4.2.1 Epoch 1: 2012-2013

Even with significant hole filling because of the low resolution from the mobile scanner used to gather the 2012 data, change detection losses suggesting rock fall appeared in the expected areas by visual inspection as well as those identified as hazardous by the RAI Score (figure 4.11). Loss clusters followed expected areas of rock fall such as along major discontinuities, under overhangs, and in areas of talus accumulation. Each area identified as a high hazard or moderate hazard by the RAI score experienced a loss, at least partially. Significant losses lower in the slope were not identified on the RAI score map even though some were as high as 20 ft from the base of the slope. Unfortunately, poor resolution was greatest in critical areas such as the highest points of the slope. Nearly all gains were points that were absent (because of cropping) or were assigned an Unclassified morphology by the RAI software; very few, at the base of the slope, were classified as talus.

4.4.2.2 Epoch 2: 2013-2014

Similar to Epoch 1, there were expected areas of loss based on discontinuities and morphology types in the center of the image, but significant losses were identified in the left and right reaches of the scan as a result of a misalignment of the scans (figure 4.12). Gains at the upper reaches of the slope aligned with points that were assigned an Unclassified morphology by the RAI software in 2013 and were absent (because of cropping) in 2014; while gains at the base of the slope were classified as talus by the RAI software.

4.4.2.3 Epoch 3: 2014-2015 Epoch

Losses in this epoch followed the pattern of losses in the previous two; most of the clusters were in locations where there were discontinuities, overhangs, and ledges (figure 4.13). The perimeter showed extensive gains, and there were patches of gains mainly encircling data holes.

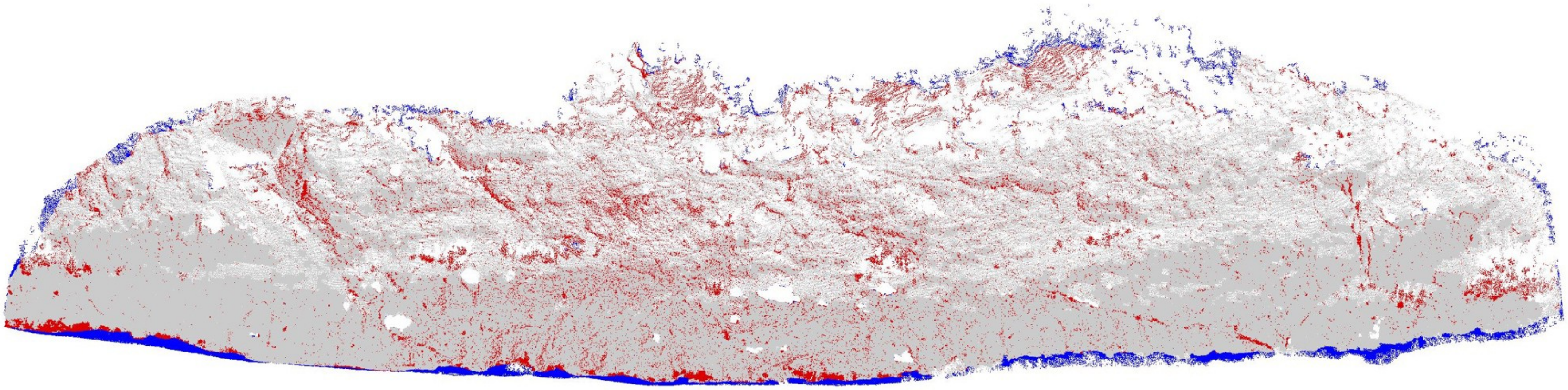

Figure 4.11 Map of the slope near MP 240.5 on the George Parks Highway in Denali, Alaska. The change data from August 2012 to August 2013 are highlighted, with red representing a loss and blue representing a gain. Gains around the perimeter may represent differences in cropping of the annual data. The map shows the change data overlying the point cloud in grey; the 2012 data were not colored RGB, so an overlay with a true color image was not generated.

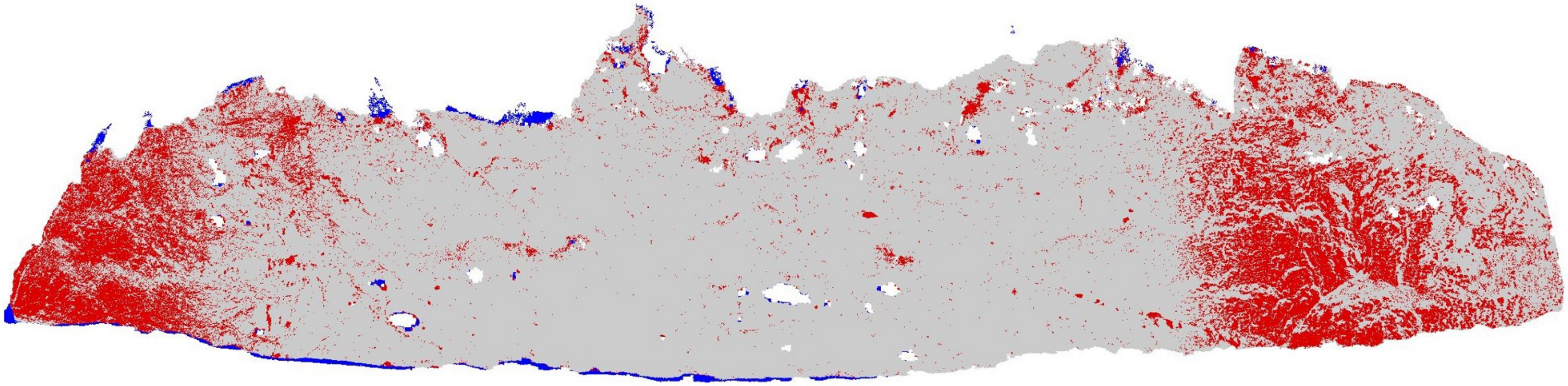

A

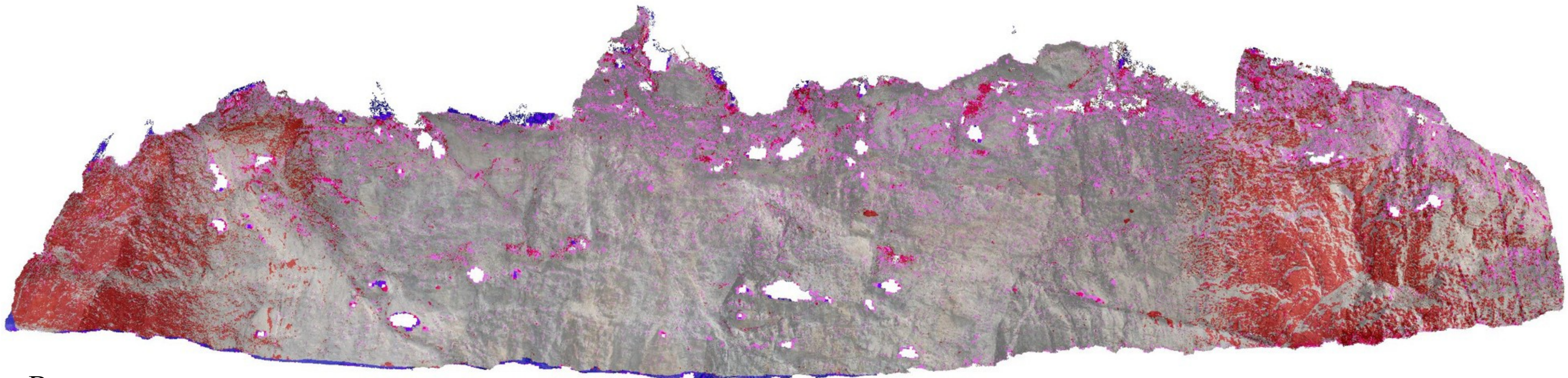

B

Figure 4.12 Map of the slope near MP 240.5 on the George Parks Highway in Denali, Alaska. The change data from August 2013 to August 2014 are highlighted, with red representing a loss and blue representing a gain. Gains around the perimeter may represent differences in cropping of the annual data. Map A shows the change data overlaying the point cloud in grey, while map B shows the change data overlaying a true color point cloud from 2013 data, with the points created during a hole-filling algorithm colored fuchsia.

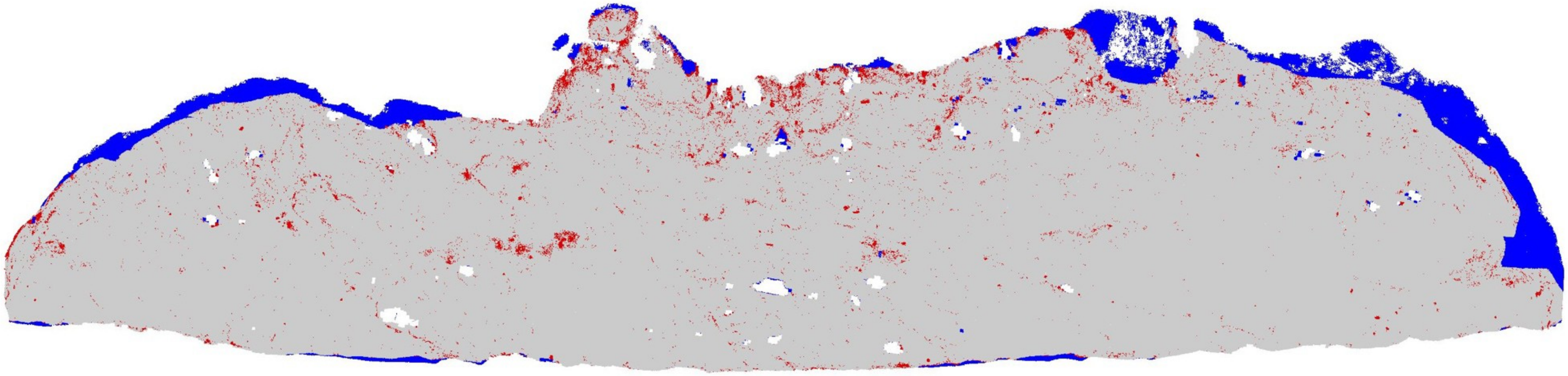

A

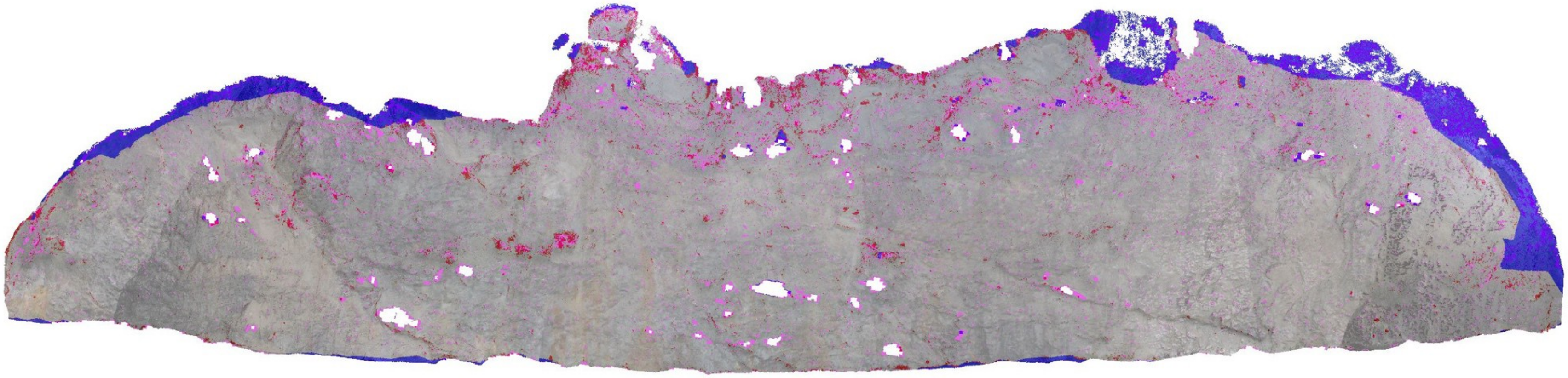

B

Figure 4.13 Map of the slope near MP 240.5 on the George Parks Highway in Denali, Alaska. The change data from August 2014 to August 2015 are highlighted, with red representing a loss and blue representing a gain. Gains around the perimeter may represent differences in cropping of the annual data. Map A shows the change data overlaying the point cloud in grey, while map B shows the change data overlaying a true color point cloud from 2014 data, with the points created during a hole-filling algorithm colored fuchsia.

4.4.2.4 Epoch 4: 2015-2017 Epoch

As expected, there were significant losses between these years (figure 4.14). The large overhanging wedge in the upper left was removed, as well the overhanging massive section in the upper right. Much of the remaining losses followed lesser overhangs identified as high and moderate hazard, and ledges with significant talus were classified. Unexpected were the significant patches of gains, not only encircling data holes but also appearing sporadically along the upper third of the slope, adjacent to significant losses.

4.4.2.5 Epoch 5: 2017-2018 Epoch

Although recently scaled (to an unknown extent), significant losses appeared around the perimeter of the large wedge that was removed on the upper left section of the slope and the discontinuities below, on the lower left (figure 4.15). Small losses were scattered across the slope face, with a slight concentration on the upper third of the slope and along the major discontinuities, particularly on the lower right side of the slope. There was a region of gains along the right edge of the slope and small patches of gains throughout, but typically where there were data holes.

4.5. Discussion

A significant hurdle in the analysis of rock fall with the RAI model in the study was the inconsistent quality of available data. The point cloud scan from 2012 was incomplete, while the 2013 scan and potentially the 2014 scan did not provide sufficient point density that could enable discussions of morphology change without significant resolution error. Additionally, limitations of the current RAI program did not allow for meaningful analysis of the metrics produced, such as volumes of morphology type and unique cell identifiers for morphology change assessment, without significant levels of programming ability and processing power.

The rock type of the studied slope did not lend itself well to a strong discussion about rockfall and the RAI model. The crystalline nature of the outcrop contributed less than ideal amounts of annual activity centered around local areas of high weathering such as on small ledges and along discontinuities; most trackable losses were likely talus or individual small blocks. The crystalline nature of the rock did, however, provide meaningful insight as to how poorly formed discontinuities on an intact face can begin to be identified by roughness.

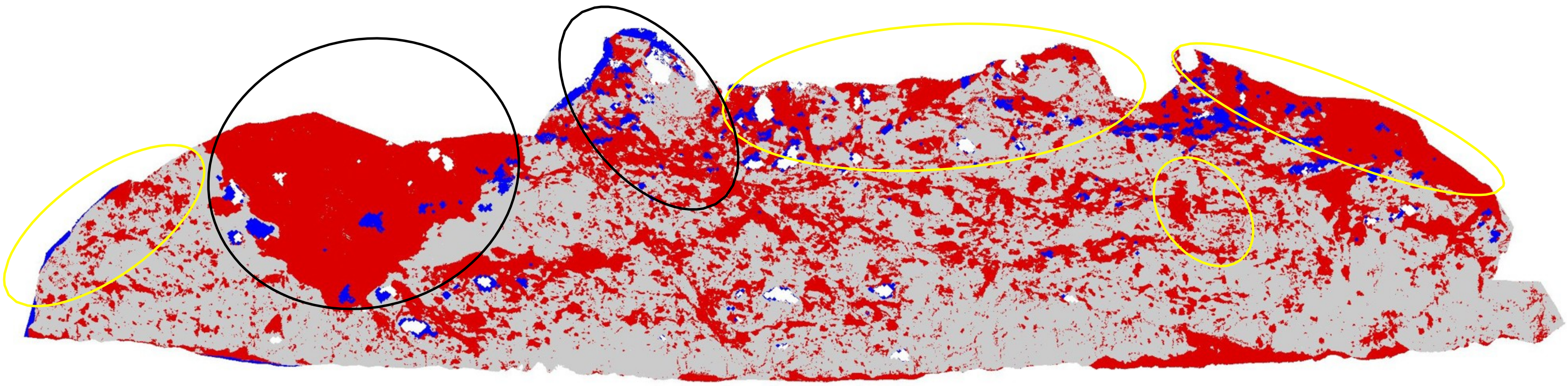

A

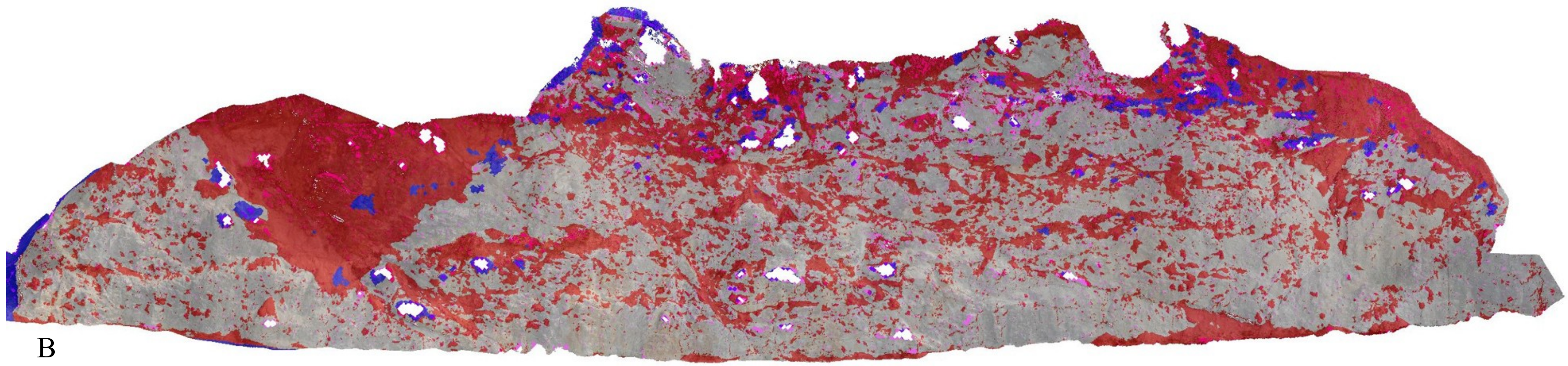

B

Figure 4.14 Map of the slope near MP 240.5 on the George Parks Highway in Denali, Alaska. The change data from August 2015 to August 2017 are highlighted, with red representing a loss and blue representing a gain; the large change is largely a result of a 2016 slope maintenance project in which scaling and trim-blasting were done on the slope in conjunction with re-paving of the highway. The planned areas for work during the project are circled, in yellow for scaling and black for trim blasting. Gains around the perimeter may represent differences in cropping of the annual data. Map A shows the change data overlaying the point cloud in grey, while map B shows the change data overlaying a true color point cloud from 2015 data, with the points created during a hole-filling algorithm colored fuchsia.

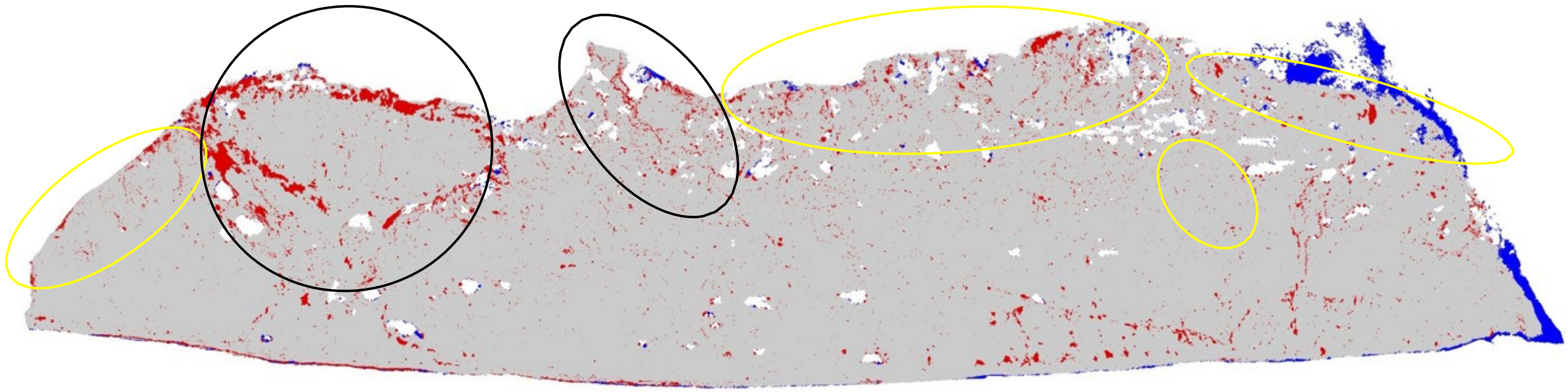

A

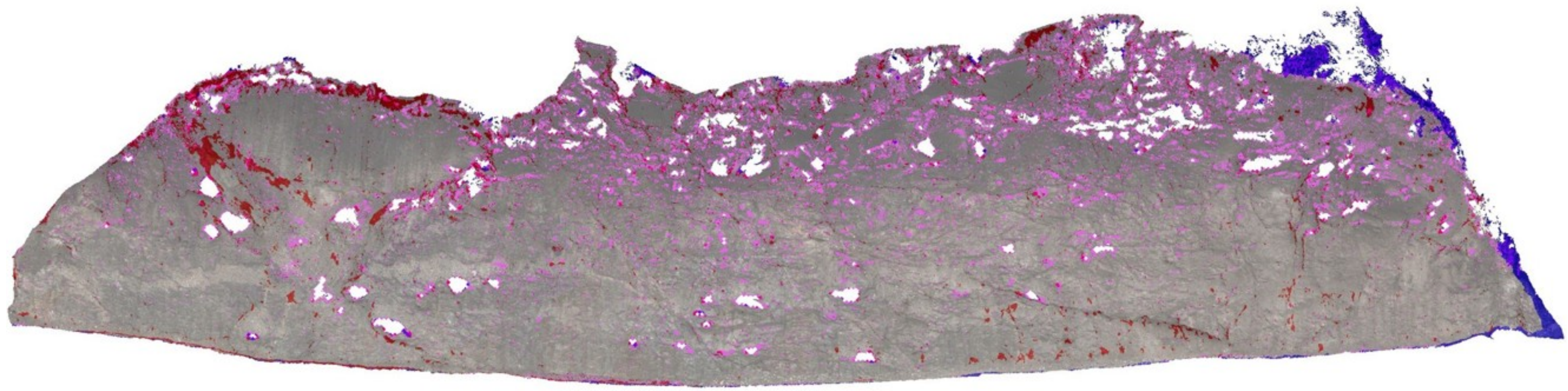

B

Figure 4.15 Map of the slope near MP 240.5 on the George Parks Highway in Denali, Alaska. The change data from August 2017 to August 2018 are highlighted, with red representing a loss and blue representing a gain. The planned areas for work during the 2016 maintenance project are circled, in yellow for scaling and black for trim blasting. Gains around the perimeter may represent differences in cropping of the annual data. Map A shows the change data overlaying the point cloud in grey, while map B shows the change data overlaying a true color point cloud from 2017 data, with the points created during a hole-filling algorithm colored fuchsia

Regardless, the overall pattern of rock fall over the five change epochs, with concessions for the resolution and misalignment errors, showed some consistency before the scaling and a less than remarkable decrease post-scaling (table 4.3). Decreased losses did occur in rock classified as higher hazard, such as widely spaced discontinuous and overhanging, but the post-scaling RAI maps highlighted that rockfall hazard from the slope did not decrease in the long term; the scaling contributed to the creation of more rock classified as overhanging.

According to the RAI model, much of the post-scaling rockfall was from talus and intact rock; these activity levels were consistent with pre-scaling levels. The significant amount of rockfall activity could be attributed to the slope attempting to reach a new equilibrium after large removals during maintenance or possibly to damage caused by the maintenance processes themselves.

Table 4.3 Annual rock fall activity data for the slope near MP 240.5 on the George Parks Highway in Denali, Alaska, from 2012 to 2018 as measured with the RAI software. Values are losses in m^3 as determined by the change detection algorithm.

	2012-2013	2013-2014	2014-2015	2015-2017*	2017-2018	Total Years
Total Loss	0.841714	1.23479	0.657163	2.863276	0.452263	5.849206
Unclassified	0.151848	0.172119	0.125202	0.757800	0.101206	1.408175
Talus	0.028666	0.048867	0.017831	0.377244	0.039587	0.512195
Intact	0.026467	0.142291	0.012279	0.398722	0.027942	0.607701
Widely-spaced Discontinuous	0.140732	0.146200	0.097521	0.508267	0.075471	0.928191
Closely-spaced Discontinuous	0.098417	0.139865	0.072456	0.455992	0.049123	0.785853
Fragmented Discontinuous	0.078136	0.130202	0.059889	0.455887	0.038691	0.732805
Steep Overhang	0.108764	0.196356	0.098499	0.909364	0.038145	1.301128
Cantilevered Overhang	0.208684	0.258890	0.023486	-1.00000	0.082098	-0.426842

*Survey was not conducted in 2016, due to a significant slope maintenance project where scaling and trim-blasting was done on the slope in conjunction with re-paving of the highway.

4.5.1. Excavation Damage

Because of a lack of a standard methodology for removing rock, scaling methods are not consistent; even the exact work done during the 2016 mitigation project represented here was unknown. Often large pry bars and air bags that are used to force rock loose can impart damage on the underlying "fresh" rock (Wyllie, 2017; Hook, 2007). In addition to direct damage to the surrounding rock, removal of key pieces that kept others locked in their position can passively damage the slope; the stress state on the remaining block(s) shifts from one of compression to tension, and the strength is greatly weakened (Hook, 2007). This was likely the case for the studied slope, as many more overhangs were present post-scaling.

4.5.2. Data Error

Errors (in the form of misidentification of change) arose because of variations in the 3-D surface created from the point cloud in subsequent years that were independent of any actual change in the geometry of the slope face. Alignment errors were significantly less than the chosen threshold for change, so any error present would be due to resolution or filtering. The most common cause of a misrepresented 3-D surface was vegetation that was incompletely removed being represented as part of the slope face; this could be partially corrected by a hole-filling algorithm but might still result in misidentification of slope failures, as outlined by Markus (2018) (Figure 4.5; 2018). Hole filling can be significant, even in a very dense and well-cleaned data set (Figure 4.16).

4.5.3. RAI Hazard

This model, while useful for quantifying rock fall hazards on a rock slope, enabling the ranking of slope hazard, failed to identify key risk factors that are incorporated into the more qualitative models that it is attempting to supersede, such as the Rockfall Hazard Rating System. While the RAI model may identify a slope as of the highest hazard, that slope may lie on a road with low traffic and a ditch wide enough to capture most or all of the presumed failures. Additionally, it fails to account for other types of failures, such as topples and slides, that may be a dominant failure mode for rock slopes with persistent failure planes parallel to the face.

An important phenomenon to take note of is that a surface, visually identifiable as one block or unit, may be delineated as multiple rock types by the RAI software because of a change in surface roughness. While this occurrence may appear to be an error, it can aid in identifying hazards by highlighting potential future failure planes (discontinuities) that are not visible to the naked eye. This also enables the geologically trained eye to pick out large blocks or wedges by noting the outline of such an object, created by the highlighting of rougher areas around the intact object. This could be enhanced by including a means to identify significant relief off of the slope face in the x and y planes in addition to the z-plane.

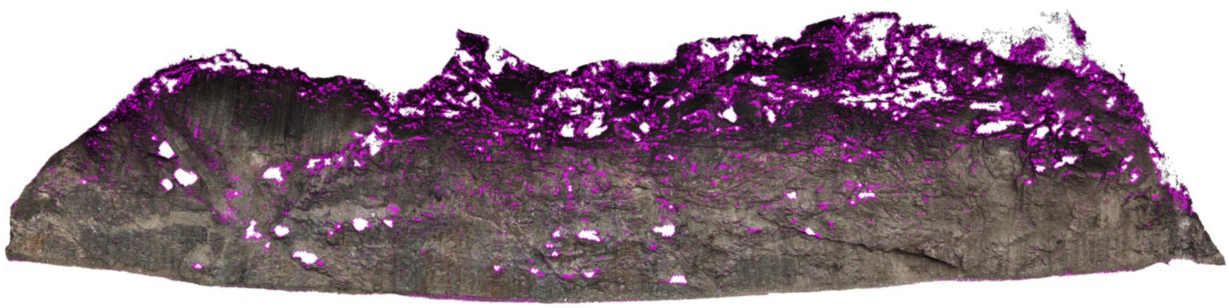

Figure 4.16 Point cloud generation of the 2018 study slope with hole filling outputs colored fuchsia.

CHAPTER 5. SUMMARY OF CHAPTERS' CONCLUSIONS

Ensuring mobility through critical transportation corridors is essential for community well-being, resilience, commerce, and tourism. Unfortunately, sustaining mobility is a significant challenge in the scenic, yet rugged Pacific Northwest. This dynamic setting means that transportation infrastructure essential for economic activity and community well-being traverse unstable terrain and is frequently subject to closures or reduced mobility from geohazards such as landslides, rockfall, debris flows, or slope instability because of thawing permafrost. Besides closure of important transportation systems, the consequences of landslide events routinely include injuries, property losses, and infrastructure damage. These consequences have critical implications for mobility, safety, and supply chain logistics. During this time, motorists and freight traffic are required to utilize limited, significantly lengthier alternative routes, which quickly become congested with increased traffic levels that are beyond their capacity to safely and efficiently navigate. Moreover, mitigation, maintenance, or repair can take weeks to months to complete, resulting in either complete loss of that section of highway or a loss of capacity during those activities. In our research, we developed a practical, data-driven framework for assessing the impacts of rockfall and debris slides on highway mobility to provide transportation planners, engineers, and managers with tools to make better-informed, quantitative decisions regarding mitigation and potential closures for repairs and maintenance. The Rockfall Impacts on Mobility (RIM) geospatial database can be utilized to develop original fragility curves that relate rockfall and debris volumes to closure times within an integrated framework that builds upon the existing Rockfall Activity Index (RAI) developed through PacTrans. This database is being developed through Web-based data mining.

The RIM database developed in this research provides several unique opportunities to understand how rockfalls and landslides affect the highway network. Example applications include the following:

- Determine economic costs associated with debris removal, repairs, and closures from rockfalls and landslides.
- Identify routes most vulnerable to closures because of landslides and rockfalls.
- Assess the effectiveness of slope mitigation techniques by identifying areas prone to repeat failures.

The database has some limitations that could benefit from additional documentation by transportation agencies. Most records indicate only whether the road was fully closed or open. Having detailed information on how long each lane and each direction was closed would be useful for developing more robust models that are based on capacity rather than on road closure. Also, future databases could consider other factors in addition to volume, such as soil type, predominate block size, and location (e.g., proximity to DOT maintenance crews) to better refine the model to predict closure time.

Analysis of the 2016 scaling mitigation indicated that rockfall activity was reduced by approximately 50 percent in the years immediately following the project. This analysis, which focused on the Glitter Gulch study site, also showed that based on rockfall activity over these years, the RAI score was useful in identifying hazardous areas. For each change epoch, the significant losses on the slope were identified by the RAI score as being of at least moderate hazard. However, significant sized failures are not scaled accordingly; there should be some metric that clumps potential failures into clusters that could have a higher rating. Specific conclusions from evaluation of rockfall mitigation efforts include the following:

- Efficacy of scaling: The low number of change epochs, limited rock type variability, and singular site of this study limited the ability to make global conclusions about the validity of scaling on unstable rock slopes. However, even with allowances for systematic errors that could be easily identified, rockfall activity was reduced by approximately 50 percent in the years immediately following the extensive maintenance project. The cost of this project, as well as the ongoing costs associated with ditch and road maintenance, should be considered; these expenses may be significant in comparison with cost of a more extensive and long-term stabilization project.
- Effectiveness of the RAI: Although this was a different rock type than the RAI classification scheme was designed for, morphologies on the slope face were well mapped. The massive, crystalline phyllite-schist was not considered poor quality in this outcrop and failed differently than a less crystalline domain. Regardless, techniques similar to a visual slope classification, such as looking for intact portions surrounded by significant relief (overhangs), could identify large blocks. While this would eliminate some of the automation, the RAI classification would still be valuable in mapping morphology for hard to see and dangerous slope sections. According to rock fall activity

over these years, the RAI score was effective at identifying hazardous areas. For each change epoch, the significant losses on the slope were identified by the RAI score as being of at least moderate hazard. However, significant sized failures were not scaled accordingly; there should be a metric that clumps potential failures into clusters that could have a higher rating. An issue for further consideration is that failure planes parallel to the slope face or that daylight infrequently can lead to some of the most catastrophic failures but are not explicitly highlighted by the RAI score. It would be prudent for emergency and infrastructure managers and planners to use a combination method, the RAI model as well as geologic assessment, for complete slope analysis.

REFERENCES

Andrew, R.D., and Pierson, L.A., (2012). Stabilization of Rockfall in Turner, K. A., Schuster, R. L., eds., Rockfall: Characterization and Control: Washington, D.C., Transportation Research Board, p. 468-492.

Basahel, H., and Mitri, H., 2017, Application of rock mass classification systems to rock slope stability assessment: A case study: Journal of Rock Mechanics and Geotechnical Engineering, v. 9, no. 6, p. 993-1009.

Cole, D., 2016, Rock climbers put their skills to work improving highway safety near Denali Park: https://www.adn.com/business-economy/energy/2016/06/25/denali-climbers-chip-away- at-crumbling-rock-walls-as-summer-traffic-flows-by-100-feet-below/ (accessed August 2018).

Dunham, L., Wartman, J., **Olsen, M.J.,** O'Banion, M.S*, & Cunningham, K. (2017). "Rockfall Activity Index (RAI): A Lidar-derived, morphology-based hazard assessment system," *Engineering Geology,* 221, 184-192**.** https://doi.org/10.1016/j.enggeo.2017.03.009

Eberhart-Phillips, D., Christensen, D., Brocher, T., Hansen, R., Ruppert, N., Haeussler, P., and Abers, G., 2006, Imaging the transition from Aleutian subduction to Yakutat collision in central Alaska, with local earthquakes and active source data: Journal of Geophysical Research: Solid Earth, v. 111, 31p.

Falkowski, S., Enkelmann, E., Drost, K., Pfänder, J. A., Stübner, K., and Ehlers, T. A.,2016, Cooling history of the St. Elias syntaxis, southeast Alaska, revealed by geochronology and thermochronology of cobble-sized glacial detritus: Tectonics, v. 35, p. 447–468.

Gigli, G., Morelli, S., Fornera, S., and Casagli, N., 2014, Terrestrial laser scanner and geomechanical surveys for the rapid evaluation of rock fall susceptibility scenarios: Landslides, v. 11, no. 1, p. 1-14.

Hook, E., 2007, Practical Rock Engineering: https://www.rocscience.com/learning/hoeks-corner/course-notes-books (accessed June 2018).

Kromer, R. A., Hutchinson, D. J., Lato, M. J., Gauthier, D., and Edwards, T., 2015, Identifying rock slope failure precursors using LiDAR for transportation corridor hazard management: Engineering Geology, v. 195, no. 3, p. 93-103.

Lato, M., Diederichs, J., Hutchinson, M., and Harrap, S., 2012, Evaluating roadside rockmasses for rockfall hazards using LiDAR data: Optimizing data collection and processing protocols: Natural Hazards, v. 60, no. 3, p. 831-864.

Markus, S., 2018, Morphological Evolution of Rock-Slopes and Assessing the Rockfall Activity Index (RAI) Methodology: University of Washington, 135 p.

Matasci, B., Stock, G. M., Jaboyedoff, M., Carrea, D., Collins, B. D., Guérin, A., Matasci, G., Ravanel, L., 2018, Assessing rockfall susceptibility in steep and overhanging slopes using three-dimensional analysis of failure mechanisms: Landslides, v. 15, no. 5, p. 859–878.Olsen, M.J., Johnstone, E., Driscoll, N., Ashford, S.A., & Kuester, F., (2009). "Terrestrial laser scanning of extended cliff sections in dynamic environments: a parameter analysis," Journal of Surveying Engineering, ASCE, 135(4), 161-169. http://dx.doi.org/10.1061/(ASCE)0733-9453(2009)135:4(161)

Olsen, M.J., Johnstone, E., Kuester, F., Ashford, S.A., & Driscoll, N. (2011). "New automated point-cloud alignment for ground based lidar data of long coastal sections," Journal of Surveying Engineering, ASCE, 137(1), 14-25. http://dx.doi.org/10.1061/(ASCE)SU.1943-5428.0000030

Olsen, M.J., Wartman, J., McAlister, M., Mahmoudabadhi, H., O'Banion, M.S., Dunham, L., and Cunningham, K., (2015). "To fill or not to fill: Sensitivity analysis of the influence of resolution and hole filling on point cloud surface modeling and individual rockfall event detection." Remote Sensing, Special Issue- Use of lidar and 3D point clouds in geohazards, 79(9),12103-12134. doi:10.3390/rs70912103

Olsen, M.J. (2020). RAMBO software.

Pierson, L.A., 2012, Rockfall Hazard Rating Systems in Turner, K. A., Schuster, R. L., eds., Rockfall: Characterization and Control: Washington, D.C., Transportation Research Board, p. 56-71.

Pierson, L.A., and Turner, K. A., 2012, Implementation of Rock Slope Management Systems in Turner, K. A., Schuster, R. L., eds., Rockfall: Characterization and Control: Washington, D.C., Transportation Research Board, p. 72-110.

Pierson, L.A., and Vierling, M. P., 2012, Mitigation Selection in Turner, K. A., Schuster, R. L., eds., Rockfall: Characterization and Control: Washington, D.C., Transportation Research Board, p. 445-456.Stead, D., and Wolter, A., 2015, A critical review of rock slope failure mechanisms: The importance of structural geology: Journal of Structural Geology, v. 74, p. 1-23.

Wahrhaftig, C., 1968, Schists of the Central Alaska Range: U.S. Geological Survey, Bulletin 1254, 22 p.

Wahrhaftig, C., and Black, R. F., 1958, Quaternary geology of the Nenana River valley and adjacent parts of the Alaska Range; Engineering geology along part of the Alaska Railroad: U.S. Geological Survey, Professional Paper 293, 118 p.

Wilson, F.H., Hults, C.P., Mull, C.G, and Karl, S.M, comps., 2015, Geologic map of Alaska: U.S. Geological Survey Scientific Investigations Map 3340, pamphlet 196 p., 2 sheets, scale 1:1,584,000, http://dx.doi.org/10.3133/sim3340.

Wyllie, D.C., 2015, Rock Fall Engineering: Boca Raton, CRC Press/Taylor & Francis Group, 243p.

Wyllie, D.C., 2017, Rock Slope Engineering: Civil Applications Fifth Edition: Boca Raton, CRC Press/Taylor & Francis Group, 620p.

BIBLIOGRAPHY

ACCAP (2016). Alaska Center for Climate Assessment and Policy, https://accap.uaf.edu/

Alaska Dispatch News (2016) Rock climbers put their skills to work improving highway safety near Denali Park, http://www.adn.com/business-economy/energy/2016/06/25/denali-climbers-chip-away-at-crumbling-rock-walls-as-summer-traffic-flows-by-100-feet-below/

Alaska Dispatch News (2016) Rock climbers put their skills to work improving highway safety near Denali Park, http://www.adn.com/business-economy/energy/2016/06/25/denali-climbers-chip-away-at-crumbling-rock-walls-as-summer-traffic-flows-by-100-feet-below/

Alaska Department of Transportation (2020). Geotechnical Asset Management Database Viewer. https://akdot.maps.arcgis.com/apps/MapSeries/index.html?appid=0be74f9ba168424eac48983da02e0250

Al-Rawabdeh, A., He, F., Moussa, A., El-Sheimy, N., Habib, A. (2016). Using an Unmanned Aerial Vehicle-Based Digital Imaging System to Derive a 3D Point Cloud for Landslide Scarp Recognition. Remote Sensing. 8, 95. DOI:10.3390/rs8020095.

Badger, T.C. and Lowell, S. 1992. Rockfall Control Washington State. In Rockfall Prediction and Control and Landslide Case Histories, Transportation Research Record, National Research Council, Washington, No 1342, 14-19.

Badger, T.C. and Lowell, S. 1992. Rockfall Control Washington State. In Rockfall Prediction and Control and Landslide Case Histories, Transportation Research Record, National Research Council, Washington, No 1342, 14-19.

Badger, T.C. and Lowell, S. 1992. Rockfall Control Washington State. In Rockfall Prediction and Control and Landslide Case Histories, Transportation Research Record, National Research Council, Washington, No 1342, 14-19.

Barlow, J., Lim, M., Rosser, N., Petley, D., Brain, M., Norman, E., Geer, M. (2012) Modeling cliff erosion using negative power law scaling of rockfalls, Geomorphology, Volumes 139–140, 15 February 2012, Pages 416–424.

Barlow, J., Lim, M., Rosser, N., Petley, D., Brain, M., Norman, E., Geer, M. (2012) Modeling cliff erosion using negative power law scaling of rockfalls, Geomorphology, Volumes 139–140, 15 February 2012, Pages 416–424.

Belowich, M., "Matanuska Coal Field. Field Guide, Anchorage Alaska," Alaska Geological Society, 2006.

Budetta P, Nappi, M (2013) Comparison between qualitative rockfall risk rating systems for a road affected by high traffic intensity, Nat. Hazards Earth Syst. Sci., 13:1643-1653, doi:10.5194/nhess-13-1643-2013

Budetta P, Nappi, M (2013) Comparison between qualitative rockfall risk rating systems for a road affected by high traffic intensity, Nat. Hazards Earth Syst. Sci., 13:1643-1653, doi:10.5194/nhess-13-1643-2013

Burns, W. J., & Madin, I. (2009). Protocol for inventory mapping of landslide deposits from light detection and ranging (LiDAR) imagery. Oregon Department of Geology and Mineral Industries.

CloudCompare (version 2.7.0) [GPL software]. (2016) Retrieved from http://cloudcompare.org/

Connor, B. and Harper, J. (2013). How Vulnerable Is Alaska's Transportation to Climate Change? Managing an Infrastructure Built on Permafrost.

Cunningham, K. and Krynicki, A. (2013). Oblique vegetation classification and removal from terrestrial laser scanning point clouds. UAF Invention Disclosure.

Cunningham, K., Hatfield, M., and Philemonoff, R. "Unmanned Aircraft Systems in Alaska Civil Research," Offshore Technology Conference, 2014.

Cunningham, K., Olsen, M., Wartman, J., Dunham, L., and Stuedlein, A. 2015. A Platform for Proactive Risk-Based Slope Asset Management – Phase II. PacTrans Final Report

Curry, J. (2018). Personal Communication.

Dunham, L. (2015) "Rock-slope activity index (RAI): A Lidar-derived process based rock-slope assessment system," M.S. thesis, Univ. of Washington.

Eltner, A., A. Kaiser, C. Castillo, G. Rock, F. Neugirg, and A. Abellán, "Image-based surface reconstruction in geomorphometry - merits, limits and developments," *Earth Surf. Dyn.*, vol. 4, no. 2, pp. 359–389, May 2016.

Fassi, F., L. Fregonese, S. Ackermann, and V. D. Troia, "Comparison between Laser Scanning and Automated 3D Modelling Techniques to Reconstruct Complex and Extensive Cultural Heritage Areas," *ISPRS - Int. Arch. Photogramm. Remote Sens. Spat. Inf. Sci.*, vol. XL-5-W1, pp. 73–80, Feb. 2013.

Fernandez, T., Perez, J.L., Cardenal, F.J., Lopez, A., Gomez, J.M., Colomo, C., Delgado, J., Sanchez, M. (2015) Use of a Light UAV and Photogrammetric Techniques to Study the Evolution of a Landslide in Jaen (Southern Spain). ISPRS – Int. Arch. Photogramm. Rem. Sens., XL-3/W3, 241-248, DOI:10.5194/isprsarchives-XL-3-W3-241-2015.

Fernandez, T., Perez, J.L., Cardenal, J., Gomez, J.M., Colomo, C., Delgado, J. (2013). Analysis of Landslide Evolution Affecting Olive Groves Using UAV and Photogrammetric Techniques. Remote Sensing. 8, 837. DOI:10.3390/rs8100837.

FHWA (2016) Geohazards, Climate Change, and Extreme Weather Events – Synthesis Report.

Greenwood, W., Zekkos, D., Lynch J., Bateman, J., Clark, M.K., Chamlagain, D. (2016). UAV-Based 3-D Characterization of Rock Masses and Rock Slides in Nepal. 50th US Rock Mechanics/Geomechanics Symposium, Houstion, Texas, 26-29 June 2016.

Hicks, D.L., 1995. A way to estimate the frequency of rainfall-induced mass movement. Journal of Hydrology (New Zealand) 33 (1), 59–67.

http://idav.ucdavis.edu/~okreylos/ResDev/LowCostVR/index.html (Dec. 15, 2016)

Jaboyedoff, M., Oppikofer, T, Abellan, A., Derron, M.H., Loye, A., Metzger, R., Pedrazzini, A. 2010."Use of LiDAR in landslide investigations: a review," *Natural Hazards*.

Juang CS, Stanley TA, and Kirschbaum DB (2019) Using citizen science to expand the global map of landslides: Introducing the Cooperative Open Online Landslide Repository (COOLR). PLOS ONE 14(7): e0218657. doi:10.1371/journal.pone.0218657

Keeney, J.T., (2016). "Using Unmanned Aerial Systems (UAS) and Photogrammetry to Remotely Assess Landslide Events in Near Real-Time". M.S. Thesis, University of Kentucky.

Kemeny, J., and Turner, A.K., (2008) "Ground-based LiDAR Rock slope mapping and assessment," Publication No. FHWA-CFL/TD-08-006.

Kemeny, J., Norton, B., Handy, J., and Donovan, J. (2008). "Three-dimensional digital imaging for the identification, evaluation and management of unstable highway slopes," Final Report for Highway IDEA project 119, TRB NAS.

Kirschbaum, D.B., Stanley, T., & Zhou, Y. (2015). Spatial and temporal analysis of a global landslide catalog. Geomorphology, 249, 4-15. doi:10.1016/j.geomorph.2015.03.016

Kirschbaum, D.B., Adler, R., Hong, Y., Hill, S., & Lerner-Lam, A. (2010). A global landslide catalog for hazard applications: method, results, and limitations. Natural Hazards, 52, 561-575. doi:10.1007/s11069-009-9401-4

Larsen, P.H., et al., Estimating future costs for Alaska public infrastructure at risk from climate change. Global Environmental Change (2008), doi: 10.1016/j.gloenvcha.2008.03.005

Lucieer, A., de Jong, S., Turner, D. (2013). Mapping landslide displacements using Structure from Motion (SfM) and image correlation of multi-temporal UAV photography. Prog. Phys. Geog. 38, 1-20, DOI:10.1177/0309133313515293.

Manousakis, J., Zekkos, D., Saroglou, H., Clark, M. (2016). Comparison of UAV-Enabled Photogrammetry-Based 3D Point Clouds and Interpolated DSMs of Sloping Terrain for Rockfall Hazard Analysis. 11th 3D Geoinfo Conference, Athens, Greece, 20-21 October 2016

Marohl, k. (2019) "Using the Rockfall Activity Index to assess the impact of scaling on rock fall activity at Glitter Gulch, Alaska," MESSAGe Technical Report Number 079, Department of Earth and Space Sciences, University of Washington.

Mason, D., Brabhaharan, P. & Saul, G. (2017) Performance of road networks in the 2016 Kaikōura earthquake: Observations on ground damage and outage effects. Proc. 20th NZGS Geotechnical Symposium. Eds. GJ Alexander & CY Chin.

Metzger, A., Cunningham, K., Olsen, M., Wartman, J., Dunham, L., and Stuedlein, A. 2014. A Platform for Proactive Risk-Based Slope Asset Management – Phase I. PacTrans Final Report

Mohamed, K. (2016). "Geohazards, Climate Change, And Extreme Weather Events—Peer Exchange Report."

Mohamed, K. (2016). "Geohazards, Climate Change, And Extreme Weather Events—

Murphy, R.R., Duncan, B.A., Collins, T., Kendricks, J., Lohman, P., Palmer, T., Sanborn, F. (2015) Use of a small unmanned aerial system for the SR-530 mudslide incident near Oso, Washington. J. of Field Robotics. DOI: 10.1002/rob.21586.

Nat. Acad. of Sci. (2016), Attribution of Extreme Weather Events in the Context of Climate Change.

NASA (2020). Landslide inventory. https://maps.nccs.nasa.gov/arcgis/apps/webappviewer/index.html?id=824ea5864ec8423fb985b33ee6bc05b7

National Climate Assessment (2016). Retrieved July 06, 2016, from http://nca2014.globalchange.gov/highlights/regions/alaska.

NGS (2016). "OPUS: the Online Positioning User Service, process your GNSS data in the National Spatial Reference System." [Online]. Available: https://www.ngs.noaa.gov/OPUS/. [Accessed: 17-Nov-2016].

Nicolson, D. T. 2005. Hazard assessment for progressive, weathering-related breakdown of excavated rockslopes. Quarterly Journal of Engineering Geology and Hydrogeology, 37, 327–346.

Niethammer, U., James, M.R., Rothmund, S., Travelletti, J., Joswig, M. (2012). UAV-based remote sensing of the Super-Sauze landslide: evaluation and results. Engineering Geology. 128: 2-11.

NRC (2003) Partnerships for Reducing Landslide Risk, National Academies Press, Washington, DC.

O’Banion, M., Allahyari, M., Olsen, M.J., “Comparison of Terrestrial Lidar and Structure from Motion Techniques for Assessment of Unstable Rock Slopes in Alaska“ 2016 Oregon State University College of Engineering Graduate Research Expo, Portland, OR. 2016

O'Banion, M., Olsen, M., Rault, C., Wartman, J., and Cunningham, K. (2018) Suitability of structure from motion for rock-slope assessment, The Photogrammetric Record, 33, pp 217-242

Occhiena, C., and Pirulli, M. (2012), "Analysis of Climatic Influences on Slope Microseismic Activity and Rockfalls: Case Study of the Matternhorn Peak (Northwestern Alps)," Journal of Geotechnical and Geoenvironmental Engineering, American Society of Civil Engineers, vol. 138, issue 8, pp. 1012-1021.

Olsen, M.J., Butcher, S., and Silvia, E.P., (2012). Real-time change and damage detection of landslides and other earth movements threatening public infrastructure, OTREC Final Report 2011-22 and ODOT Final Report RS 500-500, 80p.

Olsen, M.J.; Roe, G.V.; Glennie, C.; Persi, F.; Reedy, M.; Hurwitz, D.; Williams, K.; Tuss, H.; Squellati, A.; Knodler, M. *Guidelines for the Use of Mobile LiDAR in Transportation Applications*; TRB NCHRP Final Report 748; Publisher: TRB Washington, DC, 2013.

Petley (2012) Global patterns of loss of life from landslides, Geology, doi.org/10.1130/G33217.1

Pierson, L. A. (1991). Rockfall Hazard Rating System. Washington, DC: Federal Highway Administration.

Scott, P. (2016) How climate change affects extreme weather events, Science, 352, p. 1517

Silvia, E.P., and M. J. Olsen, “To Level or Not to Level: Laser Scanner Inclination Sensor Stability and Application,” *J. Surv. Eng.*, Nov. 2011.

SNAP (2016) Dynamical downscaling techniques yield new understandings and attention, https://csc.alaska.edu/research-highlights/dynamical-downscaling-techniques-yield-new-understandings-and-attention

Transportation Research Board (2012) Rockfall: Characterization and Control, Nat. Acad. Press.

Trop, J. M., R. B. Cole, D. Sunderlin, C. Hults, and E. Todd, “Bedrock geology of the Glenn Highway from Anchorage to Sheep Mountain, Alaska,” pp. 1–46, 2015.

Turner, A.K., Kemeny, J., Slob, S., and Hack R., (2006). “Evaluation and management of unstable rock slopes by 3-d laser scanning,” Proceedings of IAEG2006.

Turner, D., Lucieer, A., de Jong, S. (2015). Time Series Analysis of Landslide Dynamics Using an Unmanned Aerial Vehicle (UAV). Remote Sensing. 7, 1736-1757, DOI:10.3390/rs70201736.

USGS (1999) Map Showing Inventory and Regional Susceptibility for Holocene Debris Flows, and Related Fast-Moving Landslides in the Conterminous United States, Misc. Field Studies Map 2329.

Washington DNR. Landslides | WA - DNR. (2016). Retrieved July 06, 2016, from http://www.dnr.wa.gov/programs-and-services/geology/geologic-hazards/landslides.

APPENDIX A: ROCKFALLS IN THE NEWS

This appendix contains example rockfalls recorded in media articles. They were found by using Google alerts with the following keywords: landslide, rockfall, rock fall, road close, road closed, road closure. News articles were from November 2018 to July 2020. All articles accessed were confirmed on July 14, 2020

Table A.1 Example media articles on rockfall

Date	Location	Title	Link
July 7, 2020	Idaho	Stability of Rockslide being studied	https://lmtribune.com/northwest/stability-of-rockslide-being-studied/article_39bb68a1-b998-5588-95d5-bbf182b7b478.html
March 11, 2020	Australia	Storm damage repairs on Kempsey Road	https://www.miragenews.com/storm-damage-repairs-on-kempsey-road/
March 10, 2020	West Virginia	More needs to be done to make roads safer from rock falls	https://www.wvnews.com/theet/opinion/more-needs-to-be-done-to-make-roads-safer-from/article_c05bd191-f27e-50ad-ba62-74ca8328e3e6.html
March 9, 2020	Australia	Jenolan Caves Road remains shut . . . after severe damage. .	https://www.canberratimes.com.au/story/6668116/26-rock-falls-581-burnt-trees-why-part-of-nsws-jenolan-caves-road-remains-shut/?cs=14231
March 7, 2020	United Kingdom	Huge new rock falls in latest Devon red cliff landslides	https://www.devonlive.com/news/devon-news/huge-new-rock-falls-latest-3912210
March 6, 2020	Australia	26 rock falls . . .Jenolan Caves road remains shut	https://www.westernadvocate.com.au/story/6666726/26-rock-falls-581-burnt-trees-why-part-of-jenolan-caves-road-remains-shut/
February 28, 2020	Australia	Bega District Letters to the editor	https://www.begadistrictnews.com.au/story/6653134/letters-reliable-roads-critical-to-coasts-future/
February 26, 2020	Alaska	Denali Park Road Closures . . .	https://www.webcenterfairbanks.com/content/news/Denali-Park-Road-closures-raise-tourism-concerns-in-Alaska-568181041.html
February 25, 2020	Alaska	Denali National Park road closure . . .	https://www.usatoday.com/story/travel/experience/america/national-parks/2020/02/24/denali-national-park-road-closure-raises-alaska-tourism-concerns/4857441002/

February 21, 2020	United Kingdom	Worcestershire faced with disruption. . .	https://www.herefordtimes.com/news/regional/18251494.worcestershire-faced-disruption-following-floods/
February 14, 2020	West Virginia	Early morning mud slide forced traffic . . .	https://www.timeswv.com/news/early-morning-mud-slide-forced-traffic-to-one-lane/article_df10f130-4edb-11ea-a569-1fe636d7298a.html
February 14, 2020	West Virginia	Landslide devastates:	https://www.bdtonline.com/news/landslide-devastates-community-fears-further-tragedy-from-mud-debris/article_7b70d514-4ecc-11ea-a470-43db58b97f3d.html
February 13, 2020	Australia	Closures: Road and school . . .	https://www.northernstar.com.au/news/road-and-school-closures-on-the-northern-rivers/3943493/
February 12, 2020	West Virginia	DOW releases statement . . . rock slide	https://www.wdtv.com/content/news/US-19-closed-in-Morgantown-after-rock-slide-567737651.html
February 4, 2020	Oregon	Hwy 62 reopens following rockslide	https://mailtribune.com/news/top-stories/highway-62-reopens-following-rockslide
February 1, 2020	Canada	There are numerous highway closures. . .	https://www.castanetkamloops.net/news/Kamloops/287306/There-are-numerous-highway-closures-rockslides-across-BCs-Interior
Febrary 1, 2020	Ghana	Gov't to demolish buildings causing rockfalls	https://www.ghanaweb.com/GhanaHomePage/NewsArchive/Government-to-demolish-buildings-along-Peduase-Aburi-stretch-causing-rockfalls-854023
January 29, 2020	United Kingdom	Livermead rock fall. . .	https://www.devonlive.com/news/devon-news/livermead-rock-fall-latest-string-3787805
January 26, 2020	Canada	New bridge . . restoring access	https://vancouverisland.ctvnews.ca/new-bridge-installed-on-highway-4-restoring-road-access-to-island-s-west-coast-1.4784144
January 24, 2020	Canada	Highway . . . closed after rockfall	https://www.cheknews.ca/rock-debris-closes-highway-4-in-both-directions-639700/
December 27, 2019	Fiji	Fiji . . . Roads closure	https://fijisun.com.fj/2019/12/27/tc-sarai-fra-2pm-roads-update/
December 13, 2019	Alaska	Car strikes boulder . . .	https://www.adn.com/alaska-news/anchorage/2019/12/13/car-strikes-large-boulder-on-rockfall-prone-stretch-of-seward-highway/
November 17, 2019	Canada	Rockslide snarls traffic . . .	https://globalnews.ca/news/6180471/rockslide-vancouver-island/

September 9, 2019	United Kingdome	Work to begin . . .	https://www.pressandjournal.co.uk/fp/news/highlands/1836266/work-to-begin-on-stromeferry-rock-face-with-closures-and-delays-expected/
August 29, 2019	Colorado	CDOT: Summer driving safety	https://www.fortmorgantimes.com/2019/08/26/cdot-summer-driving-safety/
August 29, 2019	Utah	Rockfall at Zion . . .	https://www.thespectrum.com/story/news/2019/08/27/zion-national-park-utah-trail-close-open-rockfall-updates/2130079001/
August 9, 2019	Alaska	Denali Park Road to reopen . . .	https://www.adn.com/alaska-news/weather/2019/08/08/denali-park-road-closed-amid-heavy-rains-and-landslide-danger/
August 8, 2019	Alaska	Denali Park Road closed . . .	http://www.newsminer.com/news/local_news/denali-park-road-closed-thursday-after-heavy-rainfall/article_ca4db8a2-b96f-11e9-b56a-d3f72ea8767d.html
June 4, 2019	Alaska	A stretch of the Denali Park Road . . .	https://www.alaskapublic.org/2019/06/03/a-stretch-of-the-denali-park-road-sits-atop-a-creeping-landslide-and-its-picking-up-speed/
June 1, 2019	New Zealand	State Highway 1 closed . . .	https://www.stuff.co.nz/national/113178868/state-highway-1-closed-due-to-rockfall
May 28, 2019	Wyoming	Northern Wyoming highways . . .	https://k2radio.com/northern-wyoming-highways-closed-due-to-landslide-rock-fall/
May 27, 2019	Colorado	10.3 Million Pounds of rock . . .	https://www.thedrive.com/news/28227/10-3-million-pounds-of-rock-tumble-1000-feet-onto-colorado-highway-closing-it-indefinitely
May 26, 2019	Colorado	Colorado Highway closed. . .	https://www.theepochtimes.com/colorado-highway-closed-indefinitely-after-huge-boulders-blocks-roadway_2937552.html
May 6, 2019	Colorado	Rockslide in Western Colorado . . .	https://www.denverpost.com/2019/05/05/rockslide-western-colorado-closes-interstate-70/
March 16, 2019	Colorado	Beware of rockfall . . .	https://www.aspentimes.com/news/local/beware-of-rockfall-in-glenwood-canyon-as-spring-approaches/
March 15, 2019	Tennessee	Most roadslide sites at risk . .	https://www.tennessean.com/story/news/2019/03/15/tennessee-highway-rock-slide-assessment-tdot/3151116002/
March 15, 2019	Colorado	Rockfall season. . .	https://www.postindependent.com/news/rockfall-season-brings-another-gravitational-hazard-to-garfield-county-roadways/
March 8, 2019	Tennessee	Crews still working . . .	https://clarksvillenow.com/local/crews-still-working-to-repair-road-after-i-24-landslide/
February 24, 2019	Hawaii	Pali Hwy closed . . .	https://www.kitv.com/story/39987573/update-hdot-to-contraflow-2-lanes-of-honolulu-bound-traffic-in-kailuakaneohe-bound-direction-of-pali-hwy

February 23, 2019	Tennessee	Another slide . . .	https://www.timesnews.net/news/local-news/another-slide-in-hawkins-closes-route-66-n-again/article_4c5729a1-a4cf-53d2-9ba5-644e2b834de8.html
February 22, 2019	Hawaii	HDOT to contraflow . . .	https://www.kitv.com/story/39987573/pali-hwy-remains-closed-possibly-through-the-end-of-the-week
February 15, 2019	California	Storm leaves behind rockfalls . . .	https://www.nbclosangeles.com/news/local/storm-topanga-canyon-boulevard-boulder-rain-california/1493/
February 15, 2019	California	Rain and snow batter . . .	https://www.sfgate.com/weather/article/Fierce-storm-batters-Southern-California-Snow-13532854.php
December 6, 2018	New Jersey	Where is the State's	https://www.njherald.com/opinion/20181206/where-is-states-proof-of-need-for-i-80-rock-wall
November 29, 2018	California	Heavy rain . . rockslides	http://www.malibutimes.com/news/article_bf271d92-f3ea-11e8-a268-138c68614905.html
November 29, 2018	California	Caltrans shuts down . . .	https://abc30.com/traffic/caltrans-shuts-down-portion-of-highway-140-due-to-potential-for-mudslides-/4783799/